Title
From networks to neurons: A multilevel investigation of experience-dependent improvement in prey capture behavior in the larval zebrafish

Author
Grossrubatscher, Irene

Publication Date
2021

Peer reviewed|Thesis/dissertation

From networks to neurons: A multilevel investigation of experience-dependent improvement in prey capture behavior in the larval zebrafish

By

Irene Grossrubatscher

A dissertation submitted in partial satisfaction of the

requirements for the degree of

Doctor of Philosophy

in

Neuroscience

in the

Graduate Division

of the

University of California, Berkeley

Committee in charge:

Professor Ehud Isacoff, Chair
Professor Helen Bateup
Professor Daniel Feldman
Professor Linda Wilbrecht

Summer 2021

Abstract

From Networks to Neurons: A multilevel investigation of experience-dependent improvement in prey capture behavior in the larval zebrafish

by

Irene Grossrubatscher

Doctor of Philosophy in Neuroscience

University of California, Berkeley

Professor Ehud Isacoff, Chair

Understanding the neural mechanisms that guide behavior is one of the biggest quests in neuroscience. This question is tackled at different levels of analysis, from studying whole-brain blood oxygenation levels in humans, to minuscule receptor movements in cells. In this dissertation, I describe work aiming to explore the neural basis of behavioral improvement in the larval zebrafish from the network level, across brain areas, to the neuron level, looking at specific neuronal ensembles.

In chapter one, I introduce the study of experience dependent changes in behavior through history and describe the advantages of using the ethologically relevant prey capture behavior in larval zebrafish as a model. In chapter two, in collaboration with Claire Oldfield, I studied how experience hunting live prey affects prey capture behavior and the underlying neural activity. I show that previous experience with live prey improves hunting performance compared to larvae that have been fed with inert fish flakes. Consequently, looking at whole-plane neural activity, I observed no differences in the neural representations of prey in the visual areas, however, experienced fish showed increased correlations between output neurons of the tectum and the forebrain, and an increased probability for visual activity to evoke motor action. This led to the hypothesis that experience may lower the threshold for visual information transfer to motor areas, via an increase of activity in the forebrain. To test this hypothesis, I specifically ablated cells in the habenula, one of the forebrain structures, and observed a reduction in eye convergences and prey consumption. These findings show the involvement of the forebrain in experience-dependent improvement of prey capture for the first time. In chapter three, I describe our attempts to study experience-dependent changes in forebrain activity and network dynamics between visual areas and the forebrain at a single-cell resolution, using multi-plane two-photon imaging. This project is still at its beginnings, but I describe the adaptation of the behavioral paradigm to the two-photon microscope, and the potential of recording large populations of neurons at cellular level during a naturalistic behavior.

Dedication

To my family and my friends near and far, who have provided the freedom and support to go on this journey.

Table of Contents

List of Figures

Acknowledgements

I feel infinitely grateful and privileged to spend my years of graduate school UC Berkeley, basking in the knowledge and discoveries around me, and the community that support them This includes all the professors, Candace Groskreutz and the staff and all my peers that make the graduate program an enjoyable stimulating place.

First and foremost, I want to thank my advisor Udi Isacoff, for creating a lab environment I could thrive in. I will always admire your simultaneous kindness and humanity and god-like perspective and wisdom. Further, I really appreciated that you included us lab members in your family events, since my family always was so far. It somehow gave me strength and grounding, and I enjoyed learning about the Jewish traditions and your family's past. Here I also want to thank the rest of my thesis committee, Helen Bateup, Linda Wilbrecht and Dan Feldman for their time, support, and availability.

Next, I thank my parents, who supported me on this path, even though it kept me thousands of miles away from them. I also thank my brothers, whose presence make my absence at home less noticeable, and who always talk me through tough decisions.

Further, I thank my mentors before graduate school, who believed in me and helped me get here in the first place. Professor Giorgio Aicardi at the University of Bologna, Professor Patricia Janak, who is currently at Johns Hopkins, and Professor Loren Frank at UCSF. Next come my peers, who have guided and supported me along the way, before and throughout graduate school. Elizabeth Steinberg and Kate Vitale at the Gallo, Kenny Kay, Jason Chung, Jai Yu, Marilena Sosa, Lucas Tian and Jeffery Knowles at UCSF.

I also thank my fellow Isacoff Lab members, especially the fish team, Shi-Wei Chou and Amy Winans. Your patience and knowledge supported me in all aspects of my work, the practical and experimental aspects, and the mental and people aspects. You shaped me as a scientist and a person, and I will miss you very much. I also want to thank Adam Hoagland, for his availability to help with thinking and programming when in-promptu setup of experiments and analysis were needed. Further, I thank Sandra Wiese and all the fish facility staff whose work is invaluable, and all the fish that enabled my experiments.

I also thank my collaborators Clarie Oldfield and Lamiae Abdeladim. It was a pleasure working with you, and you continue to be my role models for powerful women pursuing meaningful careers.

Over the years, I have worked with three undergraduates, Andrea Romo, Sweta Parija and Lydia Liu, who have helped me with the most tedious tasks and whose presence have always sparked my passion for science.

Finally, I want to thank my friends, who are in the front lines in good times and in bad times. The Euro crew, with Kathrin, Maria, Pablo and Juan, the East Bay crew, with Tobias, Stacy, Devon, and Simone. Rose and Louis who are always up for adventure, and all the others I don't mention. Special thanks also go to my two main house communities, the Bombest house in San Francisco, and the Carleton house in Berkeley. The talks, walks, dinners, outdoor excursions, and dance sessions with friends were and will always be the juice that keeps me going.

Publication Related to This Work

My dissertation contains work that has been previously published, with me being a co-first author:

Oldfield CS*, Grossrubatscher I*, Chavez M, Hoagland A, Huth AR, Carroll EC, Prendergast A, Qu T, Gallant J, Wyart C and Isacoff EY (2020). Experience, circuit dynamics and forebrain recruitment in larval zebrafish prey capture. *Elife*. 2020; 9:e56619. doi: 10.7554/eLife.56619.

Chapter 1: Introduction

The zebrafish larva as a model for studying the shaping of brain function and behavior by experience

The levels of analysis in the nervous system

In the late 19th century, the Italian physician Camillo Golgi and the Spanish pathologist Santiago Ramon y Cajal held opposing views on whether the brain was a network of fibers, similar to the vascular system, or, whether it was an agglomeration of special nerve cells, called neurons. In 1873, Golgi developed a tissue staining method, “la reazione nera", where silver nitrate would penetrate only a random small percentage of the nervous tissue, revealing its structure for the first time. In his research, he observed long nerve fibers and widely arborized dendrites and could not recognize a delimitation between the various shapes. Therefore, he held on to the idea of the nervous system being a continuous net of nerve fibers — the “reticular theory”. A few years later, Ramon y Cajal used and refined the Golgi stain for his own anatomical studies in bird brains. He observed that there were gaps between the different nerve fiber structures and proposed that the nervous system was made up by discrete cells and not a continuous net[1]. This finding was seconded by other scientists of the era, and popularized as the “neuron doctrine”, which declared the “neuron” as the anatomical and functional unit of the brain.

Around the same time of the discoveries of Golgi and Ramon y Cajal, another fundamental theory of brain function developed — the functional localization theory. This theory postulated that different brain functions are encoded in different areas of the brain. The theory, rooted in the concept of phrenology, was proposed by the German neuroanatomist Franz Gall who believed that the brain was not a uniform organ. Instead, he hypothesized that the brain was an assembly of multiple organ-like structures, each of which had a specific function[2]. He postulated that the shape of the skull could indicate the degree of development of a specific function or trait. Although phrenology turned out to be wrong, Gall’s careful experiments yielded some interesting results, especially the concept that some brain functions are localized to a specific area of the brain. This idea was then picked up and confirmed by other neuroscientists such as Pierre-Paul Broca, who was working with patients with aphasia and examined their brains post-mortem. He pinpointed for the first time, an area of the brain that was essential for a specific higher function, namely speech[3].

The neuron doctrine and the functional localization theory lay at the basis of our current understanding of the structure and function of the nervous system. As a result of technological advancement and empirical observations in the following century, these two theories were confirmed and furthered by many discoveries. It became clear that single neurons could hold very specific functions, like the “bug detector” neurons found in frogs, which fire in response to small moving stimuli, such as flies[4]. It also became clear that single neurons could be part of functional circuits that sometimes were confined to a specific brain structure, and sometimes would act in networks that involving multiple structures. More recently, through the ability to monitor the simultaneous activity of multiple neurons via multicellular electrical recordings or through neuronal imaging techniques, it has been shown that specific brain functions also lie in the simultaneous activity of groups of neurons, neuronal ensembles, and that specific neurons can be a part of multiple different functional ensembles[5]. The different levels of analysis are depicted in Figure 1.1.

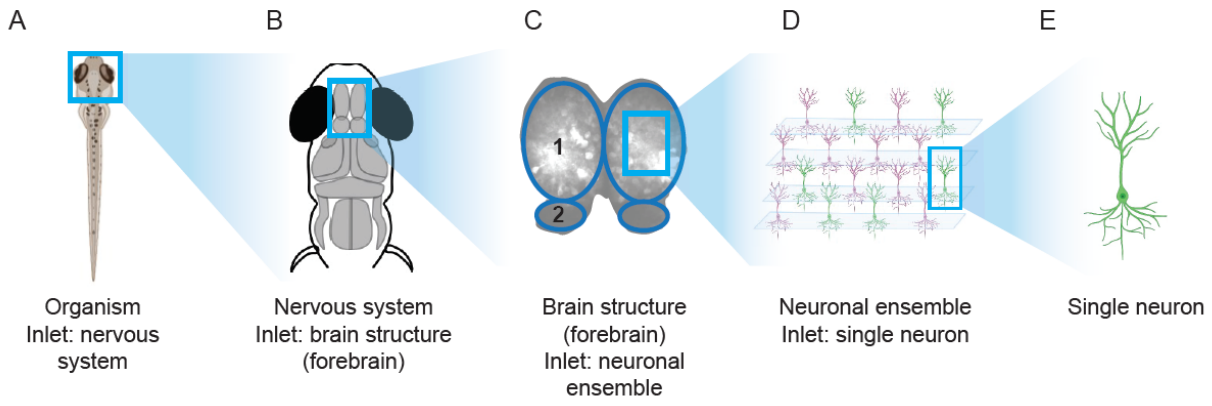

Figure 1.1. Levels of analysis.

This schematic shows the levels of analysis used in this work on the zebrafish larva model. **A)** Depiction of a whole organism, in this case the zebrafish larva, with an inlet box above the head, indicating the nervous system. **B)** A depiction of the zebrafish nervous system, with a cartoon of its main brain areas. The inlet indicates the forebrain. **C)**The forebrain is composed of two brain structures, the telencephalon (1) and the habenula (2). The inlet shows neurons in the telencephalon. **D)** Group of neurons in the telencephalon, with an active ensemble highlighted in green. Inlet on a single active neuron. **E)** Single neuron.

Today, we have long moved past the discord between Golgi and Cajal and have understood that the nervous system is constituted by billions of connected neurons, each of which is acting dynamically as part of many neuronal ensembles that in turn are part of various functional networks. It is still poorly understood how neuronal activity at these different levels creates and updates our representations of experience and guides behavior. In this dissertation, I will shed light on the neural basis of experience dependent changes in larval zebrafish prey capture, at the network, structural, and cellular levels.

The neural basis of experience-dependent changes in behavior

The human brain is made up of about one hundred billion neurons, with hundreds of trillions of connections, forming functional circuits. These circuits are in turn organized into larger networks and anatomical structures that integrate information from all parts of the nervous system. These networks then process external information coming from the sensory organs, and internal information, coming from other parts of the brain, to generate behavior. Responses to sensory experiences can be as simple as a retracting your hand when touching a hot surface, or more complex, like choosing to stop texting your latest love interest when they didn't get back to you for the third time. Therefore, behavior can be simple, such as the reflexive response to a stimulus, or can be more complicated, such as choosing what to do from a variety of options in response to a set of sensory information and integrating it over time with accumulated experience.

The integration of past experience into current behavior is called "learning", and it relies on memory, which is recollection of the past experience. Despite the popularity of the functional localization theory, memory was believed to be a distributed throughout the cortex of mammals, after a series of experiments performed by Karl Lashley and published in 1929, where he trained rats in seeking a food reward, and then lesioned different parts of their cerebral cortex. He concluded that lesions deteriorate the learning, but that the degree of deficit depended more on the

amount of cortex lesioned and not by the location[6]. This view changed dramatically in the 1950s, through observations in patients with localized brain injuries, the most famous one being Henry Gustave Molaison, or patient H.M. Patient H.M. underwent bilateral removal of his temporal lobe, including the hippocampus, amygdala and parts of the parahippocampal formation, to alleviate him from his severe epilepsy. After the surgery, he was free of seizures, but a new memory loss occurred, while other intellectual and perceptual functions, like copying drawings and repeating digits, remained intact. Careful observations and experiments performed on patient H.M. identified, for the first time, a particular area of the brain being important for memory and birthed the modern memory research[7].

Findings from patients with localized brain lesions like H.M. started the search for the brain regions underlying different types of learning, and after 50 years of research, several brain areas have been shown to be involved in different types of learning. Firstly, one needs to distinguish between short-term memory, working memory and long-term memory, where long-term memory has historically been divided into further subtypes. One current framework introduced by Larry Squire in 2004 distinguishes two types of memory, which are declarative memory, and non-declarative memory[8]. Declarative memory is the memory of facts and events, which is representational and accessible to conscious awareness, and requires the medial temporal lobe. Non-declarative memory includes other types of memory and are process specific types of information in specialized brain regions. Non-declarative memory includes procedural memory encoded in the striatum, priming and perceptual learning in the cortex, simple and classical conditioning in the amygdala and the cerebellum, and non-associative learning in the various reflexive pathways.

While discovering various brain structures underlying different types of learning, scientists also started wondering about the basis of learning on a cellular level. Ramon y Cajal and one of his early followers, Eugenio Tanzi, developed the first theories about how practice and experience could promote neuronal growth by shortening the gaps between the neurons and facilitating their interactions, coining the idea of neuronal plasticity[9]. Subsequently, chemical synapses were discovered as the junctions between two nerve cells and named and popularized by Charles Sherrington, who studied the knee jerk reflex in different animals. Sherrington described for the first time many fundamental properties of synaptic transmission, and suggested that the synapse was not just the anatomical but also the functional unit of the nervous system, and possibly related to learning and memory[10]. Only in the 1940s, Donald Hebb who was studying the effects of neurosurgery and behavior in humans and animals, developed the theory of Hebbian learning, building on the idea of plasticity. He observed that children often partially or fully recovered from cognitive impairments after brain injury, while in adults such improvements were not observed and concluded that plastic changes in the brain may be age dependent. Following up on his observations and some already existing ideas, he hypothesized that if a neuron A was in close enough proximity to repeatedly excite a neuron B, some metabolic changes would take place in one or both neurons to increase the efficiency of neuron A firing neuron B[11].

Empirical evidence for this theory only came in the 1960s, where Eric Kandel studied simple forms of non-associative learning, namely habituation and sensitization on the gill withdrawal reflex in the sea slug *Aplysia Californica*. Kandel and his collogues repeatedly stimulated the animal's syphon trough innocuous touch and observed that the animal, after repeated stimulation. retracted the syphon and gill less frequently, showing habituation[12]. They also observed that the gill retraction reflex could be facilitated by previous repeated stimulation with a noxious stimulus, which means that if previously sensitized, the neuron would respond more

strongly to a stimulus, and that, interestingly, this effect would last for weeks. By recording electrical activity from the motor and sensory neurons involved in this reflex pathway, they discovered a change in synaptic strength between the sensory neuron detection the touch, and the motor neuron causing the gill withdrawal. This change in synaptic strength, was mediated by a change in neurotransmitter release[13], resembling the "metabolic change" that Hebb had imagined. These were the first steps in understanding the cellular mechanisms underlying learning and suggested the synapse as a major player in learning and memory.

In the 1970s, Bliss and Lømo confirmed the importance of synapses in learning and memory with their discovery of long-term potentiation (LTP) in the hippocampal circuit. The hippocampus was by then known to be the most important structure involved in long term memory, and its trisynaptic circuit was discovered and initially described by Ramon y Cajal[14]. This circuit is composed of three different cell groups and the connecting nerve fibers between them. The inputs from the enthorinal cortex enter the hippocampus via the perforant path, which synapse onto the granule cells in the dentate gyrus. The granule cells, then project to the pyramidal neurons in the hippocampal region CA3 via the mossy fibers. The neurons then project to the pyramidal neurons in the region CA1 of the hippocampus via the Schaffer collaterals, see Figure 1.2. Bliss and Lømo studied this circuit in anesthetized rabbits, and observed that low frequency stimulation of the perforant pathway corresponded with a baseline low level of activity in the dentate gyrus, but following a high-frequency stimulation of the perforant pathway, subsequent low frequency stimulations would activate the dentate more and maintain a result in a larger population spike than before the stimulation, for a long period of time[15]. This activity-dependent long-lasting change in synaptic efficiency provided the experimental basis for the link between synaptic changes and memory storage.

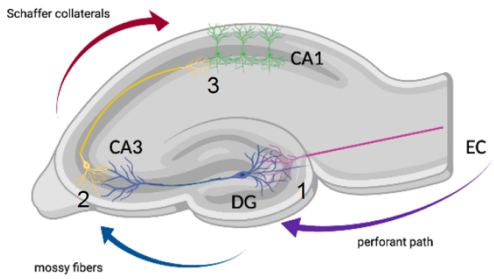

Figure 1.2. Trisynaptic loop.

Sensory information from the enthorinal cortex (EC) enters the hippocampus via the perforant path, and synapses onto the granule cells in the dentate gyrus (DG) (1). The granule cells synapse onto hippocampal area CA3 pyramidal cells via the mossy fibers (2), and the CA3 cells synapse onto the CA 1 pyramidal cells via the Schäffer collaterals (3).

This discovery was followed by a large body of work that reinforced the belief that the mechanisms underlying learning and memory lay in changes of synaptic strength. It was observed that the timing between the presynaptic input and the postsynaptic action potential determined whether synaptic strengthening or synaptic wakening, called long term depression or LTD, was induced[16]. Then, it was found that the induction of LTP was dependent on NMDA glutamate receptors, that require activation of both the presynaptic and the postsynaptic neuron in very close temporal proximity, and therefore act as "coincidence" detectors[17]. Later, it was discovered that different forms of synaptic strengthening and weaking, that depended on different types of glutamate receptors, exist in different tissues and in different areas of the brain, and that calcium influx played an important role in this process[18]. Most importantly, it was also shown that blockage of NMDA receptors in the hippocampus, and therefore presumably blockage of LTP, caused an

impairment in learning a spatial memory task in rats[19], which proved synaptic plasticity to be relevant in live organisms, and encouraged further studying of this process.

Changes in synaptic strength of excitatory neurons were shown modulated by inhibition, especially gamma-aminobutyric acid (GABA) and other neuromodulatory transmitters that can favor either synaptic strengthening or weakening. Further findings revealed that the basis of the long-term effects of LTP and LTD, lay in de-novo protein synthesis, which can be dependent or independent of gene transcription. This dependence on protein synthesis of LTP allows for another form of associative interaction between synaptic inputs, which is called "synaptic tagging". In short, proteins synthetized in response to a strong stimulation of one input pathway can be captured by a second converging input pathway in the proximity, and be used to generate changes in synaptic strength[20]. This process occurs across intervals of several hours and may facilitate the storage of memories that occur in temporal proximity to strongly stored experiences.

So far, I have summarized the functional synaptic changes induced by LTP and LTD, however, there are also structural changes in dendritic spines of the postsynaptic neurons that can be induced. This is called structural plasticity. Dendritic spines are little protrusions at the postsynaptic site of most excitatory mammalian synapses, and their dynamic nature was discovered first by detecting a decrease of spine density with age and an increase with environmental enrichment[21]. Kandel and colleagues observed such structural changes at the sensory neuron to motor neuron synapse in his studies of sensitizations and habituation, where he would observe growth of new synapses in the first case, and removal of synapses in the latter, for long term forms of memory[22,23]. Only recent technical advancements of imaging techniques allowed scientists to monitor spine dynamics during learning. It was shown that new spine formation would occur across multiple forms of learning, like the exposure to a novel experience or the acquisition of a new skill, and that only a small percentage of spines persisted over the next few weeks. The percentage of spines that remained stable increased with longer periods of exposure or training. After the reinstatement of the previously acquired learning, no novel spine growth was observed, but after learning of a novel, similar task, new spines could be detected, which suggested that spine formation is needed for new memory formation, but not needed for recall. Further it was observed that longer training caused increased spine elimination. This removal of unused connections can be interpreted as a mechanism for behavioral refinement observed in animals that had more practice[24]. Dendritic spines are found in most excitatory neurons, and their capacity for experience-dependent dynamic changes provide cortical networks with the ability to convert novel experiences into anatomical traces. Therefore, dendritic spines are an attractive candidate to translate synaptic reorganizations into durable memories.

Above, I have non-exhaustively outlined some key discoveries supporting learning and memory on a cellular level. However, memory consolidation and stabilization also happen on a network level. Evidence for this has been shown in patients like H.M., where new episodic memories, which are dependent on the hippocampus, could not be formed, but old, lifelong memories were intact. This supported Karl Lashley's distributed idea of memory, and seeded ideas of memory transfer between the hippocampus and the cortex, with gradual stabilization of memories in the cortex. The mechanism believed to underly such transfer of memories is a high frequency hippocampal rhythm called the sharp-wave ripple (SWR). These activity patterns occur spontaneously during sleep or active immobility, when the release of subcortical neuromodulators within the hippocampus is decreased and replay neuronal firing sequences that occurred during recent experience. Further, the temporal compression of the firing sequence seems to reflect a property of memory, and memory is impaired when SWRs are interrupted during a spatial memory

task[25]. SWRs are not confined to the hippocampus, but also generate sequential activation in cortical circuits, leading to network level consolidation of memories[26].

Recently, more evidence for the distributed localization of a memory trace, called the "engram", was found trough the development of novel technologies that allow for tracing and stimulation of strengthened synapses. The engram is a sparse ensemble of neurons which are 1) activated during experience, 2) undergo structural and functional modifications as a result, and 3) are reactivated upon recall of the experience. It was shown in a classical fear conditioning study in mice that cells part of an engram showed the typical changes in synaptic strength seen during LTP and were blocked by injection of protein synthesis inhibitors (PSIs). Surprisingly, opsin mediated stimulation of tagged engram cells could induce memory recall in PSI injected mice[27]. Therefore, it seems that protein synthesis dependent LTP was not necessary for memory storage, but necessary for the recall of a memory.

This summary of some milestones in learning and memory research shows that changes in synaptic efficacy via LTP and LTD at pre-existing connections represent a primary mechanism to encode a memory trace or engram. Further, LTP and LTD facilitate the formation of new synapses and the elimination of old synapses, and therefore changes in structural connectivity. There is still much to be learned about the mechanisms underlying learning at the cellular, neuronal ensemble, brain structure and circuit level, and the connections between those levels. One limitation for the multilevel studying of experience-dependent refinements of behavior is the balance between the accessibility to monitor a high percentage of neurons, which is given in invertebrates and simple vertebrates, and the complexity of the behavioral repertoire displayed by the organism. In this dissertation I propose the zebrafish larva as an attractive model for such multilevel investigations for experience-dependent behavioral improvement.

The zebrafish larva is an attractive model organism in neuroscience

Technological advancements often lie at the basis of significant discoveries. We observed this throughout history, starting with the Golgi stain that enabled the visualization of the structure of the nervous system for the first time and revealed the neuron to be its fundamental component. The development of microelectrodes for extracellular and intracellular recording was based on ideas of Luigi Galvani, who first detected that the signal between nerves and muscles was electrical by performing experiments in frog legs. This was followed by attempts to record the electric currents running through nerves and muscles, which was first obtained by using instruments like the galvanometer and the Bernstein rheotome, and followed by the development of micropipettes and microelectrodes[28], and the invention of the tungsten electrode to record from single neurons by Hubel and Wiesel in the 1950s. The development of hippocampal ex-vivo slice preparations also was seminal in the study of synaptic plasticity and is to date widely used in neuroscience.

With the discovery that calcium played a major role for the functioning of the nervous system, interest increased in being able to monitor calcium dynamics in living cells. To achieve this, the identification of a compound that would change conformation upon binding of calcium and change its fluorescent properties was needed. In 1980, the biochemist Roger Tsien developed the first selective Ca^{2+} dye, that could be used to measure changes in free intracellular calcium[29]. From there, after many years of discoveries in microscopy techniques and optimization of calcium dyes the field of neural imaging came to be, which to date is monitoring calcium dynamics, the counterpart of the action potential. Calcium imaging has since then become a widely used

technique to study the neural correlates of behavior, since it displays different properties than classical electrical recordings. Calcium dynamics are slower than the electrical potentials in neurons, which causes lower temporal resolution, while the spatial resolution is improved, strikingly enabling the visualization the active neurons in real-time, in behaving animals. Today, the calmodulin-based genetically encoded fluorescent calcium indicators (GCaMPs) are the most popular for in vivo imaging. In these proteins, circularly permuted forms of the fluorescent protein GFP are fused to calmodulin and the M13 domain of the myosin light chain kinase. If calcium is present GCaMP changes its conformation due to calcium binding to calmodulin, and leads to bright fluorescence due to rapid deprotonation of the GFP[30]. Throughout this dissertation the calcium indicator GCaMP6f was used in combination with spinning disk and 2-photon microscopy.

Another complementary technological advancement calcium imaging that revolutionized the field of neuroscience was the development of optogenetics. Here, light sensitive ion channels, originally found in algae and bacteria are expressed in neurons. Following activation of said channels with different wavelengths of light, the neurons are excited or inhibited, depending on the nature of the light-sensitive ion channel. This discovery has and is continuing to have an enormous impact on the study of neural circuits, since it allows millisecond-precise, reversible control of neural activity, and can specifically be expressed in certain brain structures, cell types or projections to probe their function and reveal causal links between neural activity and behavior. Further, the development of 3D patterned holographic optogenetic stimulation of neurons[31] has the potential to manipulate ensembles of neurons in a temporally precise way, which may lead to the ability to artificially induce recall of a memory trace or to create artificial engrams in the brain[32]. The combination of single-cell resolution calcium imaging and optogenetics seems to be especially suited to study the localized and distributed changes happening during learning. In mammals, neuronal ensembles can be observed trough imaging in vivo by constructing cranial windows, with the limitations of only reaching the superficial layers of the cortex in a small area, reaching only a small percentage of the neurons in the brain. Therefore, organisms with smaller brains and easily accessible neurons are advantageous for the studying the neural correlates of experience.

The zebrafish larva seems particularly suitable, with its small brain size of about 100000 neurons at day 5 post fertilization (dpf), brain length of about 1.5 mm, and its transparent head, which allows for non-invasive calcium imaging and optogenetic stimulation. Zebrafish (*Danio reiro*) are small bony fish of the family of teleosts. Native in the sweet waters of the southwestern Himalayas, they became popular as a model organism since the 70s for their fast development and ease of genetic manipulation. The zebrafish genome has been sequenced and shows that 70% of human genes have an orthologue in zebrafish. Further, they provide easy genetic targeting strategies of specific brain areas or neuronal subtypes types, permitting their optical chemical and genetic manipulation.The structural organization of their brain resembles that of other vertebrates and mammals with important conserved regions, like the retina, olfactory bulb, habenula, cerebellum and spinal cord. Analogous similarity exists in its neurochemical makeup, with the same neurotransmitters, such as glutamate, GABA and neuromodulatory systems (dopamine, noradrenalin, serotonin, histamine), receptors, enzymes, and metabolic machinery as that of higher vertebrates. The main difference between zebrafish and mammals is the absence of a neocortex and other higher order processing structures like the hippocampus, amygdala and piriform cortex, for which homologue structures in the zebrafish forebrain have been proposed[33,34]. Zebrafish are sensitive to a variety of stimulus modalities, including vision, audition, olfaction, touch, vestibular inputs, heat and chemosensation and display a vast repertoire of behaviors even at the larval stage, which allow for studying of experience-dependent neural dynamics[35]. Behaviors the zebrafish

already exhibits at the larval stage include motor behaviors, for example spontaneous coiling behavior, which starts at 17 h post fertilization. They respond to threatening stimuli like large dots or loud noises with escape and startle behaviors, and they respond to illumination with phototaxis. Further, they exhibit optic flow responses, like the optokinetic reflex (OKR), where movement of the eyes compensates for movement of the environment, and the optomotor response (OMR, where display of moving stripes under the fish induces swimming. As the fish go beyond three weeks of age, they start exhibiting more complex social behaviors, like schooling, decisions in groups, aggressive encounters, and mating[36].

Examples of learned behaviors in larval zebrafish are the non-associative habituation to acoustic startle[37,38], and the associative learned passivity[39,40] and various forms of classical conditioning that depend on the cerebellum[41,42], similarly as in mammals. It is noted though that behavioral performance is inconsistent in larval zebrafish, showing large degrees of behavioral variability, possibly because the neural systems still being in a unmature, transitional state[43]. The combination of the similarity of the zebrafish to higher vertebrates, its wide range of behaviors, its genetic amenability, and the accessibility of virtually all its neurons to calcium imaging and optogenetic techniques make it an attractive model for studying the neural basis sensory processing, motor control and experience-dependent refinement of behavior.

Larval zebrafish prey capture as a model for "cognition"

In larval zebrafish, prey capture was believed to be an innate behavior. It can be observed as early as first attempts on day 4 dpf, when the fish begins to swim. To perform this behavior the larva needs to take in information about prey from its environment integrate this information with its internal state, for example hunger, decide if it wants to pursue the prey and execute the motor action to perform the hunting behavior. This simple behavior includes multiple neural processing steps, like sensory perception, decision-making and motor control, and therefore constitutes an attractive model system for the study of cognitive functions at the basis of natural behaviors in zebrafish[44].

Animal behavior generally is flexible to ensure thriving and survival in a continuously changing environment. Feeding is essential to survival, and animals have developed different strategies to procure food. In predators, some species, like most mammals, require an extended period of parental care and learn from direct experience by mimicking parents or other conspecifics, while other species must hunt by themselves right after birth, like most reptiles and fish. In both cases, prey capture improves with experience. For example, snakes improve in their hunting ability[45]and, in fish it has been reported that early exposure to available prey types was critical for survival in the wild for hatchery-raised fish[46], and that exposure to live prey increased hunting success in juvenile Australian jade perch[47]. Such evidence suggests that prey capture is comprised of both innate and learned components, where the innate component may be "hard wired" as a stereotypical response to predictable stimuli. Learning enables the animal to build upon the innate components, to respond to the variable and unpredictable situations they encounter throughout their lifespan. The neural mechanisms underlying such flexible adaptations, and how they contribute to the improvement of hunting performance are still unknown.

Zebrafish are diurnal animals which strongly rely on vision. They respond to their natural prey, which is a small unicellular organism called paramecia, and other prey-like stimuli like small moving dots with an innate hunting sequence. The sequence consists of four discrete steps: 1) prey recognition (Figure 2.3. A), 2) orienting towards the prey, 3) approach (Figure 2.3. B) and 4)

capture swim or suction motion, which culminates in the engulfment of the prey (Figure 2.3. C). Two stereotypical behavioral elements are displayed exclusively the context of prey capture, which are asymmetric J-bends of the tail during prey approach and a characteristic increase of the angle between the eyes, referred to as eye convergence. The zebrafish larva converges its eyes before every hunting sequence and maintains a high ocular vergency angle throughout the prey pursuit, therefore, eye convergence can be used as a proxy for the decision to capture prey. Zebrafish have laterally positioned eyes and converge their eyes during hunting to increase their binocular visual field and purportedly helps to gage their distance from the prey[48].

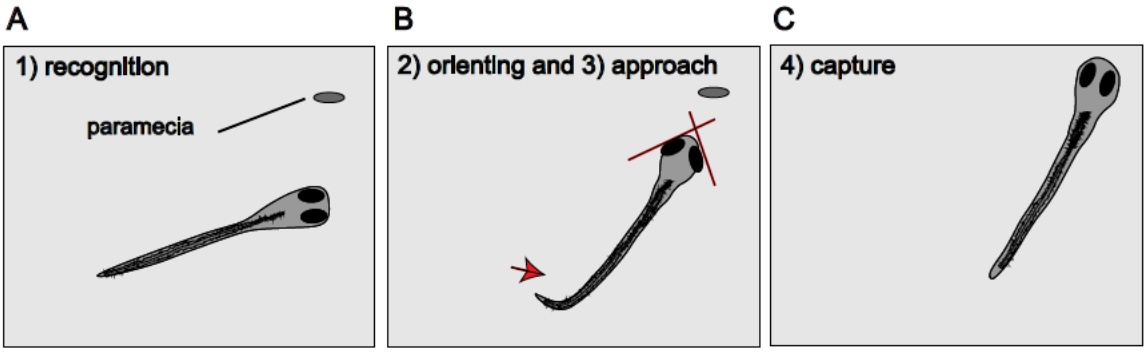

Figure 2.3. Prey capture sequence in the zebrafish larva.

A) The zebrafish larva recognizes its natural prey, the unicellular organism paramecia. **B)** The zebrafish converges its eyes, signaling its decision to pursue the prey and orients towards it by J- turn tail movements. The increase in eye angle and characteristic tail movement are shown in red. **C)** The larva strikes forward and engulfs the prey.

Prey capture is a complex behavior that involves multiple brain structures. The neural circuit underlying prey capture behavior in the zebrafish larva has been extensively studied as an example of sensorimotor integration. Visual information absorbed by the retina flows from the retinal ganglion cells (RGCs) to different relay regions in the optic tectum. The zebrafish tectum is a large layered brain structure which is homolog to the superior colliculus in mammals, and is believed to be the main hub for visual processing in the zebrafish brain, though recent results show that it may mediate additional functions, like possibly the modulation of prey capture by hunger[49,50]. Retinal ganglion cells project to 10 different arborization fields in the optic tectum, of which the area AF7, also referred to as the pretectum, responds specifically to prey like stimuli[51] and contains neurons that directly control hunting intitiation[52]. Tectal neurons are tuned to different stimulus sizes[53] and participate in local circuits for the detection of small prey-like and large looming stimuli, therefore mediating both hunting and avoidance behaviors[54–58]. From the optic tectum, information travels to the mesencephalic reticular formation (MRF), which controls the muscles mediating the eye convergence movement and to the reticulospinal neurons in the hindbrain, which recruit spinal neurons to produce J-turns[55], see Figure 2.4.. The prey capture circuit is modulated by several neuromodulatory systems. Cholinergic modulation from the nucleus isthmi was shown to be necessary for the maintenance of prey pursuit[59], and modulation of prey capture by hunger is regulated by serotonin[60].

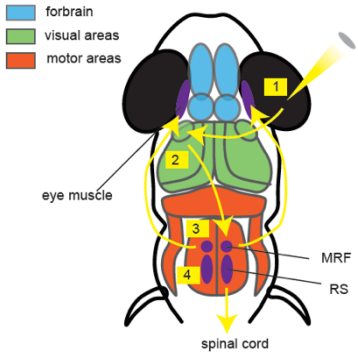

Figure 2.3. Schematic of main steps in the prey capture circuit.

Visual information activates photoreceptors in the retina (1), from there, information flows to the visual areas in the midbrain, the pretectum and the optic tectum. After various processing steps in the optic tectum not depicted here, information about prey flows to the motor areas in the hindbrain. The mesencephalic reticular formation (MRF) mediates eye convergence by controlling the ocular muscles, and the reticulospinal neurons project to the spinal cord to mediate the tail movement.

Since larval prey capture is a complex behavior dependent on a distributed circuit, it makes for an interesting model to study experience-dependent improvement across levels of analysis. To date, studies of experience-dependent changes in behavior often rely on drastic manipulations, such as blinding animals, or delivering electric shocks to achieve sufficient motivation to obtain a response. However, neurons respond differently to behaviors that are ethologically relevant[61,62], and therefore studying experience dependent changes using hunting behavior in the zebrafish larva model seems particularly relevant. Neuronal plasticity mechanisms are conserved trough species, and in the zebrafish larva it has been shown that visual stimulations induces plasticity in the retina[63], but does not cause reorganization in the layers of the optic tectum[64], showing that those are hardwired. Further studies show plasticity in the telencephalon[65,66], an area that purportedly contains homolog areas to higher processing areas like the amygdala, the hippocampus and the olfactory cortex[67–69], which could be important for experience-dependent learning. The habenula is also located in the forebrain and has traditionally been shown to be important for value-based learning. Recent studies have shown its importance in behavioral flexibility[39,70] and adaptation to learning rules[71]. Additionally, a retino-tectal-brainstem-thalamus-telencephalon-tectum pathway mediates sensory integration and behavioral gating across species, and may therefore also play a role in zebrafish[72].

In summary, I have discussed that prey capture is a natural complex behavior displayed in the larval zebrafish. It has a hard-wired, innate component, since stimulation of certain pretectal neurons can induce the capture sequence, but it may improve with experience, since such refinement has been seen in other organisms. The site and mechanism underlying behavioral refinement remains largely unknown and may lie at several locations in the circuit. The forebrain seems to be an attractive candidate region because of its involvement in learned behaviors throughout species, however, it has so far not been involved in the prey capture circuit.

Thesis summary

During my graduate research, I was interested in the neural basis for experience dependent improvement of behavior, and particularly in understanding the connections between different levels of analysis. In my first project (Chapter 2), I show in collaboration with my fellow co-first author, that experience with live prey improves hunting performance in larval zebrafish. Embedding a live prey in front of a head-fixed zebrafish allowed for monitoring behavior and neural activity in prey-naïve and prey-experienced fish. The larvae displayed eye convergences and J-turns during prey observation. Comparison of the neural activity of prey-naïve and prey-experienced larvae showed that the representation of prey in the visual areas did not change with

experience, however, prey-experienced fish were more likely to trigger a capture initiation in response to a given visual neural event and, surprisingly, displayed an increased drive from the output neurons of the OT to the forebrain. To further test the role of the forebrain in experience-dependent improvement of prey capture, I specifically ablated the habenula in experience fish and observed a reduction hunting behavior and prey consumption. I showed for the first time that the forebrain is involved in experience-dependent improvement of prey capture performance possibly by increasing the impact of information transfer from visual to motor-related areas, as a result of recruitment of forebrain activity.

This first study was conducted using live prey and imaging one plane of the brain, allowing only for a gross brain area-wide resolution. In the second part of my dissertation (Chapter 3), I describe a pilot study where I employ volumetric two-photon imaging to study hunting behavior in experienced fish, by employing a moving dot as visual stimulus. I show the reproducibility of findings from Chapter 2 with this methodology and set the stage for future more detailed studies of the neuronal ensembles underlying experience-dependent improvement in larval zebrafish prey capture on a rich dataset.

References

1. Cajal, S. R. *Histologia del sistema nervioso de los vertebrados*. (1905).
2. Folzenlogen, Z. & Ormond, D. R. A brief history of cortical functional localization and its relevance to neurosurgery. *Neurosurg. Focus* **47**, E2 (2019).
3. Dr. Paul Broca. *Science (80-.).* **os-1**, 93 LP – 93 (1880).
4. Maturana, H. R., Lettvin, j. Y., McCulloch, W. S. & PITTS, W. H. Anatomy and physiology of vision in the frog (Rana pipiens). *J. Gen. Physiol.* **43(6)Suppl**, 129–175 (1960).
5. Yuste, R. From the neuron doctrine to neural networks. *Nat. Rev. Neurosci.* **16**, 487–497 (2015).
6. Lashley, K. S. *Brain mechanisms and intelligence: A quantitative study of injuries to the brain. Brain mechanisms and intelligence: A quantitative study of injuries to the brain.* (University of Chicago Press, 1929). doi:10.1037/10017-000
7. Scoville, W. B. & Milner, B. Loss of recent memory after bilateral hippocampal lesions. *J. Neuropsychiatry Clin. Neurosci.* **12**, 103–113 (1957).
8. Squire, L. R. Memory systems of the brain: A brief history and current perspective. *Neurobiol. Learn. Mem.* **82**, 171–177 (2004).
9. Tanzi, E. Sulle modificazione morfologiche funzionali dei dendtriti delle cellule nervose. *Riv. Patol. Nerv. Ment.* **3**, 337–359 (1898).
10. Sherrington, C. *The integrative action of the nervous system*. (CUP Archive, 1952).
11. Hebb, D. O. *The Organization of Behavior*. *The Organization of Behavior* **911**, (1949).
12. Castellucci V., P. H. K. I. *et al.* Neuronal Mechanisms of Habituation and dishabituation of the gill withdrawal reflex in Aplysia. *Science (80-.).* **167**, 1745–1748 (1970).
13. Pinsker, H. M., Hening, W. A., Carew, T. J. & Kandel, E. R. Long-term sensitization of a defensive withdrawal reflex in Aplysia. *Science (80-.).* **182**, 1039–1042 (1973).
14. Andersen, P. Organization of Hippocampal Neurons and Their Interconnections. in *The Hippocampus: Volume 1: Structure and Development* (eds. Isaacson, R. L. & Pribram, K. H.) 155–175 (Springer US, 1975). doi:10.1007/978-1-4684-2976-3_7
15. Bliss, T. V & Lømo, T. Long-lasting potentiation of synaptic transmission in the dentate area of the anaesthetized rabbit following stimulation of the perforant path. *J. Physiol.* **232**, 331–356 (1973).
16. Bear, M. F. & Abraham, W. C. Long-term depression in hippocampus. *Annu. Rev. Neurosci.* **19**, 437–462 (1996).
17. Collingridge, G. L., Kehl, S. J. & McLennan, H. Excitatory amino acids in synaptic transmission in the Schaffer collateral-commissural pathway of the rat hippocampus. *J. Physiol.* **334**, 33–46 (1983).
18. Zhdanova, I. V. Sleep and its regulation in zebrafish. *Rev. Neurosci.* **22**, 27–36 (2011).
19. Morris, R. G. M., Anderson, E., Lynch, G. S. a & Baudry, M. Selective impairment of learning and blockade of long-term potentiation by an N-methyl-D-aspartate receptor antagonist, AP5. *Nature* **319**, 774–776 (1986).
20. Frey, U. & Morris, R. G. Synaptic tagging and long-term potentiation. *Nature* **385**, 533–536 (1997).
21. Connor, J. & Diamond, M. A Comparison of dendritic spine number and type on pyramidal neurons of the visual cortex of old adult rats from social or isolated environments. *J. Comp. Neurol.* **210**, 99–106 (1982).
22. Bailey, C. H. & Chen, M. Long-term memory in Aplysia modulates the total number of

varicosities of single identified sensory neurons. *Proc. Natl. Acad. Sci. U. S. A.* **85**, 2373–2377 (1988).
23. Bailey, C. H. & Kandel, E. R. Structural changes accompanying memory storage. *Annu. Rev. Physiol.* **55**, 397–426 (1993).
24. Hofer, S. B. & Bonhoeffer, T. Dendritic Spines: The Stuff That Memories Are Made Of? *Curr. Biol.* **20**, R157–R159 (2010).
25. Jadhav, S. P., Kemere, C., German, P. W. & Frank, L. M. Awake hippocampal sharp-wave ripples support spatial memory. *Science* **336**, 1454–1458 (2012).
26. Peyrache, A., Khamassi, M., Benchenane, K., Wiener, S. I. & Battaglia, F. P. Replay of rule-learning related neural patterns in the prefrontal cortex during sleep. *Nat. Neurosci.* **12**, 919–926 (2009).
27. Ryan, T. J., Roy, D. S., Pignatelli, M., Arons, A. & Tonegawa, S. Memory. Engram cells retain memory under retrograde amnesia. *Science* **348**, 1007–1013 (2015).
28. Verkhratsky, A. & Parpura, V. History of Electrophysiology and the Patch Clamp. *Methods Mol. Biol.* **1183**, 1–19 (2014).
29. Tang, Y. P. *et al.* Genetic enhancement of learning and memory in mice. *Nature* **401**, 63–69 (1999).
30. Miyawaki, A. *et al.* Fluorescent indicators for Ca 2+ based on green fluorescent proteins and calmodulin. *Nature* **388**, 882–887 (1997).
31. Pégard, N. C. *et al.* Three-dimensional scanless holographic optogenetics with temporal focusing (3D-SHOT). *Nat. Commun.* **8**, 1228 (2017).
32. Josselyn, S. A. & Tonegawa, S. Memory engrams: Recalling the past and imagining the future. *Science* **367**, (2020).
33. Mueller, T., Dong, Z., Berberoglu, M. A. & Guo, S. The dorsal pallium in zebrafish, Danio rerio(Cyprinidae, Teleostei). *Brain Res.* 95–105 (2011). doi:10.1016/j.brainres.2010.12.089.The
34. Porter, B. A. & Mueller, T. The Zebrafish Amygdaloid Complex – Functional Ground Plan, Molecular Delineation, and Everted Topology . *Frontiers in Neuroscience* **14**, 608 (2020).
35. Fero, K., Yokogawa, T. & Burgess, H. A. The Behavioral Repertoire of Larval Zebrafish BT - Zebrafish Models in Neurobehavioral Research. in (eds. Kalueff, A. V & Cachat, J. M.) 249–291 (Humana Press, 2011). doi:10.1007/978-1-60761-922-2_12
36. Orger, M. B. & de Polavieja, G. G. Zebrafish Behavior: Opportunities and Challenges. *Annu. Rev. Neurosci.* **40**, 125–147 (2017).
37. Roberts, A. C. *et al.* Habituation of the C-start response in larval zebrafish exhibits several distinct phases and sensitivity to NMDA receptor Blockade. *PLoS One* **6**, 1–10 (2011).
38. Pantoja, C. *et al.* Neuromodulatory Regulation of Behavioral Individuality in Zebrafish. *Neuron* **91**, 587–601 (2016).
39. Andalman, A. S. *et al.* Neuronal Dynamics Regulating Brain and Behavioral State Transitions. *Cell* **177**, 970-985.e20 (2019).
40. Mu, Y. *et al.* Glia Accumulate Evidence that Actions Are Futile and Suppress Unsuccessful Behavior. *Cell* **178**, 27-43.e19 (2019).
41. Aizenberg, M. & Schuman, E. M. Cerebellar-Dependent Learning in Larval Zebrafish. *J. Neurosci.* **31**, 8708–8712 (2011).
42. Harmon, T. C., Magaram, U., McLean, D. L. & Raman, I. M. Distinct responses of Purkinje neurons and roles of simple spikes during associative motor learning in larval zebrafish. *Elife* **6**, e22537 (2017).

43. Lovett-Barron, M. Learning-dependent neuronal activity across the larval zebrafish brain. *Curr. Opin. Neurobiol.* **67**, 42–49 (2021).
44. Muto, A. & Kawakami, K. Prey capture in zebrafish larvae serves as a model to study cognitive functions. *Front. Neural Circuits* **7**, 110 (2013).
45. Penning, D. A. & Cairns, S. Prey-handling behaviors of naïve Pantherophis guttatus. *J. Herpetol.* **50**, 196–202 (2016).
46. Cox, E. S. & Pankhurst, P. M. Feeding behaviour of greenback flounder larvae, Rhombosolea tapirina (Günther) with differing exposure histories to live prey. *Aquaculture* **183**, 285–297 (2000).
47. Reid, A. L., Seebacher, F. & Ward, A. J. W. Learning to hunt: the role of experience in predator success. *Behaviour* **147**, 223–233 (2010).
48. Bianco, I. H., Kampff, A. R. & Engert, F. Prey capture behavior evoked by simple visual stimuli in larval zebrafish. *Front. Syst. Neurosci.* **5**, 101 (2011).
49. Muto, A. *et al.* Activation of the hypothalamic feeding centre upon visual prey detection. *Nat. Commun.* (2017). doi:10.1038/ncomms15029
50. Heap, L. A. *et al.* Hypothalamic projections to the optic tectum in larval zebrafish. *Front. Neuroanat.* (2018). doi:10.3389/fnana.2017.00135
51. Semmelhack, J. L. *et al.* A dedicated visual pathway for prey detection in larval zebrafish. *Elife* **4**, 1–19 (2014).
52. Antinucci, P., Folgueira, M. & Bianco, I. H. A pretectal command system controls hunting behaviour. *bioRxiv* (2019). doi:10.1101/637215
53. Preuss, S. J., Trivedi, C. A., Vom Berg-Maurer, C. M., Ryu, S. & Bollmann, J. H. Classification of object size in retinotectal microcircuits. *Curr. Biol.* **24**, 2376–2385 (2014).
54. Del Bene, F. *et al.* Filtering of visual information in the tectum by an identified neural circuit. *Science (80-.).* **330**, 669–673 (2010).
55. Bianco, I. & Engert, F. Visuomotor Transformations Underlying Hunting Behavior in Zebrafish. *Curr. Biol.* **25**, 831–846 (2015).
56. Bollmann, J. H. The Zebrafish Visual System: From Circuits to Behavior. *Annu. Rev. Vis. Sci.* **5**, 269–293 (2019).
57. Barker, A. J. & Baier, H. SINs and SOMs: neural microcircuits for size tuning in the zebrafish and mouse visual pathway. *Front. Neural Circuits* **7**, 89 (2013).
58. Barker, A. J. & Baier, H. Sensorimotor decision making in the Zebrafish tectum. *Curr. Biol.* **25**, 2804–2814 (2015).
59. Henriques, P. M., Rahman, N., Jackson, S. E. & Bianco, I. H. Nucleus Isthmi Is Required to Sustain Target Pursuit during Visually Guided Prey-Catching. *Curr. Biol.* (2019). doi:10.1016/j.cub.2019.04.064
60. Filosa, A., Barker, A. J., Dal Maschio, M. & Baier, H. Feeding State Modulates Behavioral Choice and Processing of Prey Stimuli in the Zebrafish Tectum. *Neuron* **90**, 596–608 (2016).
61. Felsen, G. & Dan, Y. A natural approach to studying vision. *Nat. Neurosci.* **8**, 1643–1646 (2005).
62. Theunissen, F. E. & Elie, J. E. Neural processing of natural sounds. *Nat. Rev. Neurosci.* **15**, 355–366 (2014).
63. Wei, H., Yao, Y., Zhang, R., Zhao, X. & Du, J. Activity-induced long-term potentiation of excitatory synapses in developing zebrafish retina in vivo. *Neuron* **75**, 479–489 (2012).
64. Nevin, L. M., Taylor, M. R. & Baier, H. Hardwiring of fine synaptic layers in the zebrafish

visual pathway. *Neural Dev.* **3**, 36 (2008).
65. Jacobson, G. A., Rupprecht, P. & Friedrich, R. W. Experience-Dependent Plasticity of Odor Representations in the Telencephalon of Zebrafish. *Curr. Biol.* **28**, 1-14.e3 (2018).
66. Wu, Y.-J. *et al.* Unilateral stimulation of the lateral division of the dorsal telencephalon induces synaptic plasticity in the bilateral medial division of zebrafish. *Sci. Rep.* **7**, 9096 (2017).
67. Perathoner, S., Cordero-Maldonado, M. L. & Crawford, A. D. Potential of zebrafish as a model for exploring the role of the amygdala in emotional memory and motivational behavior. *J. Neurosci. Res.* **94**, 445–462 (2016).
68. Martín, I., Gómez, A., Salas, C., Puerto, A. & Rodríguez, F. Dorsomedial pallium lesions impair taste aversion learning in goldfish. *Neurobiol. Learn. Mem.* **96**, 297–305 (2011).
69. Mueller, T., Dong, Z., Berberoglu, M. A. & Guo, S. The dorsal pallium in zebrafish, Danio rerio (Cyprinidae, Teleostei). *Brain Res.* 95–105 (2011). doi:10.1016/j.brainres.2010.12.089.The
70. Duboué, E. R., Hong, E., Eldred, K. C. & Halpern, M. E. Left Habenular Activity Attenuates Fear Responses in Larval Zebrafish. *Curr. Biol.* **27**, 2154-2162.e3 (2017).
71. Palumbo, F., Serneels, B., Pelgrims, R. & Yaksi, E. The Zebrafish Dorsolateral Habenula Is Required for Updating Learned Behaviors. *Cell Rep.* **32**, 108054 (2020).
72. Isa, T., Marquez-Legorreta, E., Grillner, S. & Scott, E. K. The tectum/superior colliculus as the vertebrate solution for spatial sensory integration and action. *Curr. Biol.* **31**, R741–R762 (2021).

Chapter 2:

Experience, circuit dynamics and forebrain recruitment in larval zebrafish prey capture

eLife 2020;9:e56619

Linker Statement

In this chapter, I investigate the neural basis of experience-dependent improvements in larval zebrafish prey capture, which is an ethologically relevant natural behavior. This model allows for simultaneous assessment of behavior and neural activity. By monitoring neural activity in one plane of the brain that contains the main structures known to be involved in the prey capture circuit, we show that experience increases the probability of visual activity to induce motor action and the correlation between the output neurons of the optic tectum and the forebrain areas. This is the first time the forebrain has been shown to be involved in prey capture behavior. To causally test the importance of the forebrain in prey capture, I specifically ablated the habenula, one of the forebrain areas, and observed a decrease in hunting performance in experienced fish. In summary, we describe experience-dependent changes the network dynamics underlying behavioral improvement, that may depend on forebrain activity.

Experience, circuit dynamics and forebrain recruitment in larval zebrafish prey capture

Oldfield CS[1*], Grossrubatscher I[1*], Chavez M[3], Hoagland A[5], Huth AR[1], Carroll EC[5], Prendergast A[2,3,4], Qu T[5], Gallant J[1,6], Wyart C[2,3,4,#] and Isacoff EY[1,5,7,#].

[1] Helen Wills Neuroscience Institute and Graduate Program, University of California Berkeley, Berkeley CA, 94720. [2] Institut du Cerveau et de la Moelle épinière (ICM), Hôpital de la Pitié-Salpêtrière, 75013, Paris, France. [3] CNRS-UMR-7225, 75013 Paris, France. [4] INSERM UMRS 1127, 75013 Paris, France. [5] Department of Molecular and Cell Biology, University of California Berkeley, Berkeley CA, 94720. [6] Department of Psychology, University of California, Berkeley, California 94720. [7] Bioscience Division, Lawrence Berkeley National Laboratory, Berkeley CA, 94720.

Author contributions

*Clarie S. Oldfield contributed equally with Irene Grossrubatscher. Claire S Oldfield: Conceptualization, Software, Formal analysis, Investigation, Writing - original draft. Irene Grossrubatscher: Conceptualization, Software, Formal analysis, Investigation, Methodology, Writing - original draft, Writing - review and editing. Mario Chávez: Software, Formal analysis. Adam D Hoagland: Software, Formal analysis. Alex R Huth: Software, Formal analysis. Elizabeth C Carroll: Methodology. Andrew Prendergast: Formal analysis. Tony Qu: Resources. Jack L Gallant: Conceptualization, Supervision. Claire Wyart: Conceptualization, Supervision, Writing - review and editing. Ehud Y Isacoff: Conceptualization, Resources, Formal analysis, Supervision, Writing - original draft, Project administration, Writing - review and editing. All authors declare no competing interests

Summary

Experience strongly influences behavior, but little is known about how experience is encoded in the brain, and how changes in neural activity are implemented at a network level to improve performance. Here we investigate how differences in experience impact brain circuitry and behavior in larval zebrafish prey capture. We find that experience of live prey compared to inert food increases capture success by boosting capture initiation. To explore the underlying neural basis, we studied the effects of prior experience of live prey on behavior and brain activity. In response to live prey, animals with and without prior experience of live prey all show activity in visual areas (pretectum and optic tectum) and motor areas (cerebellum and hindbrain), with similar visual area retinotopic maps of prey position. However, prey-experienced animals more readily initiate capture in response to visual area activity and also have greater visually-evoked activity in two forebrain areas: the telencephalon and the habenula. Consistent with the contribution of the forebrain to prey capture, disruption of neurons in the habenula reduced prey capture performance in prey-experienced fish. Together, our results suggest that experience of prey strengthens prey-associated visual drive to the forebrain, and that this lowers the threshold for prey-associated visual activity to trigger activity in motor areas, thereby improving capture performance.

Keywords

zebrafish; prey capture behavior; neural circuit; brain; experience; calcium imaging; neural connectivity; forebrain; telencephalon; habenula.

Introduction

To transform sensory input into an optimal behavioral response, animals must extract relevant perceptual information from their environment, interpret it within their internal and external contexts, and translate it into a motor output. Prior experience modulates how this transformation occurs and whether the response is successful. A large body of work has studied how enriching or depriving sensory experience affects perceptual encoding, with both morphological and molecular changes [1]. Furthermore, teaching an animal to fear or expect a stimulus alters properties of the circuits recruited in response to the cue (e.g., [2,3]). Most studies of experience-dependent changes rely on drastic manipulation such as depriving animals of all sensory input in one modality, inducing fear association with a noxious stimulus, or depriving animals of food or water to achieve sufficient motivation to assure a response. However, neurons respond differently to ethologically-relevant stimuli [4,5], and the question of how natural experience influences brain activity and downstream native behavior [6] is becoming increasingly relevant.

One of the most critical native behaviors for survival in carnivores and omnivores is hunting for food. In many species, the basic hunting sequence is innate and triggered in full by certain sensory cues. For example, predation can be evoked in toads and fish by the sight of small prey-like moving objects [7–11] and in barn owls by ruffling prey-like noise [12]. The accomplishment of this goal-directed behavior is highly flexible and is modulated by experience in animals as phylogenetically distant as mammals (the Etruscan shrew relies on tactile experience to develop efficient predation [13]) and mollusks (Limax learn to avoid a food if it makes them sick [14]).

Here we investigated how experience-dependent circuit plasticity is implemented. We took advantage of the transparency of larval zebrafish and its ability to initiate prey capture when semi-immobilized, thereby making it possible to simultaneously image behavior and neural activity across a large portion of the brain. In zebrafish larvae, prey capture behavior is already evident at five days post-fertilization (dpf). At this stage, zebrafish respond to prey, such as paramecia, in a highly stereotyped manner: when the prey is in sight, the fish reorients its body towards it with a series of unilateral tail flicks (J-Bends) and forward swims until the fish reaches a proximal striking zone; it then darts forward to engulf the prey in a final capture swim [15–20]. Notably, the onset of this sequence is characterized by gradual eye convergence as the fish gets closer to the prey. The resulting increase of visual field area covered by binocular vision has been suggested to improve depth perception needed for precise targeting of the prey [8]. Restrained fish presented with virtual prey on a screen (a moving dot) also respond with eye convergences and tail flicks, indicating that visual inputs are sufficient to initiate the prey capture sequence [8–10,21].

Prey capture in larval zebrafish has emerged as a model for understanding how sensory information translates into motor action [10,21–26]. Visual information about prey location flows from the retina to two contralateral visual areas: the pretectum and optic tectum (OT). The pretectal area around the 7th arborization field of retinal ganglion cells (AF7, see [27]) was shown to be critical for detecting prey-like objects and triggering the prey capture sequence [10,28]. Ablation and optogenetic

studies indicate that the OT is necessary for prey capture [22,24]. Assemblies of medial periventricular neurons in the OT activate prior to eye convergence, suggesting a role in inducing the motor response to the sight of prey [21]. Furthermore, novel results have shown that the nucleus isthmi, a small cholinergic area in the cerebellum, is necessary for maintenance of a hunting routine, but not for initiation [29]. Despite recent progress, the mechanism for integration of information from pretectum and OT, and the precise activation sequence downstream of visual areas, are yet to be discovered. Moreover, it is not known whether prey capture improves with experience, and if so, how improvement might be implemented at the neural level.

Here we show that experience of live prey increases capture initiation and success in natural conditions. We investigate the brain activity elicited by prey and identify sequential activity in visual areas (pretectum and optic tectum), and motor-related areas cerebellum and hindbrain. We find that prior experience of prey increases the reliability of capture initiation in response to prey-associated visual activity. In prey-naïve and prey-experienced animals, information flow from the pretectum onto the cerebellum and hindbrain correlate with prey capture initiation. However, experience of prey increases the impact of these functional links on prey capture initiation and strengthens the coupling from visual areas to the telencephalon. In agreement with this latter point, prey-experienced animals show increased activation of the forebrain (both telencephalon and habenula) during prey capture initiation. Consistently, we show that ablation of the habenula reduces hunting in prey-experienced animals. Taken together, our findings show that prey capture behavior is enhanced by prior experience of live prey and suggest that forebrain recruitment increases output gain for the prey capture circuit in response to the same visual cues.

Results

Prior experience of prey increases prey capture initiation in larval zebrafish

To assess the effect of experience on prey capture behavior and the underlying neural activity, we compared two groups of sibling zebrafish larvae. Prior to being tested with paramecia at 7 dpf, a first group was fed live paramecia for two days (5 and 6 dpf), whereas a second group was fed inert food flakes (Figure 2.1. A). While each group may acquire feeding experience for the food on which it was "trained," only the first group obtained experience of live prey, on which both groups were later tested. We therefore refer to the first group as "prey-experienced" and the second group as "prey-naïve."

At day 7 prey capture behavior was tested in both groups by quantifying behavioral steps of the prey capture sequence: a) pursuits that are aborted before a capture swim is attempted, b) capture swim attempts that fail, and c) successful captures (Figure. 2.1. A bottom). We found that experienced fish have significantly more pursuits and successful captures than their naïve counterparts, but the same probability of attempting a capture once a pursuit was initiated (Figure 2.1. B). Experience did not change the probability of success once a capture was attempted. This analysis suggests that experience increases initiation of prey capture, but not motor performance of the capture.

We next examined prey capture in a virtual environment [8–10,21] in prey-experienced or prey-naïve fish. We presented a single moving dot of varying contrast to a fish immobilized in agar with eyes and tail free (Figure 2.1. C). We focused on initiation of prey capture by examining frequency of eye convergences, as described above. We quantified performance using the discriminability index, d', calculated from response rates to a stimulus versus the absence of a stimulus (see

Materials and Methods, Behavioral data analysis and statistics). We found that at higher contrast, prey-experienced fish responded significantly more than prey-naïve fish (Figures 2.1. D-E). This indicates that response to "virtual prey" is substantially enhanced by prior experience of live prey, even though the virtual prey is a black dot moving steadily and unidirectionally on a white screen, whereas paramecia are translucent and swim erratically in three dimensions.

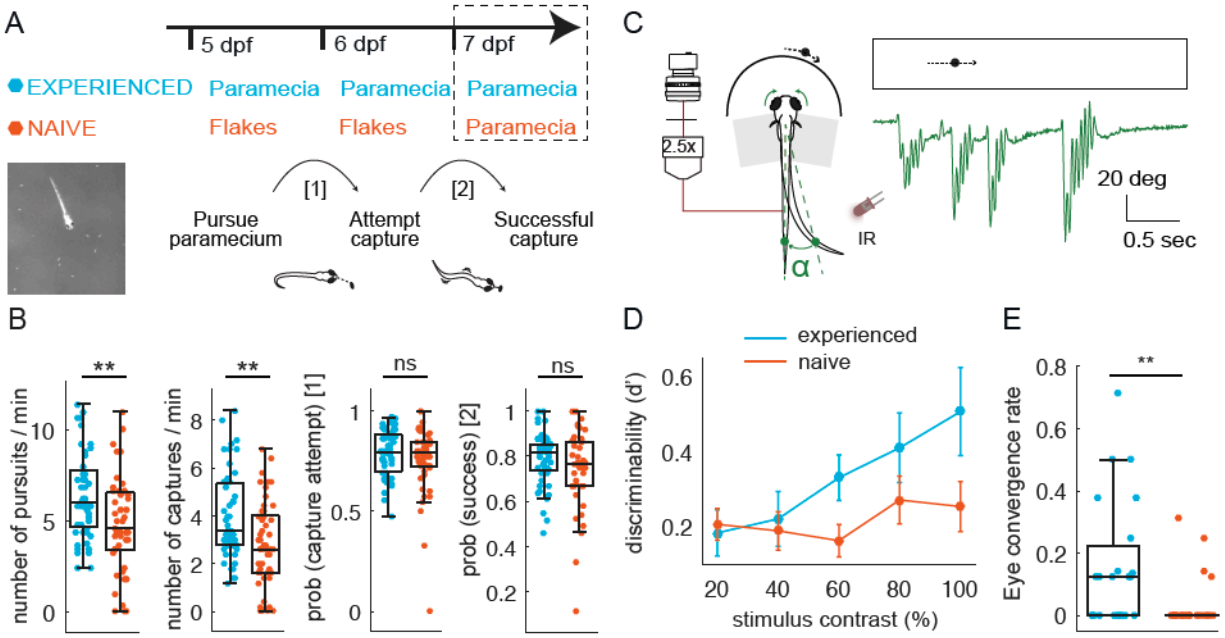

Figure 2.1. Larval zebrafish improve hunting performance with experience of live prey in both free swimming and virtual environments

A-B) Experience of live prey increases frequency of paramecia captures in a freely swimming environment. **A)** Behavioral paradigm: Fish fed paramecia ("prey-experienced") or flakes ("prey-naïve") at 5 and 6 dpf were given paramecia at 7 dpf (top, timeline). Prey capture performance was assessed by imaging single fish and paramecia (white specks in lower left image) to count pursuits aborted without a capture attempt, failed capture attempts, and successful captures (summary behavior scheme, lower, right). **B)** Summary of performance. Raw data (one symbol per fish) and a boxplot of group statistics show that experienced fish have higher frequencies of total pursuits (successful or not, $p = 0.003$), and successful captures ($p = 0.001$), but statistically indistinguishable probabilities of transitioning from pursuit to a capture attempt ($p = 0.28$), or of transitioning from capture attempt to successful capture ($p = 0.12$). Statistical comparisons used a permutation test (see Materials and Methods) with $N = 51$ each experienced and naïve fish. **C-E**) Experience of live prey increases frequencies of prey capture initiation in semi-immobilized fish. **C)** Setup: Semi-immobilized fish face a screen on which small moving dots are projected. Tail flicks and eye angle are imaged from above at 250 fps. Alpha is the angle between the point at 8/10ths of tail length from swim bladder, and midline. In green we show an example tail track during presentation of moving dot. **D)** Prey-experienced fish ($N = 23$) have significantly ($p = 0.03$) greater discriminability index (d') than prey-naïve fish ($N = 25$), Two-way ANOVA interaction between experience of live prey vs. lack thereof and contrast (see Materials and Methods for calculation of d'). **E)** At highest contrast, eye convergence rate in prey-experienced fish was significantly ($p = 0.005$) greater than in prey-naïve fish (# of times fish converged eyes / # of high contrast stimuli at highest contrast). Note high variability in response rate within groups, with experience improving virtual prey capture performance unevenly across fish, similar to [9,10].

If differences in diet (live paramecia versus inert flakes) affected fish health, there could be an effect on prey capture performance. To address this concern, we carefully examined numerous indices of fish health. We found that fish length, spontaneous swimming velocity, and swimming velocity in the presence of prey did not differ between the two groups of fish (Figure 2 S.1. A). Similarly, swim distance and rest times between swims (Figures 2 S.1. E and F), as well as rates of baseline tail flicks, eye saccades and eye convergences in the virtual environment did not differ between groups (Figure 2 S.1.B). These results indicate that differences in diet between the two groups of fish did not affect health, and that the improved capture of paramecia results from prior experience of prey.

A difference in prey capture for experienced and naïve fish could also emerge if there was a difference in hunger or motivation to hunt. To disentangle the effect of experience on feeding from hunger, we performed a flake feeding assay. We fed sibling fish either paramecia or flakes on day 5 and 6 dpf ad libitum, and then starved the fish overnight, as in our usual protocol (Figure 2.1. A). On day 7, we let fish feed on flakes for 10 minutes. We assessed the number of eye convergences during that time as a proxy for the motivation to hunt. We observed a significantly higher number of eye convergences in response to the flakes in previously flakes fed fish, suggesting that flake-fed fish are no less hungry/motivated and that the experience with flakes boosts flake "hunting" in the same way as experience with paramecia boosts paramecia hunting (Figure 2 S.1.G).

Spatio-temporal brain activity pattern associated with prey capture initiation

To understand the neuronal basis of the boost in prey capture initiation in prey-experienced fish, we imaged neuronal activity in the form of calcium transients in Tg(NeuroD:GCaMP6f) [30] transgenic zebrafish, which expressed the calcium indicator GCaMP6f broadly in the central nervous system. Imaging was performed in 7 and 8 dpf fish which were semi-immobilized in agar but with eyes and tail free, similar to the assay with virtual prey above. We monitored fluorescent calcium signals from a single plane that included the pretectal area around AF7 (see Figure 2 S.2. A), which was previously shown to be involved in prey detection [10] and in triggering the prey capture sequence [28], as well as the OT, motor-related areas, and other areas of the hindbrain and forebrain. We simultaneously imaged eye and tail movements, as well as the trajectory of a paramecium that swam freely in a slot-well in front of the fish (Figure 2.2. A-C). For each fish, we used the baseline GCaMP6f fluorescence image (Figure 2.2 D) to identify the major brain areas (Figure 2.2 E). Consistent with our assays on semi-immobilized fish above (Figure 2.1. D and E), tail flicks were similar between prey-experienced and prey-naïve fish, but prey-experienced fish exhibited significantly more eye convergences than prey-naïve fish (Figure 2.2 F).

We began by recording spontaneous neural activity and associated tail and eye movements in the absence of prey for a period of 7 minutes. We then added a single paramecium to a well in front of the fish and recorded for 11 additional minutes. We focused on brain activity associated with both spontaneous and prey-evoked eye convergence events, time-locked to the moment of strongest ocular vergence. In prey-experienced fish these events showed strong activation of visual areas (in the pretectum and in the OT) and motor-related areas (cerebellum and hindbrain) (Figure 2.2. G and H), areas that have been shown before to play roles in swim behavior and prey capture [28], [29], [31,32]. The spatio-temporal patterns of spontaneous and evoked activity were similar, except that activity was more asymmetric in the pretectum and tectal neuropil in presence of prey (i.e. more strongly activated contralateral to the paramecium) (Figure 2 S.2. B), in agreement with a moving stimulus being present in one hemifield and not the other.

We observed responses in AF7 in the pretectum and in the rostral neuropil and periventricular neurons of the OT (output neurons [33]), but not in the caudal neuropil (Figure 2.2. G). Regionalization of activity in the tectal neuropil is consistent with prey capture initiation occurring when the paramecium is in front of the fish, because, under these conditions, the prey is in the nasal visual field, and nasal retinal ganglion cells project to the rostral optic tectum [34].

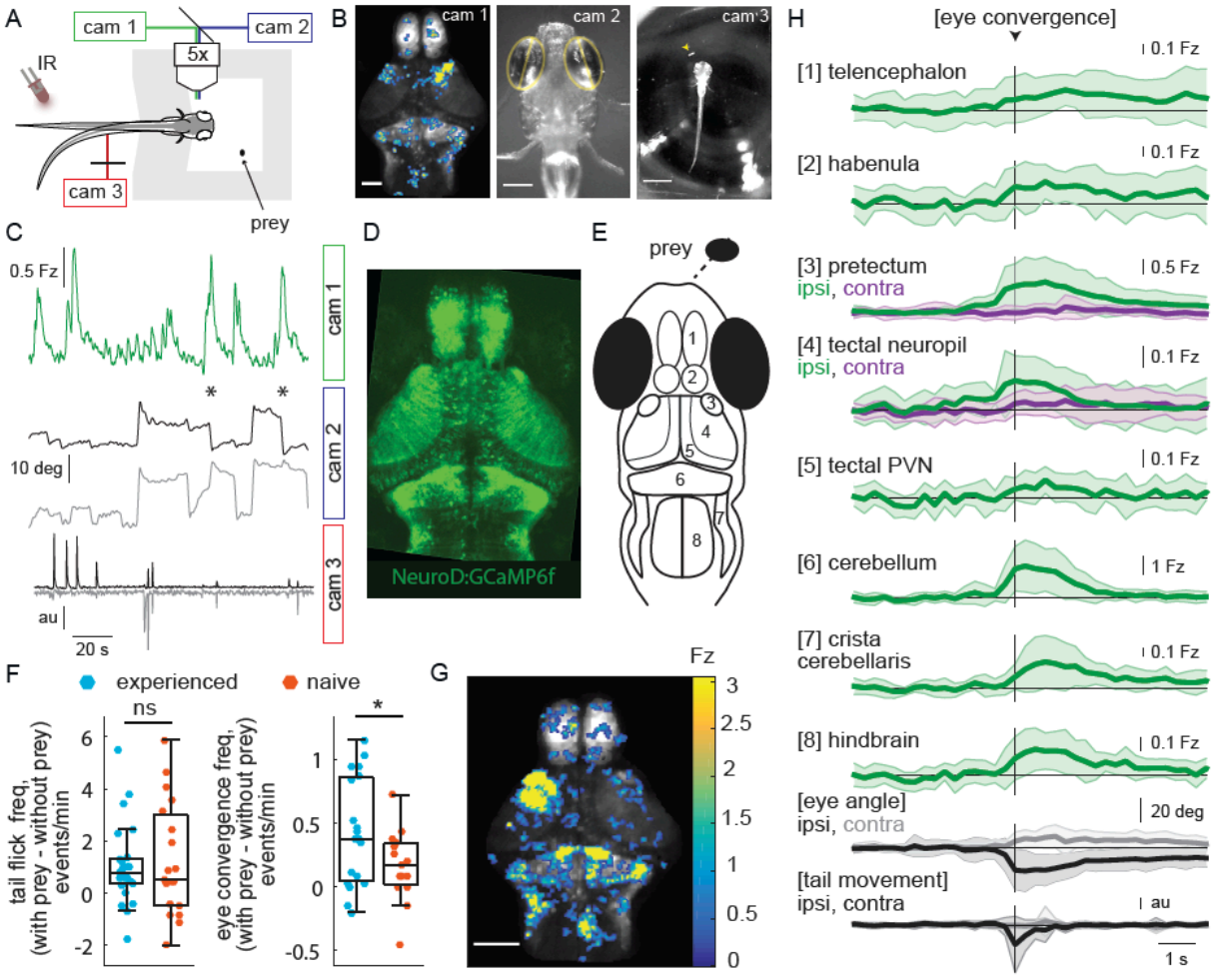

Figure 2.2. Wide-field brain imaging of prey capture initiation shows recruitment of visual and motor areas, as well as the telencephalon and habenula.

A, B) Setup for imaging of neural activity in a single plane of the whole brain while the fish observes prey **(A)** and example frames captured by three cameras **(B)**. Camera 1 (cam 1): neural activity in a single plane of the whole brain while the fish observes prey, scale bar = 200µm. Camera 2 (cam 2): eye angle, scale bar = 200µm. Camera 3 (cam 3): prey position and fish tail position, scale bar = 1 mm. Cameras were synchronized at 3.6 Hz. **C)** Example 3 minute traces from one fish for all three cameras illustrating data collected during eye convergences. Cam 1: Z-scored fluorescence in the right pretectum (smoothed with a Lowess filter, span = 7, for Fz calculation see Materials and Methods, Calcium and behavior imaging data pre-processing). Cam2: Corresponding eye angles (left eye, grey; right eye, black; convergence events, stars; smoothed with a Lowess filter, span = 9). Cam 3: tail movement (left side, grey; right side, black, see Materials and Methods). **D)** *Tg(NeuroD:GCaMP6f)* 7 dpf fish brain, dorsal view as images by cam 1. **E)** Schematic of anatomy in observation plane, numbered areas as defined in **(H)**. **F)** Prey-experienced and prey-naïve fish have statistically indistinguishable evoked (with prey – without prey) frequency of tail flicks

(left, p = 0.74), but prey-experienced fish have a significantly higher eye convergence frequency (right, with prey – without prey, p = 0.04). **G, H)** Neural activity in a prey-experienced fish around eye convergences with prey (N = 12 eye convergences). This fish showed no spontaneous eye convergences preceding addition of paramecium, suggesting that averaged activity was purely evoked by the paramecium. "Contra" and "ipsi" refer to the side with higher or lower pretectal transient amplitude peak time (see Materials and Methods). **G)** Spatial distribution of summed calcium activity over 4.2 seconds (5 frames before and 10 frames after eye convergence), when the prey was to the right side of the fish (average of 6 convergences). Scale bar = 100μm. Fz thresholded for visualization. **H)** Time-course of calcium activity for each brain area in an example experienced fish (average of 12 convergences; convergence time is vertical black line) over a period of ten seconds. We observe a significant increase in fluorescence for all brain areas except the ipsilateral side of the pretectum, comparing average fluorescence traces of baseline (frames -10 to -5 before eye convergence), to the 5 frames after eye convergence (black line in the figure). P-values are reported in Table 2 S.1. For eye angle and tail movement, black is contralateral, and grey is ipsilateral. See also Figure 2 S.1. A permutation test was used for all pairwise comparisons if not specified otherwise (see Materials and Methods, Behavioral data analysis and statistics).

Prey-naïve fish also responded to the sight of prey with eye convergences and tail flicks, albeit at a lower frequency than prey-experienced fish (Figure 2.2. F). The spatio-temporal pattern of brain activity associated with eye convergence was similar to what we observed in prey-experienced fish for both spontaneous- and prey-evoked events (Figure 2 S.2. B).

In addition to the activity expected in visual and motor-related areas, eye convergence-associated responses were observed in areas of the forebrain not previously implicated in prey capture: the telencephalon and habenula (Figure 2.2 B, 2.2 G, 2.2 H, Figure 2 S.2. C and D). We return to analyze this forebrain activity later.

Experience of prey does not affect encoding of prey position in visual areas

To determine whether experience of prey affects the ability of fish to detect and represent prey location, we compared encoding of prey location in visual areas of prey-experienced and prey-naïve fish (Figure 2.3.). Traditionally, visual responses are evaluated by repeatedly showing identical virtual stimuli, pooling trials and determining if responses in a given region of interest are reliable enough for it to be deemed "visually-responsive". However, natural stimuli have a more complex statistical structure [35], and are thought to evoke more ethologically-relevant behavioral responses [36]. We therefore used natural visual input by presenting the fish with its biological prey, a live paramecium. Since locomotion of the paramecium is not experimentally-controlled, we faced the analytic challenge of dealing with irregular visual stimulation. To address this, we applied a method developed for building predictive encoding models of human brain activity elicited by natural scenes or language, and detected by neurophysiology and functional magnetic resonance imaging [37,38]. We used regularized regression to construct a separate encoding model for each pixel that predicts the pixel's fluorescence time series based on the location of the prey (Figures 2.3. A-B). To validate the encoding models, we predicted fluorescence time series on held-out segments of the dataset that were not used for model estimation, and then computed the correlation between predicted and actual time series in this held-out set.

For pixels where prediction performance was significantly above chance, we computed the prey position that elicits the largest response and defined it as the pixel's "preferred angle" (Figures 2.3. A-C). The encoding model weights describe the spatial receptive field of the pixel (Figure 2.3. C, see Materials and Methods and Figure 2 S.3. A). Neurons in visual areas preferred positions on the contralateral side of the animal, consistent with retinal ganglion cell projections crossing the

midline and innervating contralateral visual areas. We observed strong retinotopic gradients in both the pretectum and the optic tectum, with more rostral pretectal and optic tectum locations preferring central positions of the prey and more caudal pretectal and optic tectum locations responding preferring lateral positions of the prey. Retinotopic maps were equally well-defined in prey-experienced and prey-naïve fish, with both groups of fish showing well-separated bimodal distributions for angle preferences between left and right sides (Figures 2.3. D and F). We observed no difference in encoding strength between prey-experienced and prey-naïve fish in the pretectum, tectal neuropil or tectal periventricular neurons (PVNs). See Figure 2.3. E, and Materials and Methods, Pixel-wise encoding model estimation and validation, for calculation of pixel correlation. The mean and standard deviation of preferred angle for each area were also similar between prey-experienced and prey-naïve fish (Figure 2 S.3. B), indicating similar tuning characteristics. These results indicate that prior experience of prey does not affect encoding of prey position in visual areas.

In an additional analysis, we asked whether the threshold for a visual response to prey differed between animals that did or did not have prior experience of prey. We focused on the pretectum because this is the first relay for visual information coming from the retina and because the pretectal area around AF7 has been suggested to be specifically involved in prey detection [10]. Indeed, we found that in both prey-experienced and prey-naïve fish, pretectal pixels had higher correlation values with prey position than the OT (Figure 2.3.E), for prey-experienced fish, the 25th and 75th percentile for average pixel correlation values were 0.02 and 0.09 respectively, and for prey-naïve fish 0.02 and 0.07 respectively). In addition, we observed no difference in frequency or amplitude of calcium transients in the pretectum when fish were observing a prey between prey-experienced and prey-naïve fish (Figure 2.3., figure supplement 1C). These results indicate that experience does not affect the threshold of prey detection within visual areas.

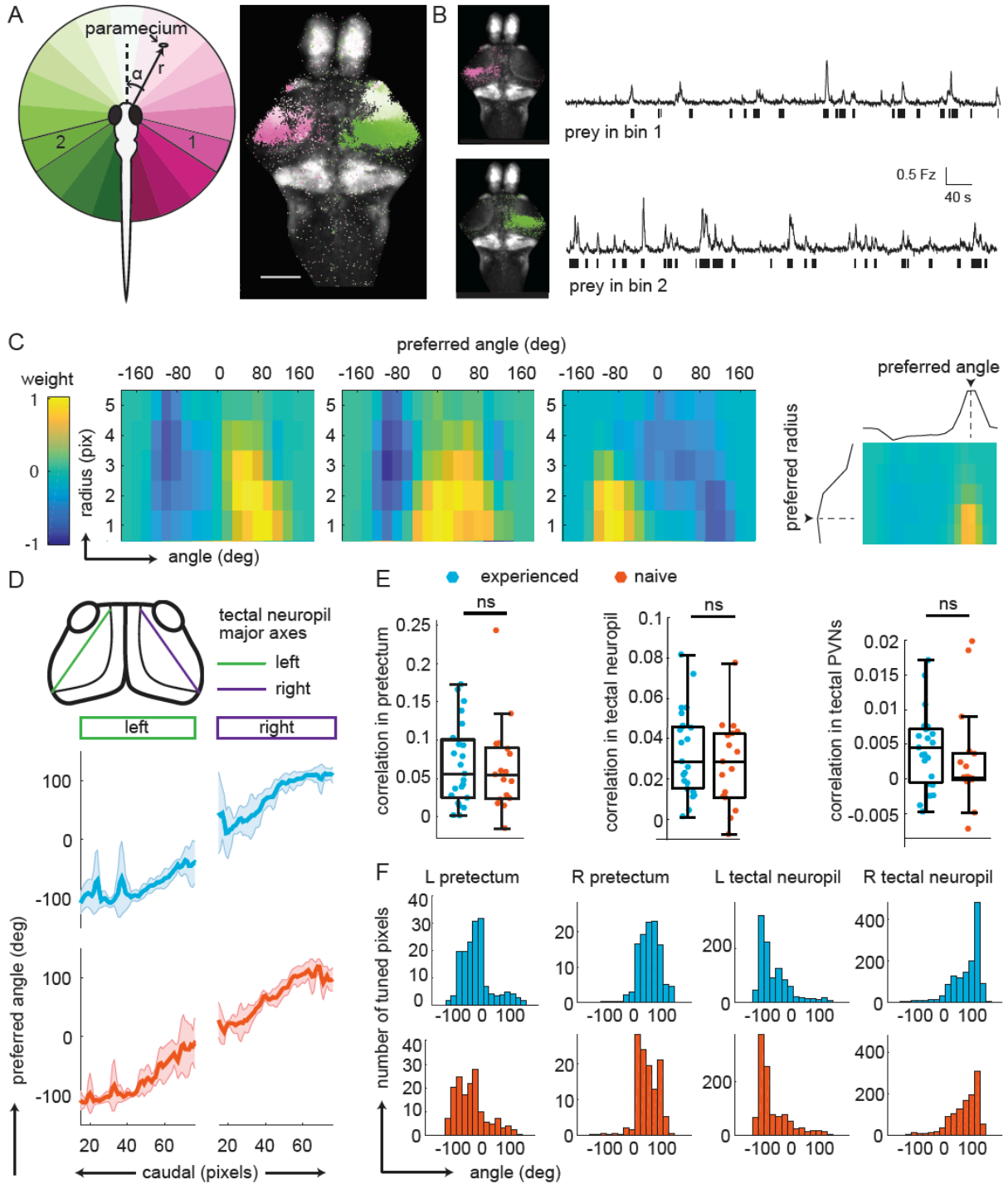

Figure 2.3. Experience does not affect prey-associated activity in visual areas.

A) Left, schematic of prey location relative to the fish in polar coordinates (angle α, radius r). Right, example retinotopic map generated by fitting an encoding model for each pixel to predict fluorescence intensity based on prey location. Significantly correlated pixels are in the color of their preferred angle.

Scale bar = 200 μm. **B)** Average fluorescence from pixels whose preferred angles are in bin 1 (120° to 101°, top) or bin 2 (-104° to 126°, bottom). Left: Anatomical location of pixels. Bars below traces indicate time points when the prey was present in the preferred angle bin. **C)** Example angular-radial receptive fields for 3 pixels in the pretectum. X-axis: angle, y-axis radius; Color represents encoding model weight for that pixel. For each receptive field, color scale is normalized to the maximum weight and centered around 0. Right: preferred angle is max of marginal. **D)** Top: anatomical location of tectal neuropil major axes (left: green, right: purple). Middle and Bottom: Average preferred angle gradient along left and right axis, shaded area is standard deviation. Middle: Prey-experienced (N = 23, blue). Bottom: Prey-naïve (N = 19, red). **E)** Average correlation values of visual area pixels in pretectum (left), tectal neuropil (middle), and tectal PVNs (right) were not significantly different between prey-experienced (N = 23) and prey-naïve fish (N = 17), p = 0.80 for pretectum; p = 0.42. **F)** Average distribution of pixels' preferred angles in each area (columns) in prey-experienced (blue, top row) and prey-naïve (red, bottom row) fish. There were no differences in average preferred angle distributions between the two groups of fish (two-sample Kolmogorov-Smirnov tests, p = 0.93 for pretectum, p = 0.94 for tectal neuropil and p = 0.95 for tectal PVNs.). See also Figure 2.3., figure supplement 1. A permutation test was used for all pairwise comparisons if not specified otherwise (see Materials and Methods, Behavioral data analysis and statistics).

Information transfer in visual areas during prey observation

Having observed that frequency of prey capture initiation is augmented by prior experience of prey, but that neural responses to prey in visual areas appear not to depend on experience, we asked whether activity in other brain regions or communication between brain regions differs in prey-experienced animals. To address this, we applied Granger-causality analysis, a method for determining if a time series of events predicts (or Granger-"causes") a second time series [39,40]. It has been classically applied to neurophysiological recordings in both animals and humans [41,42] to study the influence of one brain area or neuron upon another (Figure 2.4. A, and see Materials and Methods, Granger-causality from calcium fluorescence imaging data). In contrast to standard correlation analysis, Granger-causality provides directionality information (compare Figure 2.4. and Figure 2 S.4.), although it does not determine whether an apparent functional connection corresponds to direct or indirect anatomical connections, or whether it is serial rather than triggered in parallel by other brain areas. It should be pointed out, that the Granger-causality calculation relies on calcium activity dynamics captured at 3.6 Hz but elicited by action potentials that occur on a much faster time scale (although bursts of action potentials may occur over time scales that more closely resemble calcium dynamics). As a result, two regions that are in appearance functionally connected might seemingly peak at the same time because of slow calcium dynamics and/or image acquisition.

To validate the use of Granger-causality analysis for calcium imaging in prey capture, we first applied it within the visual system where the basic circuitry is well characterized [33,43,44]. We analyzed signals across the entire recording period. We compared baseline activity to activity evoked in the presence of a paramecium in both prey-experienced and prey-naïve fish (Figure 2.4. B). We found that the tectal neuropil (Figure 2.4. B and C, areas 3 and 4) predicts activity in tectal PVNs (Figure 2.4. B and C, areas 5 and 6). This is consistent with neuroanatomical connections between the two regions in which PVN dendrites in the neuropil receive input from upstream tectal neurons (Figure 2.4. D) [33,43,44]. Similarly, the information flow from the pretectum to tectal PVNs could be explained by pretectal neurons projecting to superficial layers of the optic tectum where PVN dendrites ramify (Figure 2.4. D) [10,33,43]. Thus, statistical causality analysis of calcium activity imaging data during prey capture agrees with known functional and anatomical connections in visual areas.

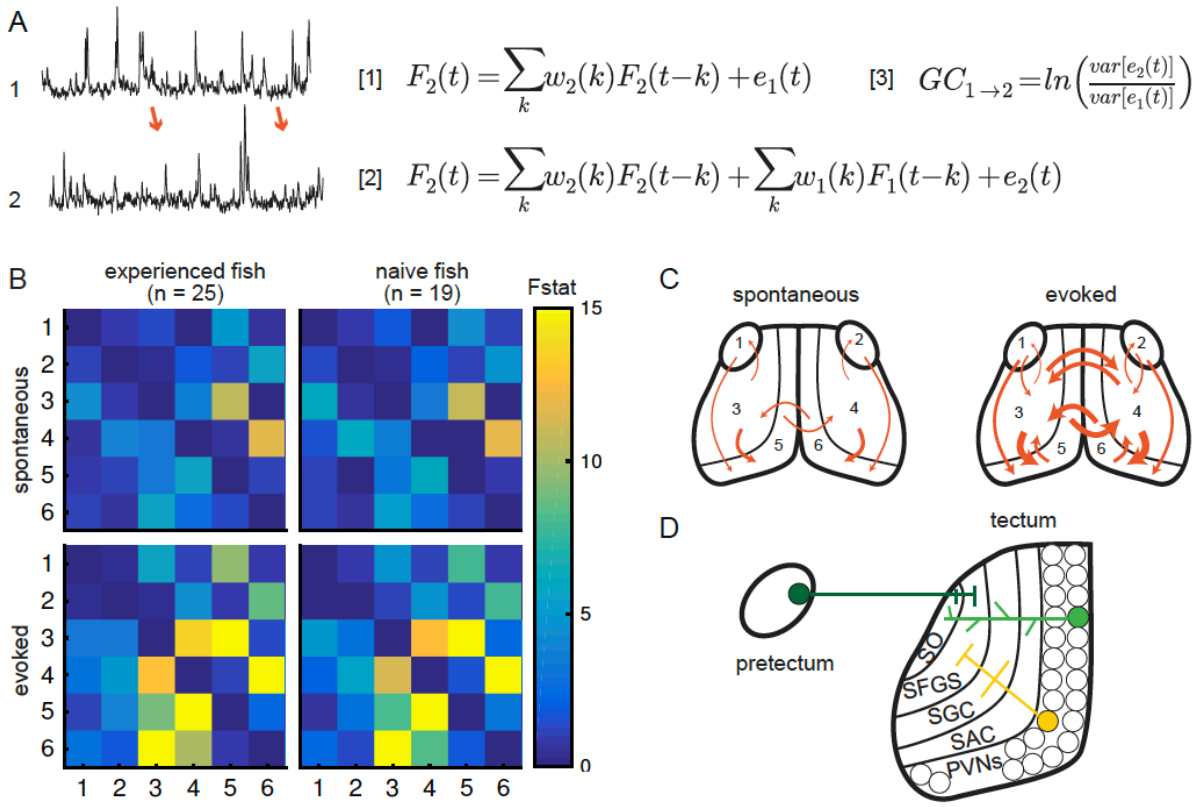

Figure 2.4. Experience does not affect directed information flow between visual areas.

A) Granger causality equations (right) to model fluorescence time-series 2 (TS2) using information from TS1 (left). TS1 and TS2: fluorescence from region 4 and 3 respectively for one representative fish. F(t) is fluorescence for time point t; w_1 and w_2 are the weights calculated for each time point; e denotes prediction error. Equations [1] and [2] are the autoregressive models for univariate and bivariate signals, respectively. Equation [3] is estimation of Granger-causality level. **B)** Average causality level within visual areas in spontaneous (no prey, top row) and evoked (prey present, bottom row) conditions, in prey-experienced (left column) and prey-naïve (right column) fish. Each box represents the F statistic which quantifies the statistical significance of the directed interaction from the region identified by the row to the region identified by the column. F statistic values ranged from 0 to 23.7. Fstat values above 15 are yellow. Brain areas shown are: 1, left pretectum; 2, right pretectum; 3, left tectal neuropil; 4, right tectal neuropil; 5, left tectal PVN; 6, right tectal PVN. Significant causal interaction causality link for Fstat > 3.88. No significant difference between prey-experienced and prey-naïve fish in either spontaneous or evoked Granger causality matrices (pair-wise T-tests, corrected using the Benjamini-Hochberg False Discovery Rate (FDR), see Materials and Methods, Behavioral data analysis and statistics; see Table 2 S.2. for p-values). **C)** Schematics of functional links in visual areas in spontaneous (left) and evoked (right) conditions. Line width proportional to Granger causality level (evoked and spontaneous maps indicate links with Fstat > 3.88). **D)** Anatomy and known connections of the optic tectum. Dark green: input from pretectum to OT. Bright green: PVNs with dendritic arborization in tectal neuropil. Yellow: axonal projections from PVNs to different layers of OT. SO, *stratum opticum*; SFGS, *stratum fibrosum et griseum superficiale*; SGC, *stratum griseum centrale*; SAC, *stratum album centrale*. See also Figure 2 S.4.

In the presence of the prey, the strength of information coupling between visual regions increased relative to baseline spontaneous activity (Figure 2.4. B, C). Specifically, we observed stronger statistical interactions between the pretectum and the OT, and between left and right hemispheres of the OT, consistent with the central role of binocular vision in prey capture (Figure 2.4. C). The anatomical basis for this functional connection needs further investigation. Interestingly, prey-experienced fish did not differ statistically from prey-naïve fish in connectivity strength in visual areas during either spontaneous activity or in presence of prey (Figure 2.4. B). This provides additional evidence suggesting experience of prey does not affect information flow between visual areas.

Connectivity between visual areas and other areas of the prey capture circuit

To determine if communication between brain areas is altered by experience of live prey, we applied Granger-causality analysis to understand region-to-region dynamic interactions and potential differences between prey-experienced and prey-naïve fish (Figure 2.5. A-B). Consistent with what is known about physical connectivity [33,43,45], activity in the tectal neuropil predicted activity in the tectal PVNs, activity in the PVNs predicted activity in the cerebellum, and activity in the cerebellum predicted activity in the hindbrain in both prey-experienced and prey-naïve fish. Other significant interactions observed in both prey-experienced and prey-naïve fish included from tectal PVNs to tectal neuropil (consistent with [43]), from cerebellum to tectal PVNs (as suggested anatomically by cerebellar output neurons that project to the optic tectum [46]), and from hindbrain to tectal neuropil (as shown in the Xenopus tadpole [47]). When comparing prey-experienced and prey-naïve fish, we found no statistical difference in the apparent functional connectivity between visual and motor-related areas, however the functional link from tectal PVNs to telencephalon was significantly greater in prey-experienced fish (Figure 2.5. A and Supplementary File 3).

To better understand how the apparent region-to-region information flow relates to prey capture initiation, we compared fish that initiated prey capture often ("strong" hunters) versus rarely ("weak" hunters). Among prey-experienced fish, strong hunters showed enhanced information flow from pretectum to the tectal neuropil, tectal PVNs, cerebellum and hindbrain, but not to the telencephalon or habenula (Figure 2 S.5. A). Together, these results suggest first, an important role of the pretectum and its connectivity to downstream visual and motor-related areas in determining frequency of prey capture initiation, and second, a possible implication of information flow from tectal PVN to telencephalon in mediating the effect of experience of live prey on subsequent initiation frequency.

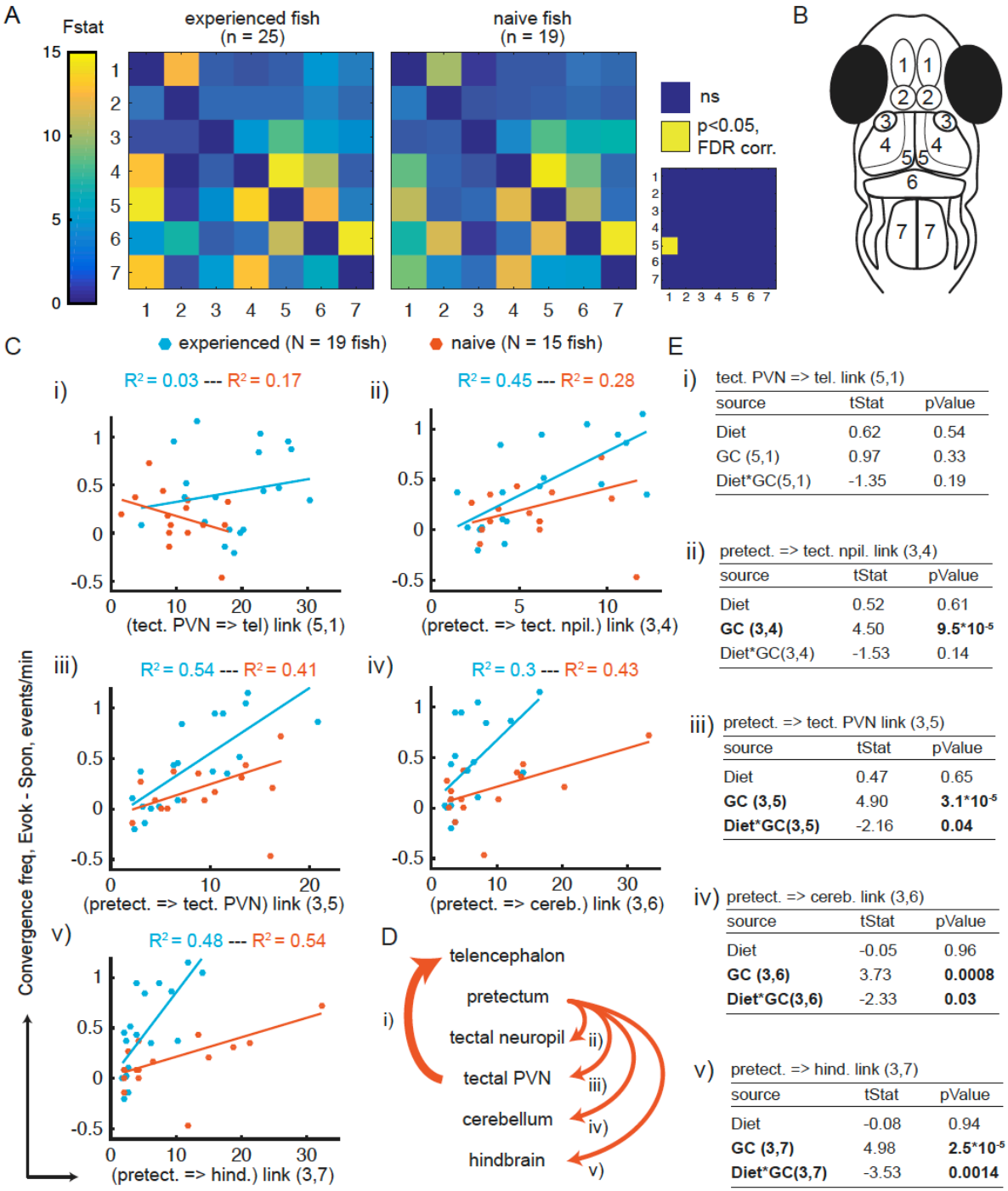

Figure 2.5. Granger causality-based estimation of interactions between visual and motor areas correlates with prey capture initiation.

A) Average Granger-causality between brain areas in prey-experienced (left) and prey-naïve (right) fish. Activity from left and right sides averaged as depicted in anatomical schematic **B)**. F statistics ranged from 0 to 34.1. Inset: Pair-wise statistical comparison of all links. Significant interactions represented in yellow ($p < 0.05$, pair-wise t-tests, FDR corrected, see Materials and Methods, Behavioral data analysis and statistics; see Table 2 S.3.for p-values). **B)** Brain areas shown in schematic are: 1: telencephalon, 2:

habenula, 3: pretectum, 4: tectal neuropil, 5: tectal PVNs, 6: cerebellum, 7: hindbrain. **C-E)** Granger-causality statistic is significantly correlated (p-values in E, "GC" row in each table) with eye convergence frequency for interactions from pretectum to downstream areas (interactions shown to be significantly stronger in "strong" hunters, see Figure 2 S.5.), but not for interaction from tectal PVNs to telencephalon (interaction shown to be significantly stronger in prey-experienced fish in A). Interaction between experience of prey ("Diet") and Granger-causality strength was significant for pretectum to tectal PVN, pretectum to cerebellum, and pretectum to hindbrain (p-values in E, "Diet*GC" row in each table). **C)** Eye convergence frequency (evoked – spontaneous) as a function of Granger-causality strength for: i) tectal neuropil→telencephalon (5,1), ii) pretectum→tectal neuropil (3,4), iii) pretectum→tectal PVN (3,5), iv) pretectum→cerebellum (3,6), v) pretectum→hindbrain (3,7). Statistics of linear regression model are in E). **D)** Schematic of links considered in C). **E)** Robust linear regression model: [Convergence Frequency ~ 1 + Diet + GC + Diet*GC], where "Convergence Frequency" is (with prey – without prey), "GC" is Granger-causality Fstat, "Diet" is prey-experienced or prey-naïve fish (categorical variable), and "Diet*GC" is interaction between experience of prey and Granger-causality statistic. N = 19 and N = 15 prey-experienced and prey-naïve fish respectively. Significant terms are bolded, GC for all links but link (5,1), and (GC*diet) interactions for links (3,5), (3,6) and (3,7).

Experience of live prey increases the probability of transitioning from sight of prey to capture initiation

Having observed an augmented drive from tectal PVNs to telencephalon in prey-experienced fish (Figure 2.5. A), and from pretectum to downstream brain areas in strong hunters (Figure 2 S.5.), we asked how experience of prey affects the relationship between these connectivity patterns and prey capture initiation frequency. For both prey-experienced and prey-naïve fish, we found a linear relationship between eye convergence frequency and dynamical drive from pretectum to tectal neuropil, tectal PVNs, cerebellum and hindbrain (Figure 2.5. C-E). Statistical causality strength was correlated with variance in behavior ($0.28 < R2 < 0.54$, Figure 2.5. C ii-v). However, there was no significant relationship with interaction strength from tectal PVNs to telencephalon (Figure 2.5. Ci-Ei). Comparing prey-experienced and prey-naïve fish, we found a significant interaction between experience of live prey and statistical causal strength in predicting prey capture initiation for links from pretectum to cerebellum and hindbrain (3 to 4-fold increase in slope for prey-experienced fish), and tectal PVNs (2-fold increase in slope) (Figure 2.5. C-E). For example, for a given level of pretectum drive to cerebellum, eye convergence frequency was higher in prey-experienced fish versus prey-naïve fish, suggesting the system is sensitized and more likely to trigger a capture. These results suggest that experience of live prey increases likelihood of triggering capture initiation for a given level of information flow from pretectum to downstream areas.

Our observations of prey-evoked activity suggest the forebrain may play a role in prey capture since the telencephalon and habenula are activated during eye convergence (Figure 2H) and the directed interaction from tectal PVNs to telencephalon is significantly stronger in prey-experienced fish (Figure 2.5. A-B). To probe involvement of the forebrain specifically in prey capture initiation, we compared pretectal transients associated with eye convergence (i.e., "fish has detected prey and initiates capture") to ones that do not lead to motor output (i.e., "fish has detected prey but does not initiate capture") (see Materials and Methods, Calcium and behavior imaging data pre-processing, for detection of pretectal transients). As expected, in both prey-experienced and prey-naïve fish activity in the cerebellum and hindbrain was only detected when there was a tail flick and eye convergence (Figure 2.6. A-C). In contrast, pretectal activation was high in both eye convergence and pretectum-only events, although it lasted longer during eye

convergence events (Figure 2.6. A). Patterns of activity in visual areas downstream of the pretectum were similar in prey-experienced and prey-naïve fish in both states, however the probability of a pretectal event being followed by an eye convergence was significantly larger in prey-experienced fish (Figure 2.6. D).

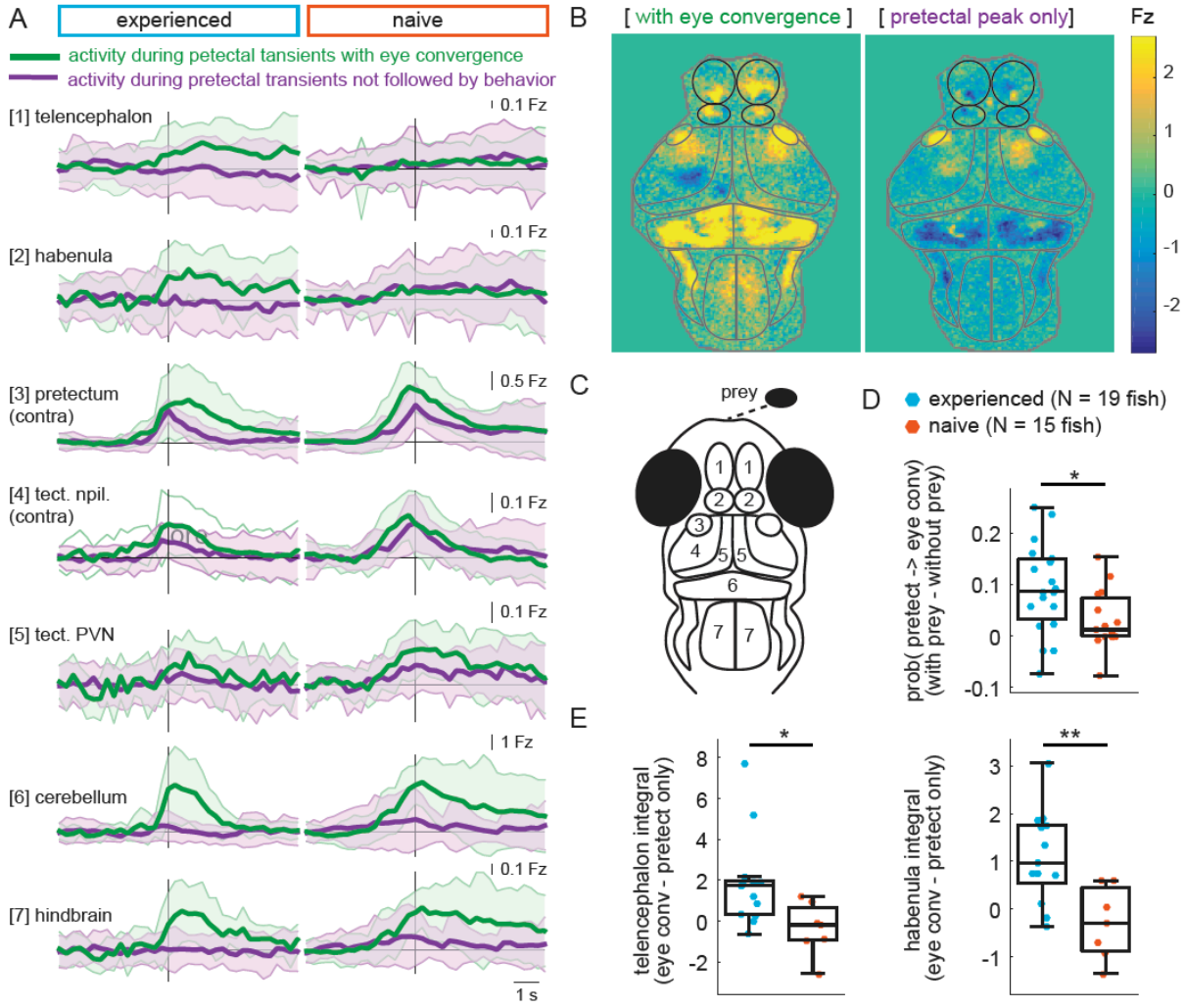

Figure 2.6. Experience of prey increases capture initiation-associated forebrain activity and lowers threshold for visual activity to trigger capture initiation.

A) Time traces of activity in seven brain regions during either a pretectum transient followed by eye convergence (green) or a pretectum transient with no behavior (purple) in a representative prey-experienced fish (left, N = 12 convergences, N = 42 pretectum-only events) and prey-naïve fish (right, N = 15 convergences, N = 20 pretectum-only events). Black vertical line represents the pretectal activity peak to which transients are aligned. "Contra" and "ipsi" refer to the side with higher or lower pretectal transient amplitude peak time (see Materials and Methods). **B)** Average brain activity maps for another representative prey-experienced fish in presence of prey, showing summed calcium activity over 4.2 seconds (5 frames before and 10 frames after event), during either pretectum transients associated with eye convergence (prey to left or right of the fish, N = 22) or pretectum transients not accompanied by behavior (N = 34). Brain areas are outlined in grey as in schematic C, and forebrain areas are additionally outlined in black. A) and B) show that forebrain areas appear active during pretectal transients associated with eye convergence, but not pretectal transients not accompanied by behavior. **C)** Schematic of anatomical areas considered in A

and B. **D)** Prey-experienced fish (N = 19) have a higher probability of pretectum transients being associated with eye convergence than prey-naïve fish (N = 15), suggesting visual events are more likely to cause motor output with experience of live prey (* indicates $p = 0.03$). Raw values of evoked and spontaneous probabilities are not significantly different in experienced *versus* naïve fish, data not shown. **E)** Prey-experienced fish (blue) have significantly more telencephalon (left, $p = 0.02$)) and habenula (right, $p = 0.004$) activity than prey-naïve fish (red) during pretectal transients associated with eye convergence relative to pretectal transients not accompanied by behavior. Box plot shows difference in fluorescence integral 5 frames before to 5 frames after events (pretectal transient with vs. without eye convergence). Fish with < 5 eye convergences were excluded, prey-experienced fish N = 13, prey-naïve fish N = 7. * and ** indicate $p < 0.05$ and $p < 0.01$ respectively. A permutation test was used for all pairwise comparisons if not specified otherwise (see Materials and Methods, Behavioral data analysis and statistics).

The only brain region where we detected a marked difference between prey-experienced and prey-naïve fish was the forebrain (Figure 2.6. A-B). We compared activity in the telencephalon and habenula between prey-experienced and prey-naïve fish and found a significant difference during pretectal transients associated with eye convergence relative to pretectal transients not accompanied by behavior (Figure 2.6. E).

These observations suggest that similar pretectal events can either remain confined in the visual areas or activate motor areas thereby triggering eye convergence. The telencephalon and/or habenula may operate as a switch that, when activated favors initiation of prey capture in response to prey-evoked visual activity.

Forebrain disruption reduces hunting initiation in prey-experienced fish

Our results so far suggest that, in prey-experienced animals, the forebrain is recruited during prey-elicited activity in a visual area and that this forebrain activity increases the probability of activation of motor areas and, thus, prey capture behavior in experienced fish. If correct, this model predicts that disruption of forebrain activity should compromise prey capture behavior. We sought to test this prediction by chemical ablation of cells in the forebrain. To do this, we expressed the gene encoding the enzyme nitroreductase (NTR) in transgenic Tg(gng8:Gal4;UAS:NTR-mCherry) larvae (Figure 2.7. A). The Tg(gng8:Gal4) line drives expression in the dorsal habenula and its projections to the interpeduncular nucleus, with a small amount of labelling of mitral cells in the olfactory bulb [48] (Figure 2.7. A and Figure 2 S.6. C). Since prey capture is a visually-guided behavior [19], which does not depend on olfactory cues [18,49], we conjectured that any effect of the manipulation on prey capture would be due to disruption of the habenula and not due to an effect on olfaction. NTR transforms the innocuous antibiotic metronidazole (MTZ) into a toxic metabolite, resulting in death of expressing cells [50] (Figure 2.7. B-C and Figure 2 S.7.). Prey-experienced larvae not expressing NTR showed no significant difference in number of eye convergences between MTZ treated and control animals (Figure 2.7. D). In contrast, fish expressing NTR showed a significant decrease in eye convergence frequency when treated with MTZ in a free-swimming prey capture assay (Figure 2.7. E) and spent a significantly lower percentage of time hunting with eyes converged (Figure 2.7. F). In accordance with this effect, MTZ had no effect on paramecia consumption in control NTR- fish (Figure 2 S.6. A), while MTZ treatment significantly reduced the number of paramecia consumed in the recorded period for NTR+ fish compared to siblings treated only with the DMSO vehicle (Figure 2 S.6. B). Swimming behavior during the acclimation and prey capture periods of the hunting assay was not affected by MTZ (Figure 2 S.6. E and F). Moreover, MTZ had no effect on paramecia consumption on day 7 dpf in naive fish, which were fed with flakes on day 5 and 6 dpf (Figure 2 S.6. G). Together, these

findings suggest that activity in the habenula is specifically required for enhanced prey capture performance in prey-experienced fish.

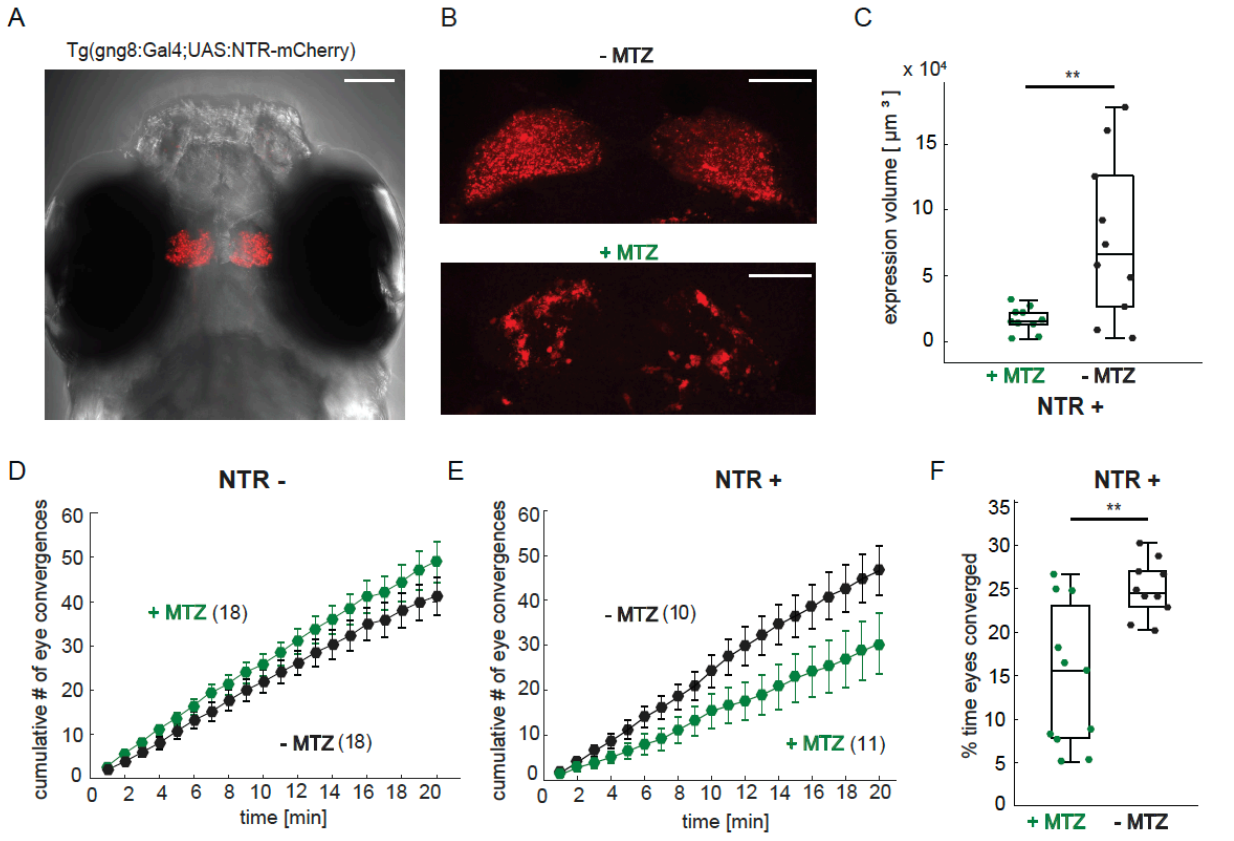

Figure 2.7. Chemical disruption of the habenula reduces hunting behavior in prey-experienced fish.

A) Representative image of 7 dpf *Tg(gng8:Gal4;UAS:NTR-mCherry)* fish, dorsal view. NTR-mCherry is depicted in red, image is a maximum intensity projection of a Z-stack. Scale bar is 100 µm. **B)** Representative images of NTR-mCherry expression (red) in the habenula in NTR+ fish after 19 hours in either 0.2% DMSO (-MTZ) (top) or 5 mM MTZ in 0.2% DMSO (+MTZ) (bottom). Images are maximum intensity projections of 5 µm/slice Z-stacks. Scale bar is 40 µm. Additional example images are shown in Figure 2 S.7.A. **C)** Volume of NTR-mCherry fluorescence is reduced in NTR-mCherry expressing fish treated with MTZ, $p = 0.003$, $N = 10$ animals per group. Differences in signal likely reflects variable transgene expression. Dependence of volume measurement on total fluorescence differs between +MTZ and -MTZ (Figure 2 S.6. B). Symbols indicate individual fish. Box plot shows median, 25th and 75th percentiles. **D, E)** Cumulative average number of eye convergences after addition of paramecia in 7 dpf control (NTR-) fish **(D)** and *Tg(gng8:Gal4;UAS:NTR-mCherry)* (NTR+) siblings **(E)**, pretreated for 19 hours with either 0.2% DMSO alone (-MTZ) or 0.2% DMSO containing 5 mM metronidazole (+MTZ) and tested for 20 minutes one hour after washout of the drug. Eye convergence rate is reduced in MTZ-treated enzyme expressing fish (NTR+/+MTZ) compared to untreated (NTR+/-MTZ) animals (Two-way repeated measures ANOVA shows an effect of treatment with $p = 0.033$), while we observe no significant difference for NTR- animals (Two-way repeated measures ANOVA, effect of treatment $p = 0.24$). (n) = number of fish in each group. Error bars show SEM. **F)** Percent time of eyes converged over 20 minutes of recording period in NTR+ fish is significantly lower in NTR+/+MTZ fish than in NTR+/-MTZ ($p = 0.004$. Symbols indicate individual fish. Box plot shows median and 25th and 75th percentiles. A permutation test is used for all pairwise comparisons unless otherwise specified (see Materials and Methods, Behavioral data analysis and statistics).

Discussion

Experience of live prey improves hunting success in larval zebrafish

After larval zebrafish hatch from their chorion and finish using the nutrient reserves from their yolk, they are left to their own devices to survive, avoid predators, and capture prey. Prey capture is generally thought to be an innate behavior in zebrafish because larvae are capable of capturing prey as early as their first attempts [15–17]. We compared hunting of paramecia between zebrafish larvae with two days of experience of live prey and sibling fish with experience of inert dry food, which are exposed to paramecia for the first time. We found that prior experience of live prey increases the frequency of successful captures, indicating that "practice" improves performance of this innate behavior. This improvement can be measured both in freely swimming fish as well as when fish are semi-immobilized for imaging and observing a live prey. Moreover, we find that experience of paramecia generalizes, increasing responsiveness to a virtual prey, even though this small black dot moving at uniform speed on a screen is quite distinct from the erratic 3D movement patterns of a translucent paramecium. While dependence of virtual prey capture on experience of live prey has not been explicitly described previously, we note that studies on prey capture in a virtual environment consistently report feeding the fish paramecia prior to testing [8–10,21,29]. Thus, experience of live prey may contribute to the ontogeny of prey capture behavior, where older (and therefore more "experienced") fish have more fluid capture maneuvers and hunt prey from a wider angular range [51]. Our finding is consistent with a recent study [52], which showed that differences in hunting kinematics result in higher hunting efficiency in experienced fish.

Genetically encoded circuits extract information relevant to predation at multiple levels of the visual processing stream. Different groups of retinal ganglion cells and optic tectum neurons respond preferentially to small prey-like objects, or looming predator-like objects in zebrafish [10,24,44,53], and frogs [7], similarly to small target motion detector neurons in insects [54,55]. This information is relayed in the tectum, whose optogenetic activation has been shown to trigger the prey capture motor response [25]. Further, recent results have shown that stimulation of single neurons in the pretectum can trigger the hunting sequence [28]. Thus, the prey-capture circuit is hard-wired in the novice hunter's brain. Nonetheless, experience of live prey may shape the circuit as shown in this work and the work mentioned above [52], and as it appears to do in juvenile fish raised in the dark who learn to forage using their lateral line system [56].

Activation of visual areas during prey observation and capture initiation

Our behavioral analysis showed an increase in prey capture initiation and successful captures in prey-experienced fish. This observation led us to test whether experience of live prey (vs. experience of dry inert food) enhances the early step of prey visualization or a later step of "decision to pursue". To distinguish between these possibilities, we imaged neural activity in semi-immobilized prey-experienced and prey-naïve fish in response to a live prey. Regression analysis of calcium signals revealed retinotopic maps that encode prey position in the pretectum and optic tectum. Previous findings show that spontaneous activity in the optic tectum changes with development and visual experience 57. We observed no difference in maps between prey-experienced and prey-naïve fish, suggesting that neural encoding of prior experience of prey lies in a step subsequent to visualization of prey.

We examined brain activity around eye convergences, the hallmark of prey capture initiation 8. In agreement with an earlier finding that AF7 responds specifically to prey-like objects and is

important for mediating the capture response 10, we observed that activation of pretectal neurons, likely surrounding AF7, consistently preceded eye convergence (Figure 2). We also found that activation of the tectal neuropil and PVNs preceded eye convergence, consistent with previous observations showing that optic tectum function is necessary for prey capture 22–24, and that assemblies of tectal neurons activate specifically when an eye convergence occurs 21. The amplitude and timing of activity observed in visual areas in the presence of prey was similar in prey-experienced and prey-naïve fish whether it elicited an eye convergence or not (Figures 2.3. and 4, and Figure 2.3., figure supplement 1). Thus, neither the mapping of prey-evoked activity in visual areas nor strength or timing of visual responses appeared to be altered by experience of live prey (vs. experience of dry inert food). We therefore turned to an analysis of motor–related areas inducing prey capture initiation.

Circuit activation during prey capture initiation

When fish initiate a prey capture sequence, they converge their eyes and flick their tail in a characteristic J-bend. Consistent with this, prey capture initiation events were associated with activation of the cerebellum and hindbrain (Figure 2). Similar to mammals, the teleost cerebellum is compartmentalized into the vestibulo-cerebellar and the non-vestibulo-cerebellar systems that control balance and locomotion respectively 58, which likely play a role in the outcome of a capture sequence. To understand how information flows from visual areas to these motor-related areas, we used Granger-causality analysis 41. We established that the strength of apparent directed information flow from pretectum to optic tectum, cerebellum, and hindbrain were significantly correlated with how frequently a fish initiated a hunting sequence (Figure 2.5. C-E). This relationship could reflect a role in triggering the motor response to the sight of prey or a change in proprioceptive feedback due to movement. A reason for favoring the former interpretation is that proprioception would be expected to be the same in prey-experienced and prey-naïve fish during an eye convergence event. Instead we observe a difference in slope of directed coupling strength relative to eye convergence frequency for information flow from pretectum to tectal PVN, from pretectum to cerebellum, and from pretectum to hindbrain (Figure 2.5. C-E). For a statistical link with a given strength from the pretectum to motor-related areas, fish with prior experience of live prey initiate prey captures more frequently than those with prior experience of dry inert food. Our results suggest that prior experience of prey increases the gain of information flow from the pretectum to motor-related areas, making a pretectum event more likely to trigger a prey capture response.

Forebrain recruitment and the experience-dependent boost in prey capture initiation

Wide-field brain activity imaging showed that prey-experienced fish had greater activity in the telencephalon and habenula when visual activity is followed by eye convergence relative to their prey-naïve siblings (Figure 2.6.). Statistical causality analysis suggested that prior experience of prey increases information flow from tectal PVNs to the telencephalon (Figure 2.5.), suggesting a role for this connection in improved prey capture performance (Figure 2.1.). Together, these results suggest forebrain regions activated by the visual system's response to prey may play a role in setting the gain of information flow through the prey capture circuit, with prior experience of prey sharpening the contrast between visual events that do or do not trigger capture behavior.

Since the above observations were correlative, we endeavored to perform a causal test of the role of the forebrain in prey capture. To do this, we turned to targeted chemical ablation using

nitroreductase in combination with metronidazole. We targeted the habenula for three reasons: availability of a habenula-specific Gal4 driver line, the fact that the habenulae receives considerable anatomical input from the ventral telencephalon (subpallium) 59, and our observation from Granger Causality analysis that activity in the habenula is predicted by activity in the telencephalon (Figure 2.5. A). We selectively disrupted neurons in the habenula following two days of exposure to live prey and observed a significant reduction in prey capture initiation and performance in fish with disrupted habenula neurons vs. siblings with an intact habenula. Our results indicate that activity in the habenula contributes to optimized prey capture performance in prey-experienced fish by increasing the gain between prey-evoked activity in visual areas and the motor areas that execute hunt behavior.

To our knowledge, while there are correlative studies for the role of the telencephalon and habenula in prey capture, no functional role for these structures had yet been demonstrated 60. The dorsal habenula in teleosts is homologous to the mammalian medial habenula and has been shown to modulate fear responses and social conflict outcomes in adult zebrafish 61,62, and integrating olfactory and optical cues in larval zebrafish 63. Our work suggests the forebrain could mediate the effect of prior experience of live prey on prey capture performance. Additional work is required to detail the mechanism of this effect. It should be noted that other brain areas may also contribute to gain control. Previous studies identified the nucleus of the medial longitudinal fasciculus (nMLF) as an important relay for motor signals controlling the prey capture circuit 22. Some pretectal neurons have direct projections to the nMLF and the hindbrain 102864. The mesencephalic reticular formation, a region controlling eye movements and convergence in goldfish 65 was also missing from our imaging plane. Neuromodulatory systems have also been implicated in regulating natural behaviors. The dopaminergic system encodes stimulus valence and regulates motivation 3; the noradrenergic locus coeruleus is thought to modulate arousal 66; different parts of the hypothalamus are thought to control a variety of motivational functions like arousal and feeding 6768. The central amygdala has recently been shown to control predatory hunting in mice, by increasing capture initiation via the periaqueductal gray 69, which is homologous to the griseum centrale of zebrafish, and receives input from the habenula 70. Further, the habenula, which is a highly conserved across species, also acts in value-based decision making throughout species 71, and this could contribute to the experience-dependent increase in prey capture performance that we find to be associated with habenula activity.

Neuromodulation could also contribute to the gain control of prey capture behavior observed in this study. The serotonergic system modulates responsiveness and arousal in fish 72 and mammals 73, as well as prey-approach behavior depending on hunger levels of the fish 74. A recent study showed that a subpopulation of neurons in the dorsal raphe in the hindbrain encodes whether zebrafish are in an hunting “exploitation” state or an “exploration” state 75. This area is another candidate for contributing to the effect of experience of live prey on behavior. Further, another study built a detailed model categorizing zebrafish behaviors, and showed that hunger influenced animals’ likelihood to seek food vs. safety 76.

In summary, we show that fish with prior experience of prey are better hunters and respond more reliably to virtual prey. Prey-experienced fish are more likely to trigger a capture initiation in response to a given visual neural event. Prey-experienced fish also display greater activity in the forebrain during visual events that trigger capture behavior relative to those that do not. Finally, prey-experienced fish show strengthened functional links from the output neurons of the optic tectum to the telencephalon. These findings suggest a role for the forebrain in prey capture, and this is supported by the observation that disruption of one of the forebrain areas, the habenula,

compromises prey capture in prey-experienced fish. We hypothesize that experience in hunting of live prey boosts prey capture performance by increasing the impact of information transfer from visual to motor-related areas as a result of recruitment of forebrain activity. The forebrain activity may contribute to gating this process, with experience sharpening contrast between visual events to create a “go” / “no-go” signal for initiating this complex motor behavior.

Materials and Methods

Key Resources Table

Reagent type	Designation	Source or reference	Identifiers	Additional information
fish line, *Danio Rerio*	AB wild type zebrafish	ZIRC	ZDB-GENO-960809-7	
fish line, *Danio Rerio*	TL wild type zebrafish	ZIRC	ZDB-GENO-990623-2	
fish line, *Danio Rerio*	TgBAC(gng8:GAL4FF);UAS:GFP	DeCarvalho, 2013		from Dr. Marnie Halpern
fish line, *Danio Rerio*	Tg(UAS-E1B:NTR-mCherry)	Curado et al., 2007; Matsuoka et al., 2016		from Dr. Didier Stainier
fish line, *Danio Rerio*	Tg(neurod1:GCaMP6F)	Rupprecht et al., 2016		from Dr. Claire Wyart
fish line, *Danio Rerio*	Tg(atoh7:gap43-RFP)	Zolessi et al., 2006		from Dr. Claire Wyart
chemical reagent	Metronidazole	Sigma-Aldrich	1442009 USP	
organism, *Paramecium Caudatum*	Paramecia	ZIRC	Paramecium starter culture	
reagent	Fish flakes	Hikari USA	First Bites Specialty fish food	

Zebrafish care and transgenic lines

Animal experiments were done under oversight by the University of California Berkeley institutional review board (Animal Care and Use Committee). Adult AB and Tüpfel long fin (TL) strains of Danio Rerio were maintained and raised on a 14 / 10 hour light cycle and water was maintained at 28.5°C, conductivity at 500µS and pH at 7.4. Embryos were raised in blue water (3 g of Instant Ocean® salts and 0.2 mL of methylene blue at 1% in 10 L of osmosed water) at 28.5°C. For imaging experiments, fish were screened for GCaMP6f expression at 2 or 3 dpf. We focused our study on early larval stages (5 to 8 dpf) when the neural circuitry of prey detection has been well studied in visual areas, and when animals are more tractable for neural activity imaging due to their transparency and small brain size. We used the Tg(NeuroD:GCaMP6f)icm05 line for all imaging experiments [30], and the Tg(atoh7:GAP-RFP) line [77] was used to compare labelling in the NeuroD line with retinal ganglion cell projections (Figure 2 S.2. A). Offspring of a Tg(gng8:Gal4;UAS:GFP) [48] crossed to a UAS:NTR-mCherry fish [78] were used for the habenula ablation experiments.

Diet and freely swimming behavior assay in wild type fish

Healthy wild type TL larval zebrafish were selected based on the inflation of the swim bladder at 4 dpf. Fish were split into two groups either fed a diet of paramecia or of fish flakes (Hikari USA inc) with 20 animals per dish. Fresh paramecia were prepared every day. We found that feeding the fish for a minimum of 6 hours per day insured that spontaneous swimming was the same across fish with different diets (Figure 2 S.1.. E and F). Fish were fed twice a day, in the morning at 9 -10 am, and in the afternoon at 1-2 pm. Dishes were cleaned out before each feed and fish were transferred to a new dish every evening at 5-6 pm. Fish were given more food than they could eat to ensure equal levels of satiation (there was always food remaining in the dishes when cleaned). At 7 dpf, one by one, fish were transferred to a 35 mm diameter dish and left to acclimate for one minute under white light. Spontaneous swimming was recorded for five minutes with a uEye CCD camera (IDS Imaging Development Systems GmbH) at 30 Hz using dark field illumination. 500µL of fresh paramecium culture was then added to the dish and prey capture behavior was recorded for five minutes. There was no significant correlation of initial number of paramecia or time of day the experiment was performed on prey capture performance in either prey-experienced or prey-naïve fish (Figure 2 S.1.C and D). We manually counted two types of events for each fish: number of pursuits initiated (eye convergence and J-bend at the same time) and successful captures. Fish that did not move at all during the spontaneous swimming test were excluded. We also compared spontaneous swimming of our two experimental groups to a third group fed pureed brine shrimp and flakes, our fish facility diet (Figure 2 S.1.. E and F). Finally, to control for differences in brain development, we estimated brain volume using the image analysis software Imaris (Bitplane AG, Switzerland) to interpolate total volume from surfaces drawn manually at 9.22 µm intervals. We found no difference between prey-experienced and prey-naïve fish (data not shown, $N = 6$ fish per group, $p = 0.25$).

Virtual prey capture assay

Our study focused on the initiation of prey capture rather than the subsequent motor-sequence. We therefore used an open-loop virtual prey capture assay, as previously described in the literature 8,9. Larval zebrafish that were fed paramecia or flakes were embedded in low-melting point agar at the end of their 6th day. Agar around the eyes and tail was carefully removed so that

only the area around the swim bladder was restrained. Fish were kept in the incubator to acclimate overnight. At 7 dpf fish were transferred to our imaging setup, a diffusive filter was fixed to the side of the dish acting as a screen ~ 10 mm away from the mid-point between the eyes. All stimuli were generated in MATLAB (Mathworks, USA) using the Psychophysics Toolbox extensions [79]. All fish were first tested for a robust optokinetic reflex evoked by moving gratings to ensure that the visual system was functional. Fish were then left to acclimate on the setup for 10 minutes. Small moving dots were projected at eye level onto the screen in front of the fish using an M2 Micro Projector (AAXA, USA). Optimal stimulus properties were chosen to maximize prey capture responses: 1 mm diameter dots of varying contrasts on a white background appeared in front of the fish and moved to the left or the right of the screen at 30 degrees / sec. Changes in speed of the stimulus due to the curvature of the screen were corrected for programmatically. The contrast of the dot was varied from 20% (light grey on white) to 100% (black on white) in 20% increments. Dots of different contrasts were presented in blocks. Fish were kept in the dark between trials (12 sec inter-trial interval), the white background screen appeared progressively 3 seconds before the onset of the trial, and at trial onset the stimulus appeared on the screen and moved to the left or to the right for a duration of 3 sec. Each contrast was tested 8 times (with 4 in each direction), and 20 blank trials were interweaved randomly with the (8 x 5 contrast types) target trials throughout the experiment, a total of 60 trials per fish. Contrast blocks were also ordered randomly. Fish were illuminated from the side with a custom-built red LED light source and behavior was imaged with a 2.5x/0.06 air objective (Carl Zeiss, Inc., Germany) using a high-speed CMOS camera (Mikrotron Eosens 1362, Germany) at 250 Hz. Behavior image acquisition and stimulus projection was synchronized by the software controlling the behavior camera (Piper, Stanford Photonics).

Imaging calcium activity induced by a live paramecium

Transgenic Tg(NeuroD:GCaMP6f) fish were embedded in agar and were placed under a one-photon spinning disc confocal microscope to acclimate for 10 minutes. They further acclimated for one minute with the 488nm laser light on continuously before the onset of image acquisition to avoid detecting the strong initial activation of visual response in response to light onset. The laser was on continuously throughout the acquisition session to avoid distracting the animal with flashing light. We limited our imaging to a single plane that contained the pretectal area around AF7 10, recording at 5x magnification (0.25NA, air objective, Zeiss Fluar) at 13-15% laser power, with an output laser light at the objective of 150 µW / cm2, and acquisition frequency at 3.6 Hz. The x / y optical resolution of the microscope used was 5.4 µm / pixel. Spontaneous activity was recorded for 1500 frames (about 7 min). A single paramecium was then added to a small well cut out in the agar in front of the fish 80. The well was sealed with a small lid of agar to keep the paramecium in front of the fish and avoid evaporation. Brain activity in response to the paramecium was recorded for 2500 frames (or 11.6 minutes). A Logitech C525 webcam (Logitech, USA) was placed under the fish to film the position of the paramecium using dark field illumination with an IR light source. A uEye CCD camera (IDS Imaging Development Systems GmbH) was attached to the microscope side port to record eye position. A notch filter 488nm (Chroma, USA) was placed in front of the webcam to block out the imaging laser light, a 488 band pass filter (Chroma, USA) was used to image GCaMP6f fluorescence and a dichroic mirror (T470lpxr, Chroma, USA) reflected wavelengths below 470 nm and above 750 nm to the uEye camera while transmitting green photons to the fluorescence camera. The webcam and the uEye camera were controlled by custom written software written in MATLAB so frames were acquired

every time a fluorescence frame was acquired. Acquisition was synchronized by a TTL pulse sent from the fluorescence imaging software Slidebook (3I, USA) to MATLAB. It has recently been suggested that the light intensities used for 1 photon light-sheet microscopy stimulate the blue and UV cones of the retina which compromises visual perception [81]. At 5x magnification, light intensity at the focal plane was 50-75μW, which is substantially less than intensities used for light-sheet microscopy. Low magnification imaging resulted some scattered blue light that we supplemented with visible blue LED side illumination, for the fish to see the paramecium in front of it and maximize responses. Data analysis is described in Materials and Methods, Behavioral data analysis and statistics and Calcium and behavior imaging data pre-processing.

Chemical ablation and free-swimming prey capture assay

We crossed Tg(gng8:Gal4;UAS:GFP) fish with Tg(UAS:NTR-mCherry) fish. At day 4 dpf, we screened for expression of nitroreductase using mCherry fluorescence, excluded fish also expressing GFP, and selected two groups of healthy fish: ones that were positive and ones that were negative for NTR. We used the same feeding protocol described above on 5 and 6 dpf. On the evening of day 6, we split the NTR positive and negative fish into two groups each and incubated them on a 48 well plate with either 5 mM MTZ (Sigma Aldrich) in 0.2% DMSO (Sigma Aldrich), referred to as +MTZ group, or 0.2% DMSO only (-MTZ group), overnight for 19 hours. The next morning, we washed the fish three times (five minutes per wash) with E3 fish water and placed them in the incubator to recover for 1 hour. After this period of recovery, fish were placed in a clear plastic 9 well plate (concave wells, diameter 11 mm, depth 10 mm) to record post-treatment feeding behavior. For our behavioral assay of predation, we placed the fish in the plate alternating in neighboring wells between the 4 groups (in a sequence of: NTR+/+MTZ, NTR+/-MTZ, NTR-/+MTZ, NTR-/-MTZ, and then repeat and so on). Fish behavior was recorded continuously for the first 30 seconds out of each 60 second period. The observation period consisted of an initial 10-minute baseline period and then 20 more minutes after paramecia were added. Fish behavior was imaged with a uEye CCD camera (IDS Imaging Development Systems GmbH) at 10 Hz frame rate, with IR illumination and incidental room light. Paramecia were added in a 200 μL volume of pre-counted paramecia. The number of paramecia at start was on average 29.7 + 8.9 (SD) and did not significantly differ between groups (Figure 2 S.6. D). Eye convergence was measured manually by counting the frequency and number of frames that the eyes were converged. Paramecia were counted in three 15-frame long windows per time point, (at frames 100-115, 200-215 and 285-300) and averaged to obtain the number of paramecia at each time point. Swim speed was measured by tracking the fish's location in the well by using a custom MATLAB (Mathworks, USA) script. For all analysis, the experimenter was blind to the genetics and treatment of the animals.

Fluorescence analysis

After the behavioral experiment, NTR+ fish were fixed in 4% formaldehyde overnight and then washed and mounted in low melting agarose. Z-stacks of both habenulae were taken on a Zeiss LSM 880 upright laser scanning confocal at equal laser intensity, making sure no pixels were oversaturated. The total volume of expressing cells was quantified by using the surface function in Imaris microscopy image analysis software (Bitplane AG, Switzerland).

Behavioral data analysis and statistics

All data was analyzed using custom-written software in MATLAB unless otherwise indicated. All pairwise comparisons were made with two-sided permutation tests using the difference in means as a test statistic [82] unless otherwise indicated. Permutation tests do not make any assumptions about the underlying distribution, do not require equal variances or equal sample size. We rearranged labels (i.e. prey-experienced or prey-naïve) on observed data points and calculated the new test statistic 100,000 times thus creating a null distribution (under the null hypothesis, labels are interchangeable). We then computed the p-value by calculating the probability of obtaining a test statistic with an absolute value at least as great as the absolute value of the observed statistic (the difference in means between the actual experimental groups) under the null distribution. Permutation tests were two-tailed, because of the comparison of absolute values. We used a significance level $\alpha = 0.05$ (or a 5% chance of incorrectly rejecting the null hypothesis). Raw data from individual fish is plotted along with a boxplot summarizing the distribution statistics of the group: the central bar is the median, the bottom and top edges of the box indicate the 25th and 75th percentiles respectively, and the whiskers extend to the most extreme data points not considered as statistical outliers (as defined by the inbuilt 'boxplot.m' function). We used a bootstrapping technique to calculate the percent increase in eye convergence frequency (Figure 2F).

Behavioral units of the prey capture sequence (pursuits and successful captures) were counted manually (Figure 2.1.). Swimming velocity and percent of time resting were determined using custom tracking code. In the virtual environment setup, eye convergence events and tail flicks were also detected manually. A hit was defined as an eye convergence event when a stimulus was presented, and a false alarm was an eye convergence when a blank stimulus was presented. Hit rate was defined as the number of hits divided by the number of stimulus trials and false alarm rate was estimated as the number of false alarms by blank stimulus trials. Blank stimuli were interleaved with stimulus trials throughout the experiment, so we used the same false alarm rate for all contrast levels. To measure eye convergence rates compared to baseline for a given fish at each contrast level, we calculated the discriminability index d' = Z(hit rate) –Z(false alarm rate), where Z is the inverse of the cumulative Gaussian distribution. d' distributions for prey-experienced and prey-naïve fish were compared using a Two-way ANOVA test.

Calcium and behavior imaging data pre-processing

Movies were registered using rigid body transformation (dftregistration from the Matlab File Exchange). Regions of interest (ROI) were drawn manually around the left and right telencephalon, habenula, pretectum, tectal neuropil, tectal PVNs, cerebellum, parallel fibers of the crista cerebellaris [45] and the hindbrain. Left and right regions that appeared to have symmetrical activity around events of interest were averaged. Images were bleach corrected by fitting a single or double exponential (depending on the best goodness-of-fit) to the mean baseline fluorescence of each ROI excluding outliers and subtracting it from each pixel's fluorescence time series. Fluorescence time-series of each pixel was then z-scored by subtracting the mean of the whole signal and dividing by the standard deviation (all Fz units in standard deviations away from the mean). We further corrected the average fluorescence traces of our ROIs for motion artifacts induced by body movements by interpolating values for all frames that had a displacement larger than 2 pixels. For Figures 5 and 6, we averaged left and right fluorescence for where signals were similar on either side. For analysis of fluorescence around pretectum transients (Figure 2.6.) we

detected pretectal peaks by thresholding the traces at 2 standard deviations from the mean and correcting for any aberrations manually and considered the highest value after thresholding as the peak. For each transient we considered the contralateral pretectum (to the prey) to be the side with the highest amplitude at peak time. We could not use prey position to determine contralateral identity because the prey was often on the midline and both eyes could detect it, and the prey moved faster than calcium transients rose to maximum meaning that a prey might evoked a transient while on one side of the fish, and already be on the other side by the time the transient has reached its peak. We extracted the average fluorescence in pretectum, optic tectum, cerebellum and hindbrain around 30 frames (~ 8 seconds) before and 30 frames after each pretectal peak. We calculated a baseline for each trace by averaging the fluorescence of the first 13 frames (~3.5 seconds).

To detect eye angle, for each frame eye contours were identified using custom written software, and an ellipse was fit to the contours. Eye angle was considered to be the angle of the major axis of the ellipse relative to the midline of the fish. Eye vergence was the angle between the two eyes. Eye convergences were detected semi-automatically by identifying frames where both eye moved sharply towards the midline, thresholding vergence at 30° [8], and correcting any aberrant detections manually. Speed of acquisition did not enable us to track fast changes in tail angle, so tail movements were detected by calculating pixel intensity changes on either side of the tail, subtracting a baseline rolling average over 20 frames. Pixel intensity changes matched tail bend amplitudes remarkably well when we scored movies by eye. Tail flick time points were detected semi-automatically by thresholding at 2 standard deviations from the mean and corrected for aberrations.

Quantifying prey position for the encoding model

We preprocessed prey-position movies by subtracting a baseline rolling average over 20 frames. Prey position was quantified using a polar representation of space around the fish. We defined 19 angle bins (or angle basis functions) of prey position relative to the fish's midline. Each bin was represented by a von Mises distribution (which is an approximation of the circular normal distribution) with centers evenly spaced from –pi to pi and the width parameter kappa set to 20. When the prey was close to the center of a bin, that angle was weighted strongly, whereas when the prey was in between two bins, the angles at the centers of those bins were weighted equally, generating a more continuous representation of prey-space. Similarly, we also defined 5 radial basis functions, which describe distance of the prey from the fish, using Gaussian distributions with centers evenly spaced from 0 to ~ 5 mm and width parameter sigma set to 40. We then took the product of each angle basis function and each radial basis function, yielding a total of 95 two-dimensional spatial basis functions that vary in both angle and radius. Each frame of the prey video was then projected onto each of these basis functions, producing 95 prey location time series. For a particular prey location time series the value is high for times when the prey is near the specified angle and radius and zero at other times.

Pixel-wise encoding model estimation and validation

Linearized finite impulse response (FIR) encoding models 37,38 that predict pixel fluorescence based on the location of prey were estimated for each pixel in each fish. For each pixel 1) we constructed the stimulus input matrix that represents prey location over time: To account for calcium indicator kinetics, and neural response delays relative to movement of the prey, each of the 95 prey-location time series were delayed from -5 to + 15 frames (-1.4 sec to 4.2

sec), yielding a total of 1900 features that were used to predict pixel fluorescence. The shifted prey location time series were concatenated, and the mean of each 1900 feature time series was then subtracted to avoid fitting an intercept term in the regression. 2) We used ridge regression to estimate the model coefficients that quantify the relationship between prey location and pixel fluorescence. To enable unbiased assessment of model prediction performance we used a 10-fold cross-validation (the outer-layer validation) approach to fit and validate the encoding models. First, the full dataset for each fish was divided into 10 sequential temporal segments. For each fold, one segment was reserved for model validation and the other 9 segments were used to estimate the model weights by way of L2-regularized linear regression (ridge regression). 3) We estimated the regularization parameter for each of the 10 outer-layer folds using a second lever of cross-validation. We tested 20 regularization parameters α, log spaced between 1 and 1,000. For each parameter α, the following procedure was repeated 50 times: we randomly selected and removed 400 time points (10 blocks of 40 consecutive time points each) from the model estimation dataset. Model weights were then estimated using the remaining time points and used to predict responses in the 400 selected time points. After this procedure was repeated 50 times a regularization-performance curve was obtained for each outer-fold layer by averaging the 50 prediction performance values for each regularization parameter. The regularization parameter with the best prediction performance was selected. 4) We re-computed model weights using the entire model estimation dataset (consisting of the 9 segments of data for this cross-validation fold). 5) We predicted fluorescence for the held-out segment of data using the estimated weights. Both weights and predicted fluorescence were saved. 6) We repeated steps 3 to 5 for each of the 10 outer-layer cross-validation folds. 7) After all 10 folds had been completed the predicted segments were concatenated to form a complete prediction dataset of the same size as the original fluorescence data. The Pearson correlation between the complete predicted time series and actual fluorescence time series was then computed for each pixel. For further analysis of pixel selectivity 8) we averaged together the estimated model weights from each of the 10 cross-validation folds (average across delays to obtain spatial receptive fields from Figure 2.3.C, average across radii to obtain preferred angle, or average across radii and angles to obtain preferred delay, etc). 9) Statistical significance of predictions was computed by comparing estimated correlations to the null distribution of correlations between two independent Gaussian random variables of the same length. Resulting p-values were corrected for multiple comparisons within each fish using the false discovery rate (FDR, $q<0.05$) procedure [83]. All model fitting was performed using custom software written in Python (https://github.com/alexhuth/ridge).

Granger-causality from calcium fluorescence imaging data

On the basis of our previous study [42], we studied Granger-causality between neuronal GCaMP6f fluorescence signals with the framework described below. According to the concept of Granger-causality [40,84], a variable F_1 causes F_2 ($F_1 \rightarrow F_2$) if the prediction of F_2 is improved when information from F_1 is included in the prediction model for F_2. GC measure is typically based on autoregressive (AR) models. In a bivariate AR modeling, a stationary signal $x_2(t)$ can be expressed as a linear regression of its past values according to the formula:

$$F_2(t) = \sum_{k=1}^{q} a(k)F_2(t-k) + e_1(t)$$

where $a(k)$ are the regression coefficients of the univariate AR model, q is the model order, and e1(t) is the respective prediction error. By introducing the information from the stationary signal $F_1(t)$, the formula can be rewritten as:

$$F_2(t) = \sum_{k=1}^{q} b_2(k)F_2(t-k) + \sum_{k=1}^{q} b_1(k)F_1(t-k) + e_2(t)$$

where $b_1(k)$ and $b_2\,(k)$ are the new regression coefficients of the bivariate AR model, and e2(t) is the new prediction error obtained by including also the past of $F_1(t)$ in the linear regression of $F_2(t)$. Statistical influence (Granger causality) between $F_1(t)$ and $F_2(t)$ is evaluated by the log ratio of the prediction error variances for the bivariate and univariate model:

$$GC_{1\to 2} = ln\left(\frac{var[e_2(t)]}{var[e_1(t)]}\right)$$

By construction, GC is a positive number; the higher $GCI_{1\to 2}$, the stronger the influence of $F_1(t)$ on $F_2(t)$ is. Such influence is often considered to reflect the existence of an information flow outgoing from the system $F_1(t)$ towards the system $F_2(t)$ [40,84]. Finally, GC is generally an asymmetric measure (i.e. $GCI_{1\to 2} \neq GCI_{2\to 1}$), which allows inferring causal or driver-response relationships.

The regression coefficients of the AR models were computed according to the ordinary-least-squares minimization of the Yule-Walker equations [84,85]. The model order q was selected according to the Akaike criterion [86]. This criterion finds the optimal q that minimizes the following cost function $C(q) = \mathrm{T}\ln(det(\Sigma_2)) + \frac{T(TN+qN^2)}{T-qN-N-1}$, where Σ_2 is the noise covariance matrix of the bivariate AR model, N = 2, and T is the number of samples of the time series. Basically, this cost function balances the variance accounted for by the AR model against the number of coefficients to be estimated. We fixed the common model order of q = 5 frames for all fish (mean of optimal order values obtained for individual fish) [87].

We estimated GC between GCaMP6f fluorescence signals in spontaneous (without prey) and evoked (with prey) conditions over 1500 frames (7 min) and 2500 frames (11 min) respectively (normalized to zero mean and unitary variance). Each zebrafish's brain was thus characterized by a full connectivity pattern by quantifying GC influences between identified ROIs. The strength of a functional link between two regions was estimated with the value of the F-statistic, which quantifies the statistical significance of the directed interaction under the assumption of non-directed effect. Statistical differences between groups were evaluated using a Welsh-test for each link [84,85]. Only p-values corresponding to percentiles inferior to a statistical threshold of $\alpha = 0.05$ FDR-BH corrected for multiple comparisons were retained.

Robust multi-variate linear regression to relate prey capture initiation to Granger-causality links. We used multivariate linear regression to model the relationship between prey capture initiation frequency (response variable), and Granger-causality links strength and experience (two predictor variables). We used the "robust" option in the MATLAB fitlm function, which reiteratively weights each data point to reduce the effect of outlier response points on the fit. A bisquare function was used for re-weighting.

Acknowledgements

We thank Dr. Marnie Halpern for generously providing the Tg(gng8:Gal4) fish line; Kait Kliman, Mel Boren, Sonia Castillo and Allison Kepple for maintaining fish lines at UC Berkeley; Natalia Maties, Bodgan Buzurin and Sophie Nunes Figueiredo for maintaining transgenic lines at the ICM zebrafish facility; Holly Aaron, Jen Lee and Feather Yves from the Berkeley Molecular Imaging Center at UC Berkeley. Intelligent Imaging Innovations provided valuable advice and assistance with the optical system. We thank Adna Dumitrescu for developing approaches to test prey consumption and Amy Winans, Carlos Pantoja and Shih-Wei Chou for thoughtful feedback on the manuscript. We thank Vincent Guillemot from the ICM Biostatistics/Bioinformatics core facility, and Chris Holdgraf from UC Berkeley for providing advice on statistics. We also thank UC Berkeley undergraduate researchers Andrea Romo, Sweta Parija and Lydia Liu for help with data analysis. This research was developed with funding from the Defense Advanced Research Projects Agency (DARPA), Contract No. N66001-17-C-4015 to J.G. and E.Y.I., with support from the National Institutes of Health Nanomedicine Development Center for the Optical Control of Biological Function (2PN2EY018241) to E.Y.I., an Optoloco starting grant from ERC (#311673) to C.W., a Research-in-Paris postdoctoral fellowship and an EMBO postdoctoral fellowship (# ALTF 549-2013) to AP, and a Boehringer Ingelheim Fonds fellowship and Chateaubriand graduate student fellowship to C.S.O.

Supplemental Materials

Supplemental Figures

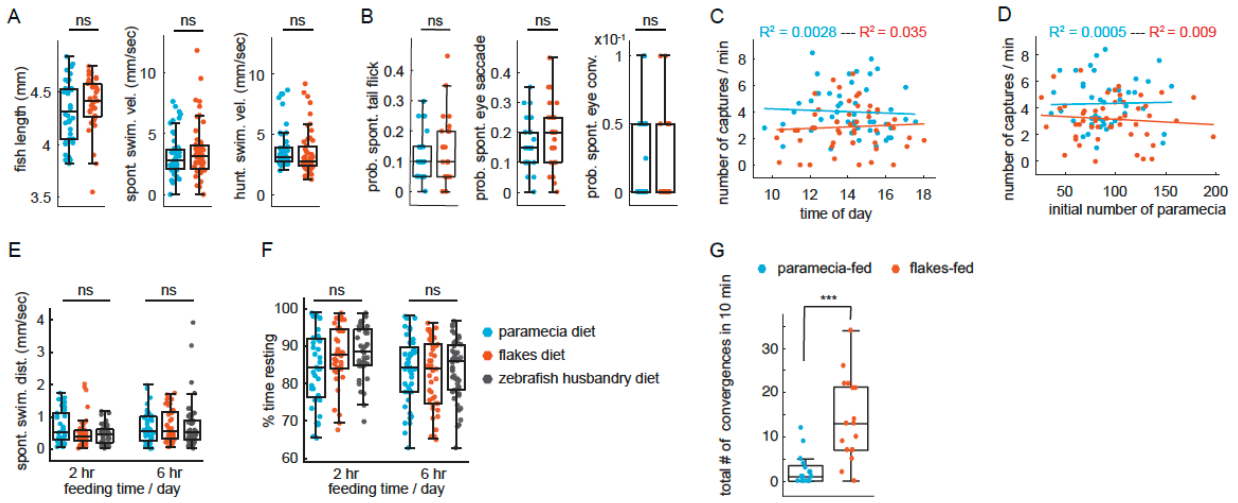

Figure 2 S.1. Lack of impact of other factors on prey capture performance.

A) No difference in health or swim behavior due to differences in diets: statistically indistinguishable fish length ($p = 0.28$), spontaneous swim velocity ($p=0.30$), and swim velocity in presence of prey ($p = 0.39$). **B)** Virtual prey capture. No difference between prey-experienced and prey-naïve fish in spontaneous tail flicks, eye saccades or eye convergences in absence of virtual prey stimulus ($p = 0.48$, $p = 0.29$, $p = 0.76$, respectively). **C, D)** No effect on prey capture performance of time of day **(C)** or initial number of paramecia **(D)**. **E, F)** No effect of diet on swimming. Spontaneous swimming velocity **(E)** and percent of time spent resting **(F)** are similar in fish fed paramecia, flakes or pureed brine shrimp + dry food (husbandry diet) for 2 hours or 6 hours/day (one-way ANOVA test for **E)** spontaneous swimming velocity 2 hours, Fstat = 2.95, $p = 0.06$; spontaneous swimming velocity 6 hours, Fstat = 0.19, $p = 0.83$; one-way ANOVA test for **F)** % time resting 2 hours, Fstat = 2.95, $p = 0.06$; % time resting 6 hours, Fstat = 0.29, $p = 0.75$). **G)** Fish previously fed with paramecia ($N = 16$) and fish previously fed with flakes ($N = 17$) on day 5 and 6 dpf are exposed to flakes on day 7 dpf for 10 minutes. Flakes-fed fish show a significantly higher amount of eye convergence during the recorded period than paramecia-fed fish, $p < 0.0001$. A permutation test was used for all pairwise comparisons if not specified otherwise (see Materials and Methods, Behavioral data analysis and statistics).

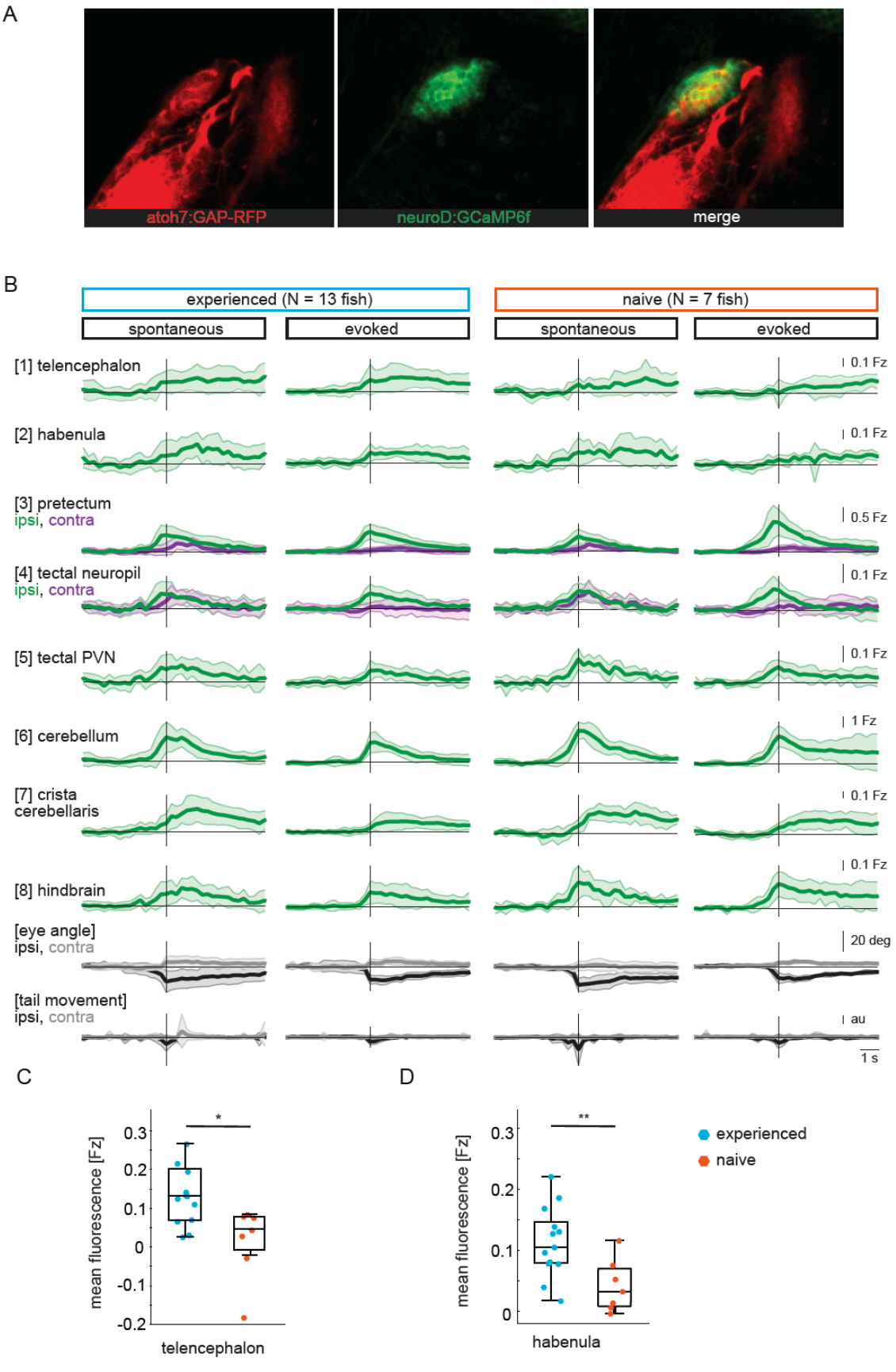
A
atoh7:GAP-RFP
neuroD:GCaMP6f
merge
B
experienced (N = 13 fish)
naive (N = 7 fish)
spontaneous
evoked
spontaneous
evoked
[1] telencephalon
[2] habenula
[3] pretectum
ipsi, contra
[4] tectal neuropil
ipsi, contra
[5] tectal PVN
[6] cerebellum
[7] crista cerebellaris
[8] hindbrain
[eye angle]
ipsi, contra
[tail movement]
ipsi, contra
0.1 Fz
0.5 Fz
1 Fz
20 deg
au
1 s
C
mean fluorescence [Fz]
telencephalon
D
habenula
experienced
naive

Figure 2 S.2. GCaMP6f expression pattern and time traces.

A) Pretectum area of a 7 dpf *Tg(ath5:mRFP;NeuroD:GCaMP6f)* fish. NeuroD-driven expression of GCaMP6f (green) includes pretectal neurons with cell bodies in close proximity to AF7, that expresses mRFP (red) under the ath5 promoter. **B)** Composite GCaMP6f fluorescence time courses for prey-experienced (N = 13) and prey-naïve (N = 7) fish associated with eye convergence (vertical black line) for brain areas and behavioral measures shown in Figure 2H. Fish selected to have > 5 eye convergences in presence of prey (evoked). Activity in contralateral tectal neuropil higher than ipsilateral tectal neuropil in evoked but not spontaneous condition. Difference between amplitude at peak convergence between contralateral and ipsilateral significant for prey-experienced ($p = 0.049$) and prey-naïve ($p = 0.02$) fish. "Contra" and "ipsi" refer to the side with higher or lower pretectal transient amplitude peak time (see Materials and Methods). **C, D)** Quantification of evoked (in presence of paramecia) forebrain activity in **(B)** for telencephalon (1) and habenula (2) over 5 frames (1.4 s) after eye convergence. We observe higher activity in prey-experienced fish than in prey-naïve fish in both the telencephalon **(C)** and the habenula **(D)** ($p = 0.025$ and 0.009, respectively (permutation test, see Materials and Methods, Behavioral data analysis and statistics).

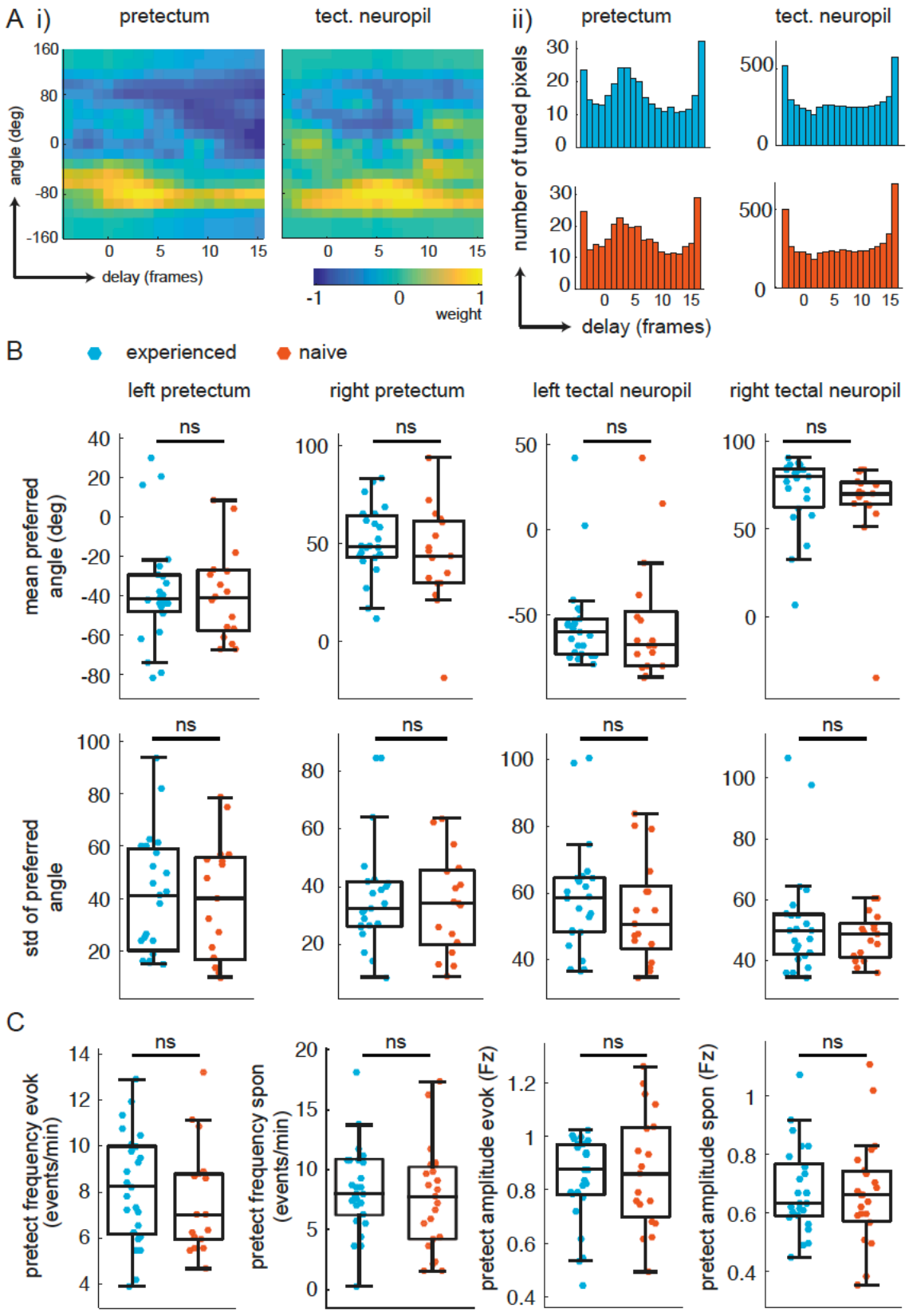

Figure 2 S.3. Similar retinotopic maps and pretectal events in prey-experienced and prey-naïve fish.

A) Delay analysis. i) Receptive fields for delay (x-axis, 1 frame is 0.28 seconds) and angle (y-axis) for example pixel in pretectum (left) and tectal neuropil (right). Notice weight is smeared in x-axis for tectal neuropil. ii) distribution of preferred delay weight in the pretectum (left) and the tectal neuropil (right) for prey-experienced (top, blue, N = 23) and prey-naïve (bottom, red, N = 17) fish are very similar. **B)** The mean and standard deviation of the preferred angle distributions were indistinguishable between prey-experienced and prey-naïve fish. (preferred angle p = 0.93 left pretectum, p = 0.31 right pretectum, p = 0.91 left tectal neuropil, p = 0.68 right tectal neuropil. Standard deviation p = 0.96 left pretectum, p = 0.34 right pretectum, p = 0.42 left tectal neuropil, p = 0.21 right tectal neuropil) **C)** Average event frequency in left and right pretectums was not different between prey-experienced and prey-naïve fish in either evoked (p = 0.20, left) or spontaneous (p = 0.56, second from left) conditions. Average pretectum event amplitude was not different between prey-experienced and prey-naïve fish in evoked (p = 0.54, second from right) or spontaneous (p = 0.67, right) conditions. A permutation test was used for all pairwise comparisons if not specified otherwise (see Materials and Methods, Behavioral data analysis and statistics).

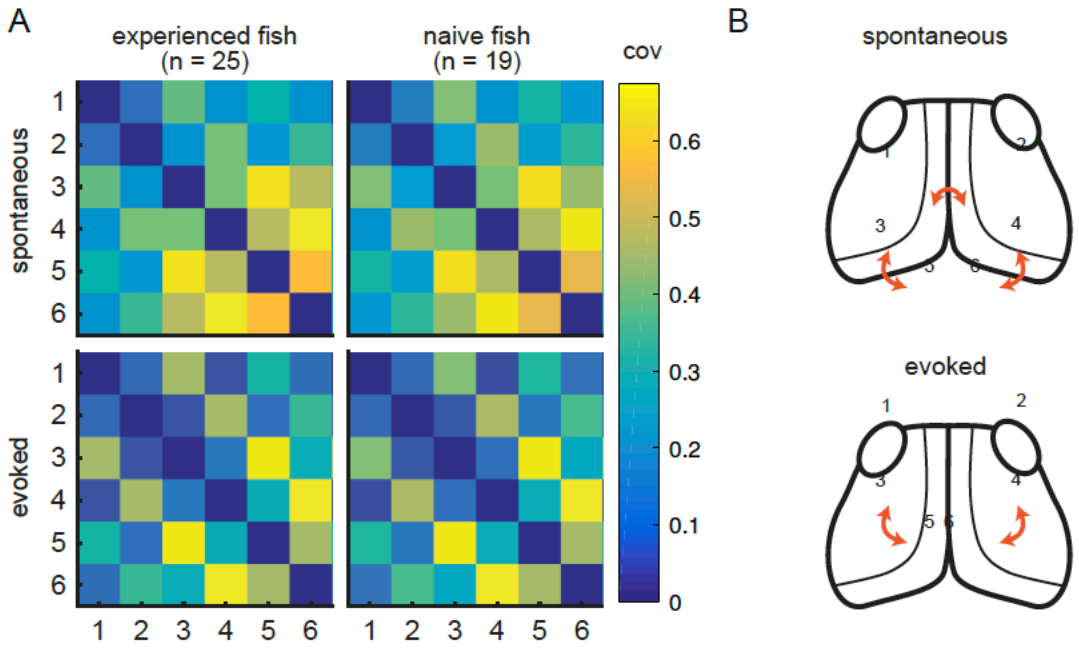

Figure 2 S.4. Experience does not affect circuit covariance in visual areas.

A) Pair-wise covariance (a non-directed measure of interaction) was calculated between the visual areas in spontaneous (top row) and evoked (bottom row) conditions and prey-experienced (left column) and prey-naïve (right column) fish. There were no statistical differences between prey-experienced and prey-naïve fish in the spontaneous or the evoked conditions (pair-wise T-tests, FDR corrected). **B)** Links with linear correlation values higher than 0.5 for spontaneous (top) and evoked (bottom) conditions are represented by the orange arrows.

Figure 2 S.5. Comparison of weak vs strong hunters.

A) Prey-experienced fish ranked by frequency of evoked eye convergence (with prey – without prey) into strongest quartile (N = 5, left) and weakest quartile (N = 5, right). Average Granger-causality matrices for same regions as Figure 5. Inset: Pair-wise statistical comparison (T-tests) of all links (see Supplemental File 3 for p-values).

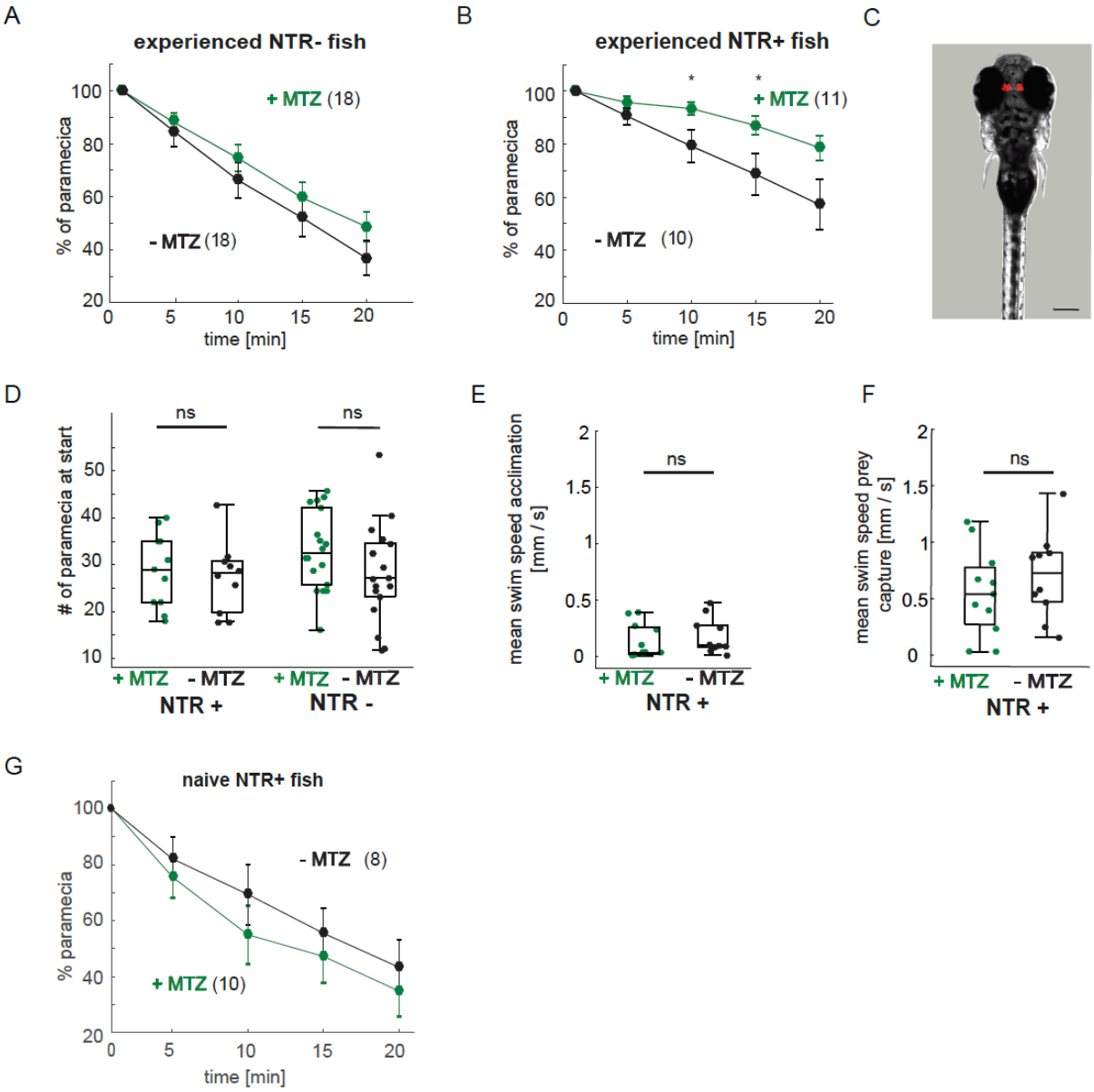

Figure 2 S.6. Expression pattern of Tg(gng8:Gal4;UAS:NTR-mCherry) fish, paramecia consumption and swim behavior.

A-B) Paramecia consumption over 20 minutes. A) NTR- fish showed no significant difference between +MTZ or -MTZ treated groups (Two-way repeated measures ANOVA, effect of treatmet p = 0.33). Error bars are SEM. B) Nitroreductase expressing NTR+/+MTZ fish consume paramecia more slowly than NTR+/-MTZ fish (minute 10: p = 0.036; minute 15: p = 0.040; minute 20: p = 0.051; Two-way repeated measures ANOVA, effect of treatment: p = 0.073). C) Expression of NTR-mCherry in Tg(gng8:Gal4;UAS:NTR-mCherry) fish is specific to the habenula. Image is a maximum intensity projection of a Z-stack, NTR expression is shown in red. Scale bar is 200 µm. D) The number of paramecia initially added to the wells was not significantly different between the +MTZ and -MTZ treated groups, for either the NTR+ fish (p = 0.69, left side) or NTR- fish (p = 0.74, right side). Every dot represents one fish, boxplots show median and 25th and 75th percentiles. E-F) No significant difference in average swim speed between +MTZ and -MTZ fish in NTR+ animals during the 10 minutes acclimation period before addition of paramecia (E) (p = 0.46) or during the 20 minutes prey capture period after addition of paramecia (F) (p

= 0.29). Dots represent individual fish, boxplots show median and 25th and 75th percentiles. G) Habenula ablation does not affect paramecia consumption in non-experienced fish. Two-way repeated measures ANOVA shows no effect of treatment, p = 0.37. Error bars are SEM. A permutation test was used for all pairwise comparisons unless specified otherwise (see Materials and Methods, Behavioral data analysis and statistics).

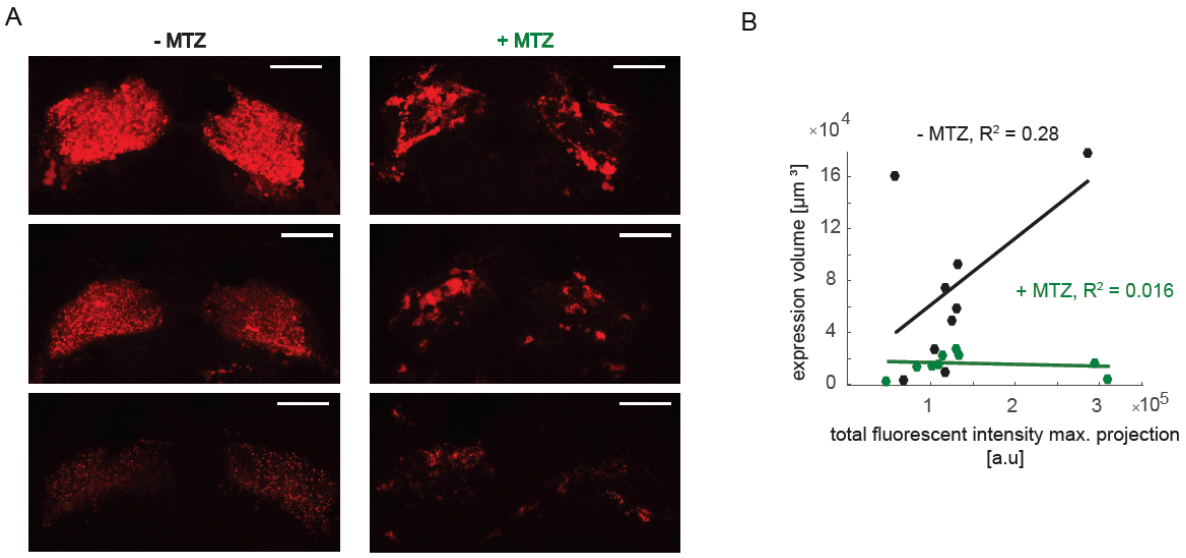

Figure 2 S.7. Differences in mCherry signal intensity and correlation with expression volume.

A) Examples of mCherry pattern in healthy control habenulae of NTR+ fish treated with vehicle only (-MTZ) and metronidazole-treated (+MTZ). Although brightness levels vary, the -MTZ controls show a typical diffuse pattern, whereas the +MTZ-treated animals have a blotchy distribution. Scale bar represents 40 µm. **B)** Relation between total fluorescent intensity in maximum projection of Z-stacks and calculated expression volume. Symbols represent individual fish, a permutation test was used for all pairwise comparisons unless specified otherwise (see Materials and Methods, Behavioral data analysis and statistics).

Supplemental Tables

Brain region	p-Value
Telencephalon	0.027
Habenula	0.003
Pretectum (contra)	< 0.001
Pretectum (ipsi)	0.697
Tectal neuropil (contra)	0.011
Tectal neuropil (ipsi)	0.018
Tectal PVN	< 0.001
Cerebellum	< 0.001
Crista cerebellaris	0.001
Hindbrain	< 0.001

Table 2 S.1. P-values for permutation test comparison of average fluorescence trace before and after eye convergence in experienced fish for different brain regions (Figure 2H).

Visual Areas - Evoked						
Region	**1**	**2**	**3**	**4**	**5**	**6**
1		0.38	0.21	0.48	0.18	0.35
2	0.3		0.12	0.43	0.18	0.36
3	0.18	0.39		0.32	0.48	0.07
4	0.15	0.33	0.23		0.3	0.36
5	0.11	0.29	0.3	0.26		0.09
6	0.23	0.19	0.29	0.16	0.16	

Visual Areas - Spontaneous						
Region	**1**	**2**	**3**	**4**	**5**	**6**
1		0.49	0.24	0.49	0.46	0.35
2	0.4		0.37	0.43	0.4	0.16
3	0.1	0.46		0.34	0.43	0.29
4	0.09	0.09	0.36		0.13	0.5
5	0.18	0.01	0.42	0.4		0.44
6	0.31	0.46	0.3	0.41	0.48	

Table 2 S.2. P-values for comparisons of Granger-causality links in the visual areas (matrices presented in Fig 4.). For each link, differences between experienced and naïve fish are assessed. Threshold for significance after FDR-BH correction is p = 0.0017 (see Materials and Methods).

Visual and motor areas - Experienced and Naïve fish (Fig. 5A), evoked							
Region	**1**	**2**	**3**	**4**	**5**	**6**	**7**
1		0.11	0.03	0.36	0.39	0.22	0.15
2	0.36		0.1	0.18	0.33	0.18	0.35
3	0.16	0.21		0.24	0.49	0.27	0.13
4	0.01	0.01	0.32		0.49	0.24	0.28
5	3.00E-04	0.07	0.02	0.21		0.06	0.36
6	0.04	0.01	0.04	0.49	0.31		0.2
7	0.01	3.00E-03	0.02	0.4	0.11	0.19	
Visual and motor areas - Strong vs Weak hunters (Fig. 5, fig. suppl. 1A), evoked							
Region	**1**	**2**	**3**	**4**	**5**	**6**	**7**
1		0.21	0.17	0.48	0.33	0.09	0.17
2	0.22		0.23	0.23	0.16	0.3	0.3
3	0.16	0.46		3.00E-12	6.00E-09	3.00E-03	4.00E-04
4	0.07	0.16	0.49		0.14	0.17	0.07
5	0.37	0.16	0.33	0.11		0.29	0.4
6	0.21	0.34	0.37	0.28	0.02		0.07
7	0.43	0.34	0.47	0.35	0.31	0.17	

Table 2 S.3. P-values for comparisons of directed (causal) interactions between visual and motor areas between experienced and naïve fish (matrices presented in Fig 5A), and strongest and weakest hunters among experienced fish (matrices presented in Fig 5, figure supplement 1A). Threshold for significance after FDR-BH correction is top: p = 3.E-04, and bottom p = 0.003. Links that are significantly different between groups are highlighted in yellow.

References

1. Feldman, D. E. Synaptic mechanisms for plasticity in neocortex. *Annu Rev Neurosci* **32**, 33–55 (2009).
2. Letzkus, J. J. *et al.* A disinhibitory microcircuit for associative fear learning in the auditory cortex. *Nature* **480**, 331–335 (2011).
3. Matsumoto, M. & Hikosaka, O. Two types of dopamine neuron distinctly convey positive and negative motivational signals. *Nature* **459**, 837–841 (2009).
4. Felsen, G. & Dan, Y. A natural approach to studying vision. *Nat. Neurosci.* **8**, 1643–1646 (2005).
5. Theunissen, F. E. & Elie, J. E. Neural processing of natural sounds. *Nat. Rev. Neurosci.* **15**, 355–366 (2014).
6. Sommerfeld, N. & Holzman, R. Suction feeding performance and prey escape response interact to determine feeding success in larval fish. *bioRxiv* (2019). doi:10.1101/603316
7. Ewert, J. P. *et al.* Neural modulation of visuomotor functions underlying prey-catching behaviour in anurans: Perception, attention, motor performance, learning. *Comp. Biochem. Physiol. - A Mol. Integr. Physiol.* **128**, 417–461 (2001).
8. Bianco, I. H., Kampff, A. R. & Engert, F. Prey capture behavior evoked by simple visual stimuli in larval zebrafish. *Front. Syst. Neurosci.* **5**, 101 (2011).
9. Trivedi, C. A. & Bollmann, J. H. Visually driven chaining of elementary swim patterns into a goal-directed motor sequence: a virtual reality study of zebrafish prey capture. *Front Neural Circuits* **7**, 86 (2013).
10. Semmelhack, J. L. *et al.* A dedicated visual pathway for prey detection in larval zebrafish. *Elife* **4**, 1–19 (2014).
11. Matsunaga, W. & Watanabe, E. Visual motion with pink noise induces predation behaviour. *Sci. Rep.* **2**, 1–7 (2012).
12. Payne, R. S. Acoustic location of prey by barn owls (Tyto alba). *J. Exp. Biol.* **54**, 535–573 (1971).
13. Anjum, F. & Brecht, M. Tactile experience shapes prey-capture behavior in Etruscan shrews. *Front. Behav. Neurosci.* **6**, 1–8 (2012).
14. Elliott, C. J. H. & Susswein, a J. Comparative neuroethology of feeding control in molluscs. *J. Exp. Biol.* **205**, 877–896 (2002).
15. Borla, M. A., Palecek, B., Budick, S. & O'Malley, D. M. Prey capture by larval zebrafish: Evidence for fine axial motor control. *Brain. Behav. Evol.* **60**, 207–229 (2002).
16. McElligott, M. B. & O'Malley, D. M. Prey tracking by larval zebrafish: Axial kinematics and visual control. *Brain. Behav. Evol.* **66**, 177–196 (2005).
17. McClenahan, P., Troup, M. & Scott, E. K. Fin-tail coordination during escape and predatory behavior in larval zebrafish. *PLoS One* **7**, 1–11 (2012).
18. Patterson, B. W., Abraham, A. O., MacIver, M. a & McLean, D. L. Visually guided gradation of prey capture movements in larval zebrafish. *J. Exp. Biol.* **216**, 3071–3083 (2013).
19. Johnson, R. E. *et al.* Probabilistic Models of Larval Zebrafish Behavior: Structure on Many Scales. *bioRxiv* (2019). doi:10.1101/672246
20. Mearns, D. S., Donovan, J. C., Fernandes, A. M., Semmelhack, J. L. & Baier, H. Deconstructing Hunting Behavior Reveals a Tightly Coupled Stimulus-Response Loop. *Curr. Biol.* (2020). doi:10.1016/j.cub.2019.11.022

21. Bianco, I. & Engert, F. Visuomotor Transformations Underlying Hunting Behavior in Zebrafish. *Curr. Biol.* **25**, 831–846 (2015).
22. Gahtan, E. Visual Prey Capture in Larval Zebrafish Is Controlled by Identified Reticulospinal Neurons Downstream of the Tectum. *J. Neurosci.* **25**, 9294–9303 (2005).
23. Smear, M. C. *et al.* Vesicular Glutamate Transport at a Central Synapse Limits the Acuity of Visual Perception in Zebrafish. *Neuron* **53**, 65–77 (2007).
24. Del Bene, F. *et al.* Filtering of visual information in the tectum by an identified neural circuit. *Science (80-.).* **330**, 669–673 (2010).
25. Fajardo, O., Zhu, P. & Friedrich, R. W. Control of a specific motor program by a small brain area in zebrafish. *Front. Neural Circuits* **7**, 67 (2013).
26. Muto, A. & Kawakami, K. Prey capture in zebrafish larvae serves as a model to study cognitive functions. *Front. Neural Circuits* **7**, 110 (2013).
27. Burrill, J. D. & Easter, S. S. Development of the retinofugal projections in the embryonic and larval zebrafish (Brachydanio rerio). *J Comp Neurol* **346**, 583–600 (1994).
28. Antinucci, P., Folgueira, M. & Bianco, I. H. A pretectal command system controls hunting behaviour. *bioRxiv* (2019). doi:10.1101/637215
29. Henriques, P. M., Rahman, N., Jackson, S. E. & Bianco, I. H. Nucleus Isthmi Is Required to Sustain Target Pursuit during Visually Guided Prey-Catching. *Curr. Biol.* (2019). doi:10.1016/j.cub.2019.04.064
30. Rupprecht, P., Prendergast, A., Wyart, C. & Friedrich, R. W. Remote z-scanning with a macroscopic voice coil motor for fast 3D multiphoton laser scanning microscopy. *Biomed. Opt. Express* **7**, 1656 (2016).
31. Dunn, T. W. *et al.* Brain-wide mapping of neural activity controlling zebrafish exploratory locomotion. 1–89 doi:10.7554/eLife.12741
32. Ahrens, M. B. *et al.* Brain-wide neuronal dynamics during motor adaptation in zebrafish. *Nature* **485**, 471–477 (2012).
33. Scott, E. K. & Baier, H. The cellular architecture of the larval zebrafish tectum, as revealed by gal4 enhancer trap lines. *Front. Neural Circuits* **3**, 1–14 (2009).
34. Karlstrom, R. O., Trowe, T. & Bonhoeffer, F. Genetic analysis of axon guidance and mapping in the zebrafish. *Trends Neurosci.* **20**, 3–8 (1997).
35. Simoncelli, E. P. & Olshausen, B. A. Natural image statistics and neural representation. *Annu Rev Neurosci* **24**, 1193–1216 (2001).
36. Wu, M. C.-K., David, S. V & Gallant, J. L. Complete functional characterization of sensory neurons by system identification. *Annu. Rev. Neurosci.* **29**, 477–505 (2006).
37. Nishimoto, S. *et al.* Reconstructing visual experiences from brain activity evoked by natural movies. *Curr. Biol.* **21**, 1641–1646 (2011).
38. Huth, A. G., Heer, W. A. De, Griffiths, T. L., Theunissen, F. E. & Jack, L. Natural speech reveals the semantic maps that tile human cerebral cortex. *Nature* (2016). doi:10.1038/nature17637
39. Friston, K. J. Functional and effective connectivity in neuroimaging: A synthesis. *Hum. Brain Mapp.* **2**, 56–78 (1994).
40. Granger, A. C. W. J. Investigating Causal Relations by Econometric Models and Cross-spectral Methods. *Econometrica* **37**, 424–438 (1969).
41. Seth, A. K., Barrett, A. B. & Barnett, L. Granger Causality Analysis in Neuroscience and Neuroimaging. *J. Neurosci.* **35**, 3293–3297 (2015).
42. De Vico Fallani, F., Corazzol, M., Sternberg, J. R., Wyart, C. & Chavez, M. Hierarchy of

neural organization in the embryonic spinal cord: Granger-causality graph analysis of in vivo calcium imaging data. *IEEE Trans. Neural Syst. Rehabil. Eng.* **23**, 333–341 (2015).
43. Nevin, L. M., Robles, E., Baier, H. & Scott, E. K. Focusing on optic tectum circuitry through the lens of genetics. *BMC Biol.* **8**, 126 (2010).
44. Preuss, S. J., Trivedi, C. A., Vom Berg-Maurer, C. M., Ryu, S. & Bollmann, J. H. Classification of object size in retinotectal microcircuits. *Curr. Biol.* **24**, 2376–2385 (2014).
45. Bae, Y. K. *et al.* Anatomy of zebrafish cerebellum and screen for mutations affecting its development. *Dev. Biol.* **330**, 406–426 (2009).
46. Heap, L. A., Goh, C. C., Kassahn, K. S. & Scott, E. K. Cerebellar output in zebrafish: an analysis of spatial patterns and topography in eurydendroid cell projections. *Front. Neural Circuits* **7**, 53 (2013).
47. Hiramoto, M. & Cline, H. T. Convergence of multisensory inputs in xenopus tadpole tectum. *Dev. Neurobiol.* **69**, 959–971 (2009).
48. deCarvalho, T. N., Akitake, C. M., Thisse, C., Thisse, B. & Halpern, M. E. Aversive cues fail to activate fos expression in the asymmetric olfactory-habenula pathway of zebrafish. *Front. Neural Circuits* (2013).
49. Muto, A. *et al.* Activation of the hypothalamic feeding centre upon visual prey detection. *Nat. Commun.* (2017). doi:10.1038/ncomms15029
50. Pisharath, H., Rhee, J. M., Swanson, M. A., Leach, S. D. & Parsons, M. J. Targeted ablation of beta cells in the embryonic zebrafish pancreas using E. coli nitroreductase. *Mech. Dev.* (2007). doi:10.1016/j.mod.2006.11.005
51. Westphal, R. E. & O'Malley, D. M. Fusion of locomotor maneuvers, and improving sensory capabilities, give rise to the flexible homing strikes of juvenile zebrafish. *Front Neural Circuits* **7**, 108 (2013).
52. Lagogiannis, K., Diana, G. & Meyer, M. P. Learning steers the ontogeny of an efficient hunting sequence in zebrafish larvae. *bioRxiv* (2019). doi:10.1101/2019.12.19.883157
53. Temizer, I., Donovan, J. C. & Baier Herwig, S. J. L. A Visual Pathway for Looming-Evoked Escape in Larval Zebrafish. *Curr. Biol.* **25**, 1823–1834 (2015).
54. Barnett, P. D., Nordstrom, K. & O'Carroll, D. C. Retinotopic Organization of Small-Field-Target-Detecting Neurons in the Insect Visual System. *Curr. Biol.* **17**, 569–578 (2007).
55. Wiederman, S. D., Shoemaker, P. a & O'Carroll, D. C. Correlation between OFF and ON channels underlies dark target selectivity in an insect visual system. *J. Neurosci.* **33**, 13225–13232 (2013).
56. Carrillo, A. & McHenry, M. J. Zebrafish learn to forage in the dark. *J. Exp. Biol.* **219**, 582–589 (2016).
57. Avitan, L. *et al.* Spontaneous Activity in the Zebrafish Tectum Reorganizes over Development and Is Influenced by Visual Experience. *Curr. Biol.* (2017). doi:10.1016/j.cub.2017.06.056
58. Volkmann, K., Rieger, S., Babaryka, A. & Köster, R. W. The zebrafish cerebellar rhombic lip is spatially patterned in producing granule cell populations of different functional compartments. *Dev. Biol.* **313**, 167–180 (2008).
59. Turner, K. J. *et al.* Afferent connectivity of the zebrafish habenulae. *Front. Neural Circuits* **10**, 1–18 (2016).
60. Ewert, J. P. *et al.* Forebrain and midbrain structures involved in prey-catching behaviour of toads: Stimulus-response mediating circuits and their modulating loops. in *European Journal of Morphology* (1999). doi:10.1076/ejom.37.2.172.4743

61. Agetsuma, M. *et al.* The habenula is crucial for experience-dependent modification of fear responses in zebrafish. *Nat Neurosci* **13**, 1354–1356 (2010).
62. Chou, M. *et al.* Social conflict resolution regulated by two dorsal habenular subregions in zebrafish. **352**, 599–602 (2016).
63. Jetti, S. K., Vendrell-Llopis, N. & Yaksi, E. Spontaneous activity governs olfactory representations in spatially organized habenular microcircuits. *Curr. Biol.* **24**, 434–439 (2014).
64. Helmbrecht, T. O., dal Maschio, M., Donovan, J. C., Koutsouli, S. & Baier, H. Topography of a Visuomotor Transformation. *Neuron* (2018). doi:10.1016/j.neuron.2018.10.021
65. Luque, M. A., Perez-Perez, M. P., Herrero, L. & Torres, B. Involvement of the optic tectum and mesencephalic reticular formation in the generation of saccadic eye movements in goldfish. *Brain Res. Rev.* **49**, 388–397 (2005).
66. Carter, M. E. *et al.* Tuning arousal with optogenetic modulation of locus coeruleus neurons. *Nat. Neurosci.* **13**, 1526–1533 (2010).
67. Mahler, S. V, Moorman, D. E., Smith, R. J., James, M. H. & Aston-Jones, G. Motivational activation: a unifying hypothesis of orexin/hypocretin function. *Nat. Neurosci.* **17**, 1298–1303 (2014).
68. Wee, C. L. *et al.* A bidirectional network for appetite control in zebrafish. *bioRxiv* (2019). doi:10.1101/631341
69. Han, W. *et al.* Integrated Control of Predatory Hunting by the Central Nucleus of the Amygdala. *Cell* **168**, 311–324.e18 (2016).
70. Olson, I., Suryanarayana, S. M., Robertson, B. & Grillner, S. Griseum centrale, a homologue of the periaqueductal gray in the lamprey. *IBRO Reports* **2**, 24–30 (2017).
71. Hikosaka, O. The habenula: from stress evasion to value-based decision-making. *Nat. Rev. Neurosci.* **11**, 503–513 (2010).
72. Yokogawa, T., Hannan, M. C. & Burgess, H. A. The Dorsal Raphe Modulates Sensory Responsiveness during Arousal in Zebrafish. **32**, 15205–15215 (2012).
73. Boulougouris, V. & Tsaltas, E. Serotonergic and dopaminergic modulation of attentional processes. *Prog. Brain Res.* **172**, 517–542 (2008).
74. Filosa, A., Barker, A. J., Dal Maschio, M. & Baier, H. Feeding State Modulates Behavioral Choice and Processing of Prey Stimuli in the Zebrafish Tectum. *Neuron* 1–13 (2016). doi:10.1016/j.neuron.2016.03.014
75. Marques, J. C., Li, M., Schaak, D., Robson, D. N. & Li, J. M. Internal state dynamics shape brainwide activity and foraging behaviour. *Nature* (2020). doi:10.1038/s41586-019-1858-z
76. Johnson, R. E. *et al.* Probabilistic Models of Larval Zebrafish Behavior Reveal Structure on Many Scales. *Curr. Biol.* (2020). doi:10.1016/j.cub.2019.11.026
77. Zolessi, F. R., Poggi, L., Wilkinson, C. J., Chien, C.-B. & Harris, W. a. Polarization and orientation of retinal ganglion cells in vivo. *Neural Dev.* **1**, 2 (2006).
78. Davison, J. M. *et al.* Transactivation from Gal4-VP16 transgenic insertions for tissue-specific cell labeling and ablation in zebrafish. *Dev. Biol.* (2007). doi:10.1016/j.ydbio.2007.01.033
79. Brainard, D. H. The Psychophysics Toolbox. *Spat. Vis.* **10**, 433–436 (1997).
80. Muto, A., Ohkura, M., Abe, G., Nakai, J. & Kawakami, K. Real-time visualization of neuronal activity during perception. *Curr. Biol.* **23**, 307–311 (2013).
81. Wolf, S. *et al.* Whole-brain functional imaging with two-photon light-sheet microscopy MiXCR : software for comprehensive adaptive immunity profiling. *Nat. Publ. Gr.* **12**, 379–

380 (2015).
82. Good, P. *Permutation, Parametric and Bootstrap Tests of Hypotheses*. (Springer, 2005). doi:10.1007/978-0-387-98135-2
83. Benjamini, Y. & Hochberg, Y. Controlling the False Discovery Rate : A Practical and Powerful Approach to Multiple Testing. *J. R. Stat. Soc.* **57**, 289–300 (1995).
84. Bressler, S. L. & Seth, A. K. Wiener-Granger Causality: A well established methodology. *Neuroimage* **58**, 323–329 (2011).
85. Gourevitch, B., Le Bouquin-Jeannes, R. & Faucon, G. Linear and nonlinear causality between signals: Methods, examples and neurophysiological applications. *Biol. Cybern.* **95**, 349–369 (2006).
86. Akaike, H. A new look at the statistical model identification. *IEEE Trans. Automat. Contr.* **19**, 716–723 (1974).
87. Pereda, E., Quiroga, R. Q. & Bhattacharya, J. Nonlinear multivariate analysis of neurophysiological signals. *Progress in Neurobiology* **77**, 1–37 (2005).

Chapter 3:

Volumetric imaging of neural activity during observation of "prey-like" moving dots in prey-experienced zebrafish larvae

Linker Statement

This chapter describes pilot study in continuation of the work reported in the previous chapter. I strived to increase temporal and spatial resolution of neural imaging to further investigate the experience-dependent changes in prey capture performance on a neuronal ensemble level. In close collaboration with Dr. Lamiae Abdeladim, currently a postdoctoral fellow in the Adesnik laboratory at UC Berkeley, I employed a fast-scanning two-photon imaging technique that allowed for imaging multiple planes of the zebrafish brain at single cell resolution. This setup did not allow for embedding a live prey in front of the fish, and therefore I adapted the virtual prey capture assay described in Chapter 2 to this imaging apparatus. In this chapter, I describe the microscopy setup, the visual stimulation protocol, the zebrafish behavior, and some neural activity results on one example experienced fish. By combining cutting-edge imaging technology, visual stimulation, and behavioral monitoring, I enabled measuring of activity of hundreds of neurons while a live animal was engaged in a natural behavior and have mad important strides towards understanding the neuronal ensembles supporting behavioral improvement in this behavior.

Introduction

Learning about how experience guides behavior is currently limited by our inability to monitor large numbers of neurons in live behaving animals. Brain-wide methods often lack single-cell resolution, and especially in mammals the large size and opaque nature of the brain force to focus on small fractions of the neuronal population and often are confined to only a few brain structures at a time. The larval zebrafish, with its small, transparent brain presents a unique advantage, and recently the development of novel imaging techniques, for example light sheet microscopy, has allowed for measuring activity of virtually the whole neuronal population in the brain of the larval zebrafish[1–3]. This has proven to be extremely valuable for the identification of the neuronal circuits underlying behavior[2,4–6], and to connect the neural basis of behavior across levels of analysis. However, many of these studies employ relatively simple behaviors, that do not require the complex integration.

In the previous chapter, I showed that experience with prey improves hunting performance in the larval zebrafish and pinpointed the forebrain, both the telencephalon and the habenula, as potentially important sites for experience-dependent plasticity during prey capture behavior. We observed an increase forebrain activity during eye convergence, and a decrease in hunting behavior upon disruption of the habenula. Further, we saw an increased drive from the tectal PVN neurons to the telencephalon only in experienced fish. The exact nature of these changes at a cellular level remains unknown, because of the limitations in speed and resolution our experimental setup.

Here I describe the combination of a fast-focusing, multi-plane imaging technique and a virtual prey capture assay, designed to enable the study the neural basis of the experience-dependent improvement of hunting, and to shed light on the neural ensembles underlying this natural behavior. I focused on the forebrain, to understand the dynamics of the experience-dependent increase in activity observed in chapter 2. The questions I was interested in were: Where are the cells that fire before or during the eye convergence? Does a specific firing pattern encoding the decision to capture prey exist in the telencephalon or habenula? Are there changes in correlation between the habenula and the telencephalon during the eye convergence in experienced fish? In addition, I also wanted to image a larger field of view, containing the forebrain as well as tectal areas and the cerebellum, to further study the changes of neuronal dynamics during prey capture. This report only describes the beginning of a project, and contains a description of the methods, some preliminary behavioral and preliminary neural imaging data, obtained from one example fish. A continuation of this investigation including further data collection and analysis will be necessary to answer any of the above stipulated questions. This report is intended as summary of the work done so far, and an outlook on the potential of using this technique on the zebrafish prey capture model.

Tg(NeuroD:GCaMP6f) positive larvae were fed with paramecia on day 5 and 6 post fertilization (dpf) as previously described[7] (Figure 3.1. A). On day 7 dpf morning, they were mounted in 3% agarose in a custom well, with eyes and tail freed (Figure 3.1. B) and let acclimate for 3-6 hours prior to the experiment.

For the data shown here, a fish was mounted on the setup and never moved, while six consecutive epochs were recorded (Figure 3.1D), with short breaks in between, to assess prey capture responses during the experiment. This helped gauging the responsiveness of the fish, since large behavioral variability has been observed in previous studies not shown here, and in similar studies done by others[5]. We wanted to maximize our chances to get many convergence responses

and detect a low responding fish early. At the beginning of each experiment, we tested what y-position of the moving dot elicited the largest neuronal response in the optic tectum and used that y-position as starting position for the stimulus. It had previously been shown that dots of size 2 - 10 degrees of the visual field (°), moving at a speed of 30°/s elicit naturalistic hunting behavior[5,8,9], and that fish generally prefer to approach their prey from the bottom angling their body at 45°below the fish, therefore suggesting the importance of finding the ideal y-coordinate for visual stimulus presentation. We displayed a small moving dot of size 4° at three heights in front of the fish for 20 trials per height, since we had previously found that y-coordinate of the stimulus greatly influenced response rate (data not shown). A trial consisted of a 5 second (s) baseline period, 5.4 s of stimulus on period, and 18.2 s of post stimulus period (Figure 3.1. C). Upon observing only few large convergence events after epoch 1, we increased the dot size to 10°, also presenting it at three heights. We found similar response rates in epoch 2 and observed that most of the responses occurred at the lowest height, right in front of the fish, where we previously had observed the largest neural response to the stimulus in the optic tectum. Consequently, we displayed 30 trials each of dot sizes 2°, 4° and 8° in a random order for the following four epochs, for a total of 120 stimuli of each size.

Across all recording epochs, we observed small convergence events, not previously seen in free swimming prey capture assays and semi-immobilized assays with live prey, and larger, typical convergences that lasted multiple frames. Most large convergences occurred in epoch 3, and the fish responded similarly to the three different stimulus sizes as expected, since they should all appear prey-like. Overall, the fish responded with eye convergence to 8% of the stimuli, consistent with what has been seen previously in similar setups[5].Further, we noted that convergences occurred at different times throughout the each trial, and that in general, convergences happened more frequently at during the visual stimulus (Figure 3.1. G), but that there was a second peak in the distribution of convergences around second 10 - 15 seconds after stimulus offset. Separating large and small convergences showed that especially the large convergences did not occur during the stimulus time (Figure 3.1. G-I). Further studies will be necessary to exactly determine the parameters inducing the most naturalistic convergence responses, here we observed small and large convergences in response to various stimulus sizes, occurring during the stimulus time and with a delay.

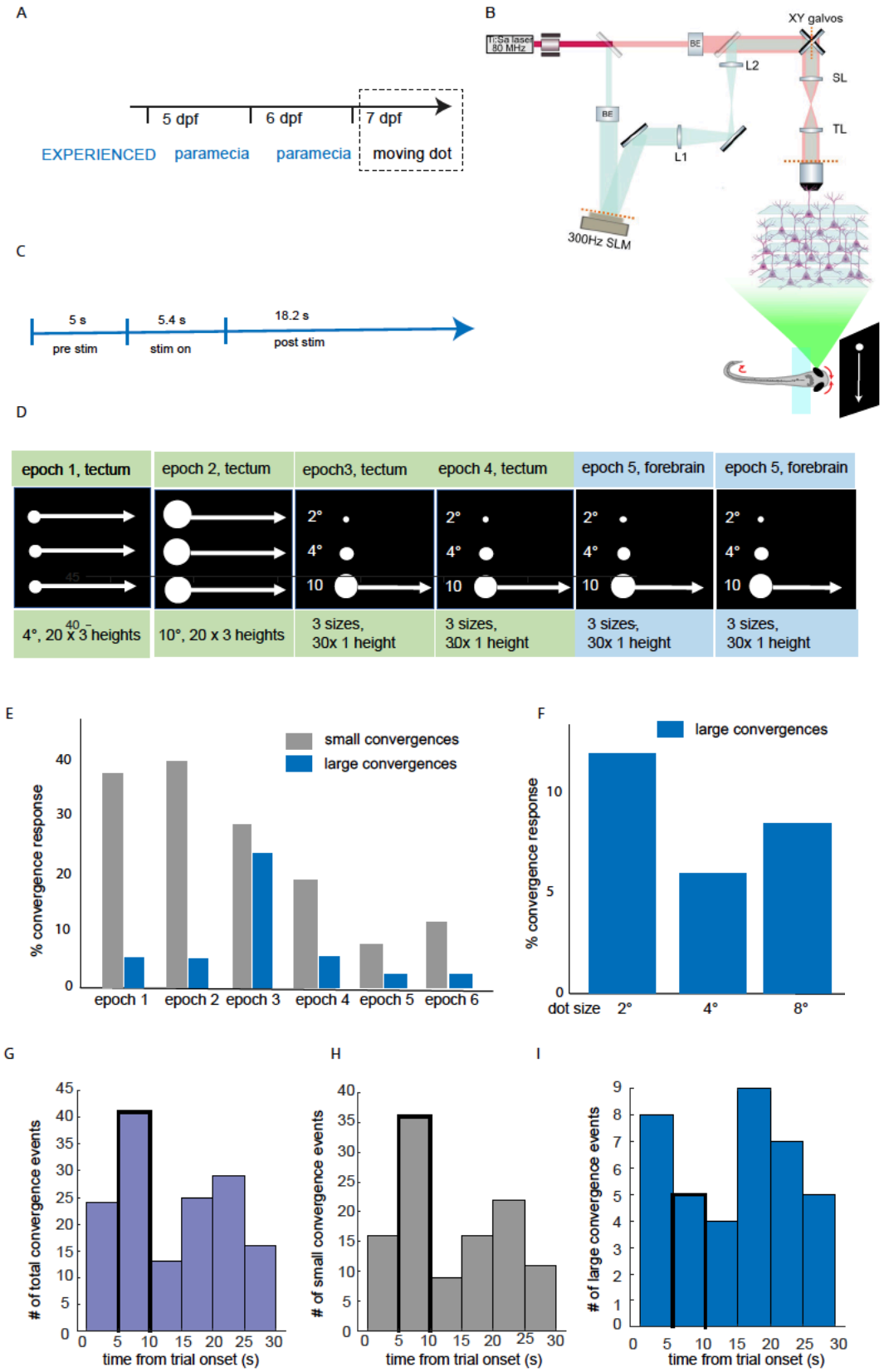

Figure 3.1. Behavioral responses to "prey like" moving dot stimuli.

A) Feeding protocol. B) Schematic of imaging setup, showing the microscope and the semi-immobilized zebrafish. C) Schematic of the timing of each behavioral trial. D) Description of stimuli and imaged brain area for each recording epoch. E) Quantification of convergence responses by epoch and size. F) Quantification of large convergence responses by stimulus type for epochs 3-6. G-I) Histograms of convergence times for all convergences, small convergences, and large convergences. The box in bold indicates the times the visual stimulus is on.

The zoomed-out view reveals promising for single-cell resolution analysis of circuit dynamics

We recorded in the zoomed-out view for 4 epochs. The imaging planes include the habenula in planes 1-3, and the telencephalon, the pretectum, the tectal neuropil, the tectal PVN neurons and a part of the cerebellum (Figure 3.2. A). The imaging quality shows promise for single cell analysis, which will enable studying visual areas – forebrain interactions. Here, I only show a gross analysis of the average of the six planes and confirm our previous finding of a significant increase of fluorescence in the forebrain and cerebellum ROIs around convergence time. Here I obsere no change in activity in the pretectum and right neuropil, but the left tectal neuropil also shows a significant increase (Figure 3.2 B and C). This analysis is preliminary and must be confirmed with more animals. Further, it has been performed on raw data, therefore a motion artifact is noticeable, and may confound the result.

A

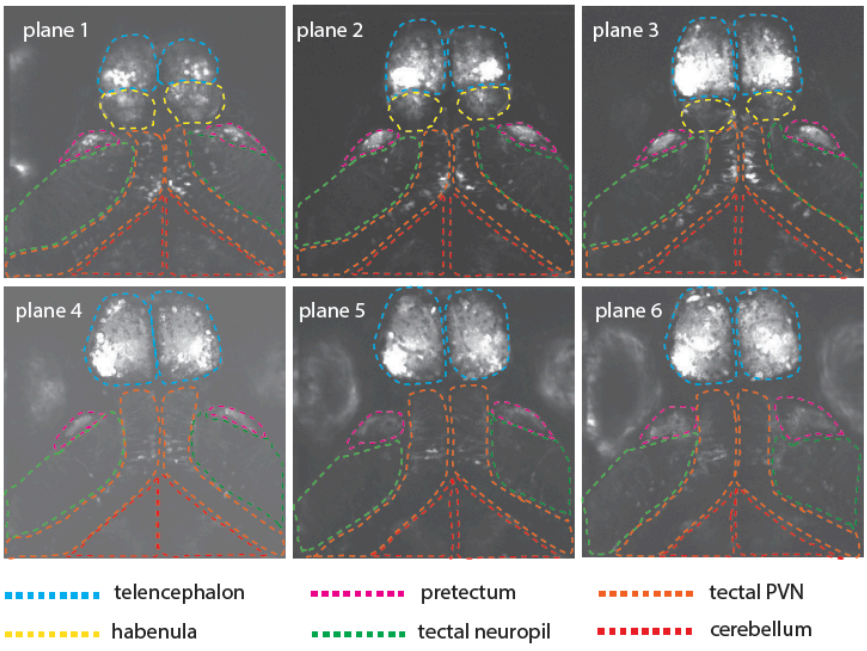

B

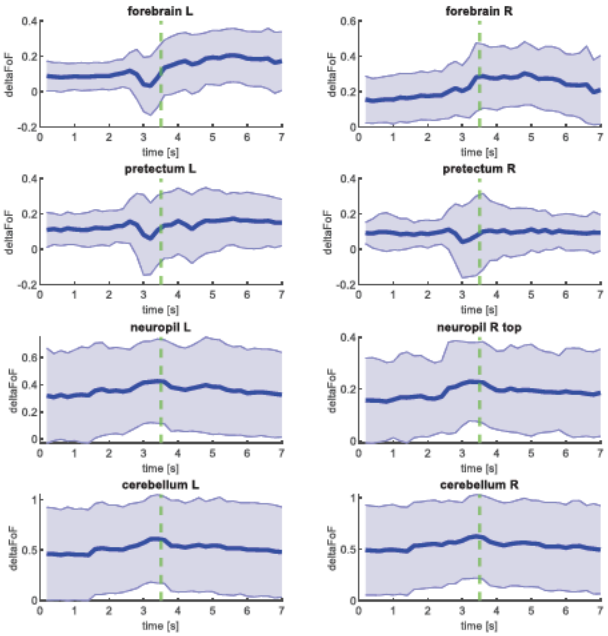

C

ROI	p value
forebrain L	0.0005
forebrain R	0.0002
pretectum L	0.4319
pretectum R	0.3468
neuropil L	0.0094
neuropil R	0.0177
cerebellum L	0.0038
cerebellum R	0.2943

max convergence

Figure 3.2. Neural activity in the zoomed-out view.

A) View of the six recorded imaging planes. Images are average intensity Z-projections of 1000 motion corrected frames in a representative animal. **B)** Average fluorescence change around time of eye convergence computed over average of six planes. Habenula and telencephalon have been included in the same ROI. N= 35 convergences. **C)** p-values of permutation test comparing mean fluorescence during second 1-2, before convergence, to the second right after the maximum convergence.

The forebrain view reveals activity of hundreds of neurons

For epochs 5 and 6 we recorded a zoomed-in view of the forebrain, including the habenula in planes 1-3. We identified hundreds of distinguishable single-cell ROIs even in the densely packed forebrain of the zebrafish (Figure 3.3.). Unfortunately, this fish displayed only four convergence events across the 180 recorded trials, and therefore I did not proceed with analysis.

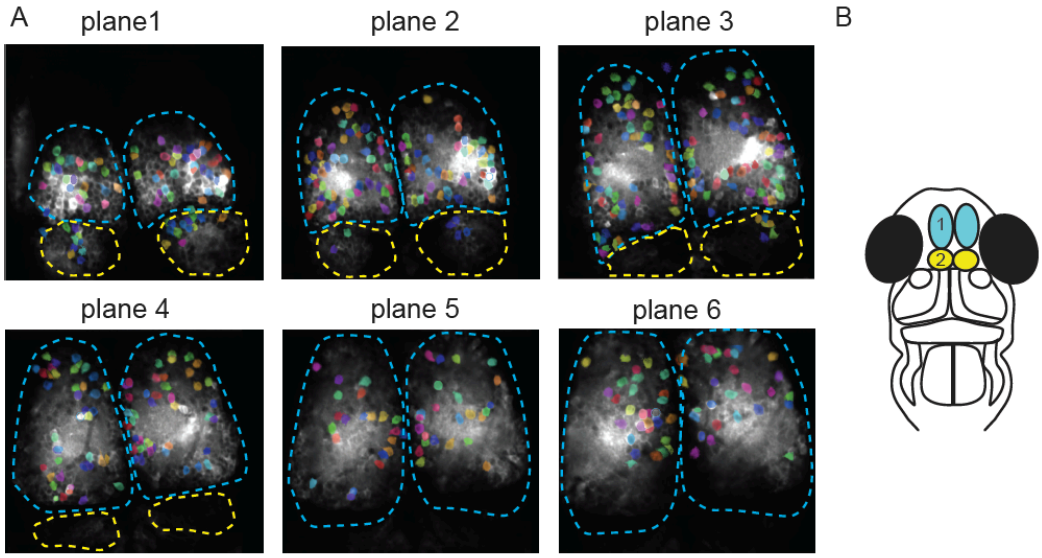

Figure 3.3. Neural activity in the forebrain view.

A) View of the six recorded imaging planes in the forebrain. Colored spots are single cells detected by Suite2p software, displayed on an average intensity z-projection of the plane. The outlines of telencephalon (blue) and the habenula (yellow) are shown with dashed lines. **B)** Schematic of forebrain view, showing the telencephalon (1) in yellow and the habenula (2) in blue.

Discussion

Few hunting responses to visual stimuli are a challenge for this experiment

In the experiment shown here and a few other pilot experiments with data not shown here, we observed a general convergence response rate to prey-like visual stimuli of 8%. In previous studies, a preference for stimuli the size 2-5° was shown to be ideal to elicit capture responses More precisely, for small dark spots on white background in direction left to right, response rates of 4-10% were observed, while for right to left moving stimuli, the rates were 13-20%[5,8]. Similarly, for a white dot on black background, response rates of 5% in direction left to right and 7% in direction right to left were reported previously[5].In our study, we used a white moving dot on black background and presented stimuli in left to right direction. We tested stimuli ranging from 2-10° degrees of the visual field and did not detect a strong preference for a specific stimulus size (Figure 3.1. F). We hypothesize that the direction and color of the stimulus may play a role in reduced convergence behavior, while the presentation of multiple dot sizes may have brought a slight advantage. Further, we previously used a curved screen (Ch. 2) allowing keeping the distance of the dot to the eyes of the fish more constant and a black dot which may be more ethological. In the two-photon imaging experiments, we used a flat screen and a white dot on a black background. In these experiments, the dot may appear different sizes depending on how far it is from the larva's eye and the white dot may be less ethological. Unfortunately, a black dot on a white background was not compatible with our current imaging setup because of the light sensitivity of the detectors, but in the future, it may be of advantage in showing the dots moving from right to left.

In addition, we observe two types of convergent eye movements. One large and sustained, as it is observed in freely swimming fish hunting paramecia, and the other very small often involving only one eye and lasting only one frame. These small convergences have not been reported in the literature before and may be a byproduct of the artificial stimuli. It is unclear if they can be counted as real convergence events. However, they seem to be more tightly time-locked to the onset of the stimulus than the larger convergences (Figure 3.1. E and G-H). In general, we observe a bout of capture responses in the five seconds of the stimulus duration, and then a second increase in responses 10 -20 seconds after the stimulus onset. More data is required to confirm these results, and a camera capable of recording and saving behavioral data at a higher speed may be needed. In summary, we show that zebrafish larvae respond to prey-like moving dots with naturalistic movements at low frequency, therefore long recordings will be necessary obtain enough behavioral events.

Movement is a challenge for imaging neural activity in a behaving animal

During the neural recordings we observed movement artifacts in both the zoomed-in and the zoomed-out view. This is a classic challenge for recordings of neuronal activity in live behaving animals, that has not completely been solved. We used the imaging software Suite2p for image registration[10], and observed good performance for the x-y movements, however, we also observed movements in the z-plane especially at times of eye convergence, or when the fish was struggling to escape the agar. Movements in the z-plane reveal challenging to correct even for the most advanced algorithms, therefore it may we worthwhile considering an even higher percent of agarose to mount the fish or paralyzing the larva with bungarotoxin for future experiments.

Overall, our setup revealed extremely efficient for volumetric recording of large populations of densely packed neurons in live behaving zebrafish and shows promise for studying the neural basis of other behaviors in zebrafish and other organisms.

Future directions

In this chapter, I describe the development of an imaging setup suited to image large populations of neurons in 3D at single cell resolution. While this project is still in an early stage, this report can serve as a roadmap for future researchers and shows the potential to uncover the ensemble neuronal response laying at the basis of a natural decision. Zebrafish prey capture lies in the sweet spot of a simple enough and complex enough behavior, requiring integration of external and internal sensory stimuli for gating its stereotyped execution. Further, its improvement with practice offers a unique opportunity for further studies of experience dependent improvement at many levels. Prey capture behavior, together with the accessibility and small size of the zebrafish brain, it may be an ideal preparation to image and manipulate “thoughts” at a single cell resolution. Further, this imaging setup and behavior may allow for causally testing the involvement of specific groups of neurons using optogenetics. In combination with 3D holographic optogenetic techniques it may offer the unique opportunity to manipulate patterned activity of neuronal ensembles to bias behavior, and at its most extreme, put thoughts in an organism’s head.

Materials and Methods

Zebrafish care and transgenic lines

Animal experiments were done under oversight by the University of California Berkeley institutional review board (Animal Care and Use Committee). The adult strain of Tg(NeuroD:GCaMP6f)^{icm05} Danio rerio[11] in the AB background was maintained and raised on a 14/10 hr light cycle and water was maintained at 28.5°C, conductivity at 500 µs and pH at 7.4. Embryos were raised in blue water (3 g of Instant Ocean salts and 0.2 mL of methylene blue at 1% in 10 L of osmosed water) at 28.5°C. For imaging experiments, fish were screened for GCaMP6f expression at 3 or 4 dpf. We used this line for all imaging experiments.

Two-photon-calcium imaging and visual stimulation

Larvae were mounted in 3% agarose on day 7 post fertilization and let acclimate in the incubator at 28.5°C for three to six hours before the experiment. Imaging was performed using a custom-built two-photon microscope, developed by Dr. Lamiae Abdeladim. This microscope achieves high-speed volumetric two-photon imaging by combining resonant galvo raster scanning (8kHz Cambridge Technology) and a high refresh rate (300Hz) spatial light modulator (SLM, Medowlark Optics). The SLM is conjugated to the scanners through a 4f system[8] and is triggered to switch to a different defocus phase pattern (i.e different Z-plane) at the end of each 2D frame acquisition. Imaging was performed at 920 nm with average laser power at sample of 10–20 mW. Images were acquired in two views, one zoomed-out (512 x 512 pixels, 0.8 µm/px) showing the forebrain, optic tectum and part of the cerebellum and one zoomed-in (512 x 512 pixels, 0.5 µm/px), focused on the forebrain only (Figures 3.2. and 3.3. A). For each larva, six focal planes were acquired by frame scanning at 5 Hz per plane, with a z-spacing of 10 µm. Visual stimuli were white moving dots of sizes 2 - 10° of visual space, moving at 30°/s, described as ideal stimuli to elicit prey capture behavior[5,9]. The stimuli were shown on a flat LCD screen that was positioned at a viewing distance of 1.6 mm from the fish. Visual stimuli were designed in MATLAB (MathWorks) using Psychophysics toolbox[10]. For all experiments, visual stimuli were presented in pseudo-random order from left to right across ~130° of frontal visual space, with 28.6 seconds of inter stimulus interval (Figure 3.1.C). Eye movements were tracked at 2.7 Hz using an inverted microscope (5X Olympus objective and a 100mm achromatic doublet as a tube lens) imaging onto a camera (Basler ACa2500), which was synchronized to the imaging setup using a hardware trigger. Microscope control and stimulus presentation were implemented using MATLAB (MathWorks). Behavioral events were tracked manually.

Calcium imaging analysis and statistics

All calcium data analysis was performed using MATLAB scripts. Extraction of fluorescence data and definition of ROIs were performed either manually using Fiji image analysis platform[12] or the software suite2p[10], which also implemented motion correction. The time-varying fluorescence signal $F(t)$ for each cell was extracted by computing the mean value of all pixels within the corresponding ROI binary mask at each time-point (imaging frame). The proportional change in fluorescence ($\Delta F/F_0$) at time t for all ROIs was calculated as $\Delta F/F_0 = F_{(t)} - F_0 \ / \ F_0$, where F_0 is a reference fluorescence value, taken as the 5th percentile of $F(t)$ over the whole duration of the trial. Statistical analyses were performed in MATLAB R2018b (MathWorks), and

all statistical tests, p-values, N-values are reported in the text. The permutation test used here is described previously[7].

References

1. Marques, J. C., Li, M., Schaak, D., Robson, D. N. & Li, J. M. Internal state dynamics shape brainwide activity and foraging behaviour. *Nature* (2020). doi:10.1038/s41586-019-1858-z
2. Ahrens, M. B. *et al.* Brain-wide neuronal dynamics during motor adaptation in zebrafish. *Nature* **485**, 471–477 (2012).
3. Ahrens, M. B. & Engert, F. Large-scale imaging in small brains. *Curr. Opin. Neurobiol.* **32**, 78–86 (2015).
4. Andalman, A. S. *et al.* Neuronal Dynamics Regulating Brain and Behavioral State Transitions. *Cell* **177**, 970-985.e20 (2019).
5. Antinucci, P., Folgueira, M. & Bianco, I. H. A pretectal command system controls hunting behaviour. *bioRxiv* (2019). doi:10.1101/637215
6. Bianco, I. & Engert, F. Visuomotor Transformations Underlying Hunting Behavior in Zebrafish. *Curr. Biol.* **25**, 831–846 (2015).
7. Oldfield, C. S. *et al.* Experience, circuit dynamics, and forebrain recruitment in larval zebrafish prey capture. *Elife* **9**, (2020).
8. Bianco, I. H., Kampff, A. R. & Engert, F. Prey capture behavior evoked by simple visual stimuli in larval zebrafish. *Front. Syst. Neurosci.* **5**, 101 (2011).
9. Filosa, A., Barker, A. J., Dal Maschio, M. & Baier, H. Feeding State Modulates Behavioral Choice and Processing of Prey Stimuli in the Zebrafish Tectum. *Neuron* 1–13 (2016). doi:10.1016/j.neuron.2016.03.014
10. Pachitariu, M. *et al.* Suite2p: beyond 10,000 neurons with standard two-photon microscopy. *bioRxiv* 61507 (2016). doi:10.1101/061507
11. Rupprecht, P., Prendergast, A., Wyart, C. & Friedrich, R. W. Remote z-scanning with a macroscopic voice coil motor for fast 3D multiphoton laser scanning microscopy. *Biomed. Opt. Express* **7**, 1656 (2016).
12. Schindelin, J. *et al.* Fiji: an open-source platform for biological-image analysis. *Nat. Methods* **9**, 676–682 (2012).